5-2005

Stratigraphic and Structural Analysis of Coals in the Ferron Sandstone Member of the Mancos Shale and Fruitland Formation: Relationship to Coal Reservoir Permeability and Coalbed Methane Production

Jason Lynn Kneedy

STRATIGRAPHIC AND STRUCTURAL ANALYSIS OF COAL IN THE FERRON SANDSTONE MEMBER OF THE MANCOS SHALE AND FRUITLAND FORMATION: RELATIONSHIP TO COAL RESERVOIR PERMEABILITY AND COALBED METHANE PRODUCTION

by

Jason Lynn Kneedy

A thesis submitted in partial fulfillment
of the requirements for the degree

of

MASTER OF SCIENCE

in

Geology

Approved:

James P. Evans Major Professor	Bradley D. Ritts Committee Member
Thomas E. Lachmar Committee Member	Laurens S. Smith Interim Dean of Graduate Studies

UTAH STATE UNIVERSITY
Logan, Utah

2005

ABSTRACT

Stratigraphic and Structural Analysis of Coals in the Ferron Sandstone Member of the Mancos Shale and Fruitland Formation: Relationship to Coal Reservoir Permeability and Coalbed Methane Production

by

Jason Lynn Kneedy, Master of Science

Utah State University, May 2005

Major Professor: Dr. James P. Evans
Department: Geology

Coal reservoir quality in the Ferron Sandstone Member of the Mancos Shale, and in the Fruitland Formation is dependent on coal cleat characteristics. Coal reservoir permeability increases as a result of high cleat density. From careful outcrop examination, we were able to identify several factors that increase cleat density. Vitrain coal typically has the highest fracture density as a result of having well-developed face cleats and conchoidal fractures. Clarain coal contains face and butt cleats. Cleat density in clarain is also controlled by mechanical layer thickness. As mechanical layer thickness decreases, cleat density increases. Durain and fusain coals typically contain no well-developed cleat system, although their presence can affect mechanical layer thickness in adjacent coals, as they may form bounding units. Cleat density increases in the damage

zone of faults and in the hinge-line of folds. Cleat-controlled reservoir permeability has beneficially affected methane production in one portion of the Drunkards Wash Gas Field, Utah, and appears to have negatively influenced methane production in the coalbed methane field. (125 pages)

ACKNOWLEDGMENTS

I wish to extend a special thank you for the research grants received from the Geological Society of America Coal Division, the A.L. Medlin Scholarship Award, the Alexander and Geraldine Wanek Research Award, the American Association of Petroleum Geologists, and the Classen Family Grant. I greatly appreciate the tuition coverage, teaching and research assistant positions granted from the Utah State University, College of Science. We appreciate the insight and field data supplied from ConocoPhillips geologist, Tom Cloud. UF3, a consulting company headed by Jim Evans, provided me with additional research opportunities and monetary support, allowing for the extension of our study into portions of southwest Colorado. Special thanks to my thesis committee members, Jim Evans, Brad Ritts, and Tom Lachmar, who have contributed helpful suggestions to this research project. I have enjoyed and learned a lot from the enthusiastic and knowledgeable professors, staff, and students in the Geology Department at Utah State University.

My major advisor, Jim Evans, is very insightful, intelligent, and easy to work with. Jim has prompted me to keep rolling, but has never been pushy. I appreciate Jim working around my busy family, work, and commuter schedule. Thank you Jim.

Thank you Shannon for being so supportive and helpful during the endless nights I spent at the computer. Thank you for being my field assistant and Geo-Mom during the hot days spent in central Utah. To my three kids, Sheyanne, Colt, and Ryker, thank you for being good kids. I would thank my mom, dad, grandparents, brother, and sisters for prompting me to set high goals, and supporting me in my academic endeavor.

Jason Lynn Kneedy

CONTENTS

LIST OF TABLES

LIST OF FIGURES

CHAPTER 1

INTRODUCTION

Production of coalbed methane from the Rocky Mountain region is one of the most active new concepts in developing natural gas in the United States (Montgomery et al., 2001). Recent drilling in the Drunkards Wash field, near Price, Utah, in the Upper Cretaceous Ferron Sandstone Member of the Mancos Shale, has resulted in one of the most successful plays of this kind (Anderson et al., 2003). Drunkards Wash is the largest gas field in Utah, and is the 18th largest natural gas field in the United States (Energy Information Administration, 2004), with 2003 total gas production reaching 79,210,724 MCF (thousand cubic feet) (Utah Oil, Gas and Mining, 2004). Estimated ultimate recoveries in Drunkards Wash range from 1.5-4.0 tcf (trillion cubic feet) (Montgomery et al., 2001).

The success of the Drunkards Wash field has resulted in a significant beneficial economic impact to the state of Utah. In 2001, over $51 million in royalties were paid to the federal government (Isaacson, 2003). Of this, nearly $25.5 million was returned to the state of Utah (Isaacson, 2003) for spending at its discretion. The State School and Institutional Trust Lands Administration (SITLA) owns the majority of land and mineral rights in Drunkards Wash field (Isaacson, 2003). Royalties paid to SITLA rose from about $2 million in the early 1990's to $26.7 million in 2003 as a result of coalbed methane production in Drunkards Wash (Isaacson, 2003).

Production of coalbed methane is largely a function of coal fracture permeability. The density, connectivity, and hydraulic properties of fractures and faults within the coal

and adjacent stratigraphy often control overall reservoir permeability. To date, little work has been performed that examines the fracture characteristics in the Ferron Sandstone Member coalbed methane system.

We examine coalbed methane reservoir outcrop analogs in the Ferron Sandstone Member, approximately 30 km south of Drunkards Wash, and in the San Juan Basin, in southwest Colorado, in order to gain insight into the nature of coal fractures and their ultimate controls on overall reservoir permeability. Numerous predictable factors affect coalbed reservoir permeability. These factors include cleats, coal type, structural controls, and joint intersections between coal and adjacent stratigraphy. These factors are described and analyzed in Chapter 2. In Chapter 3, we use our understanding of the controls on coalbed fracture characteristics to determine why a portion of the Drunkards Wash coalbed methane field is less productive than expected. Conclusions from this study are presented in Chapter 4.

References

Anderson, P.B., D. Tabet, and G. Hampton, 2003, Coalbed Gas Deposits of Central Utah: AAPG Field Trip #18 Guide, Rocky Mountain Section AAPG.

Energy Information Administration (EIA), 2004, U.S. Crude Oil, Natural Gas Liquid Reserves: 2004 Annual Report. Appendix B. http://www.eia.doe.gov/pub/oil_gas/data/publications/crude.

Isaacson, Alan, 2003, Utah Economic and Business Review: Bureau of Economic and Business Research, David Eccles School of Business, University of Utah, November/December, v. 63, no. 11 and 12.

Montgomery, S.L., D.E. Tabet, and C.E. Barker, 2001, Upper Cretaceous Ferron Sandstone: Major coalbed methane play in central Utah: American Association of Petroleum Geologists Bulletin, v. 85, p. 199-219.

Utah Division of Oil, Gas and Mining, 2004, Gas Field Statistics.

http://ogm.utah.gov/oilgas/STATISTICS/1prod.htm

CHAPTER 2

ANALYSIS OF COAL CLEATING IN THE FERRON SANDSTONE MEMBER, UTAH; AND THE FRUITLAND FORMATION, COLORADO[1]

Abstract

The Ferron Sandstone Member of the Mancos Shale in central Utah and the Fruitland Formation in southwest Colorado contain coals which are a methane source and reservoir for several coalbed methane fields along the Ferron trend, including Drunkards Wash, the largest coalbed methane field in Utah, and the northwest San Juan Basin gas field in Colorado. Coal fracture (cleat) systems are a fundamental control on coalbed methane production.

We examined factors that affect coal cleating in the Ferron Sandstone Member, Utah, and to a lesser extent, in the Fruitland Formation coals in the San Juan Basin, Colorado. Composition is one primary control on the presence and density of cleats in a coal bed. Vitrain and vitrain-rich coals contain the highest density of coal cleats, though typically only a face cleat is developed. Clarain coal contains a well-developed face and butt cleat set, in which cleat density is controlled by mechanical layer thickness. As ash content in clarain coal increases, bed parting frequency increases. These bed partings act as bounding units, and define a mechanical layer thickness; hence, high ash content in clarain coals decreases average mechanical layer thickness and increases cleat density. Carbonaceous shale is commonly found interbedded with and surrounding coal in both

[1]Coauthored by Jason Kneedy and James P. Evans

study areas. Carbonaceous shales do not typically develop face or butt cleats. Due to their ductile properties, joints from adjacent sandstones and coal cleats commonly terminate at even thin carbonaceous shale layers.

The presence of folds and faults also affects cleat density. Cleat density is enhanced in the vicinity of a fold hinge and in the damage zone of faults. In the faults we examined, fault parallel permeability is increased within the fault-damaged zone. Migration paths across a fault may be drastically reduced as a result of lateral juxtaposition.

Regional joints may break through, weaken, terminate, or multiply upon intersecting coal or carbonaceous shale. Regional joint continuation characteristics vary as a result of the thickness of the beds involved. If the sandstone to coal thickness ratio is greater than 4:1, then joints typically breakthrough both the sandstone and the coal. If this critical ratio is not met, then joint termination, weakening or multiplication is the dominate patterns seen when joints in adjacent sandstone intersect coal zones. Understanding joint continuation patterns in adjacent sandstone, increases understanding of reservoir connectivity, migration paths, and may prove useful when designing fracture stimulation techniques.

Introduction

Coal cleats are natural fractures in coal. Description of coal cleats and speculation on their origin dates from the early nineteenth century (Mammalt, 1834; Milne, 1839; cited in Kendal and Briggs, 1933). In the early 1990's, as coalbed methane

became an economically valuable resource, a renewed interest in coal cleat systems arose. Coal matrix permeability is too low for commercial production of gas. Coalbed methane systems are largely dependant on cleats (Scott et al., 1996; Ayers, 2002) as they provide the majority of the interconnected macroporosity in coal. Understanding the characteristics of the cleat systems and the associated mechanisms of their formation is essential for effective coalbed methane exploration and field management. Numerous authors (e.g., Spears and Caswell, 1986; Close and Mavor, 1991; Laubach and Tremain, 1991; Tremain et al., 1991; Grout, 1991; Levine, 1993; Law, 1993; Laubach et al., 1997) have examined some aspect of coal cleat characteristics and/or development. Although some contention exists in the literature, numerous advances have been made as a result of this effort.

We examined coal cleat characteristics within the Ferron Sandstone Member of the Mancos Shale in east-central Utah, and in the basal coal exposures of the Fruitland Formation in southwest Colorado. Analysis of coal cleats in two field areas increased the amount of accessible coal outcrops and provided a means of comparison of coal cleat characteristics that extends beyond a single field. Core samples of continuous sandstone, siltstone, coal, and carbonaceous shales sequences where examined from both areas. After examination and analysis of coal cleats and stratigraphy from the two different formations, we have identified numerous coal cleat characteristics, joint propagation patterns, and stratigraphic complexities that will lead to a better understanding of the coal cleat and reservoir dynamics affecting coalbed methane production.

Geologic Setting

Ferron Sandstone Member of the Mancos Shale

Coalbed methane (CBM) fields in the Ferron play are located along the western flank on the San Rafael Swell and to the east of the Wasatch Plateau of central Utah. The coalbed gas is produced from within the Ferron Sandstone Member of the Mancos Shale (Ryer, 1981; Anderson et al., 1997; Montgomery et al., 2001). Approximately 30 km south of the Ferron CBM fields, the Ferron Sandstone Member is exposed along a ~170 km northeasterly trending outcrop belt in Emery and Sevier counties (Ryer, 1981). We examined coal outcrops throughout this trend in order to study the characteristics of coal cleating and stratigraphy (Fig. 2-1).

The Ferron Sandstone Member lies conformably above the 120 to 200 m thick Tununk Shale Member of the Mancos Shale. Above the Ferron Sandstone, the Lower Bluegate Shale Member of the Mancos Shale ranges from 490 to 730 m thick (Fig 2-2) (Garrison et al., 1997). Along the depositional trend, the Ferron Sandstone ranges from 55 to 90 m thick in the north, and reaches maximum thicknesses between 90 and 180 m in the south where it is exposed in Emery and Sevier counties (Ryer, 1981). Sand in the Ferron Sandstone Member was sourced from the Sevier orogenic belt to west-northwest during Turonian-Conacian (Late Cretaceous) time (Anderson et al., 1997) and was deposited into the Sevier foreland, which also accommodated the Mancos Sea along the western margin of the Cretaceous, Western Interior Seaway (Gardner, 1992). Fluvial-deltaic deposition of the Ferron Sandstone Member resulted in a series of stacked, transgressive-regressive cycles (Anderson et al., 1997), which are apparent in the form of

interbedded sandstones, mudstones and coals. The wedge-shaped Ferron Sandstone Member pinches out into distal shale deposits several kilometers east of the outcrop and Drunkards Wash field area.

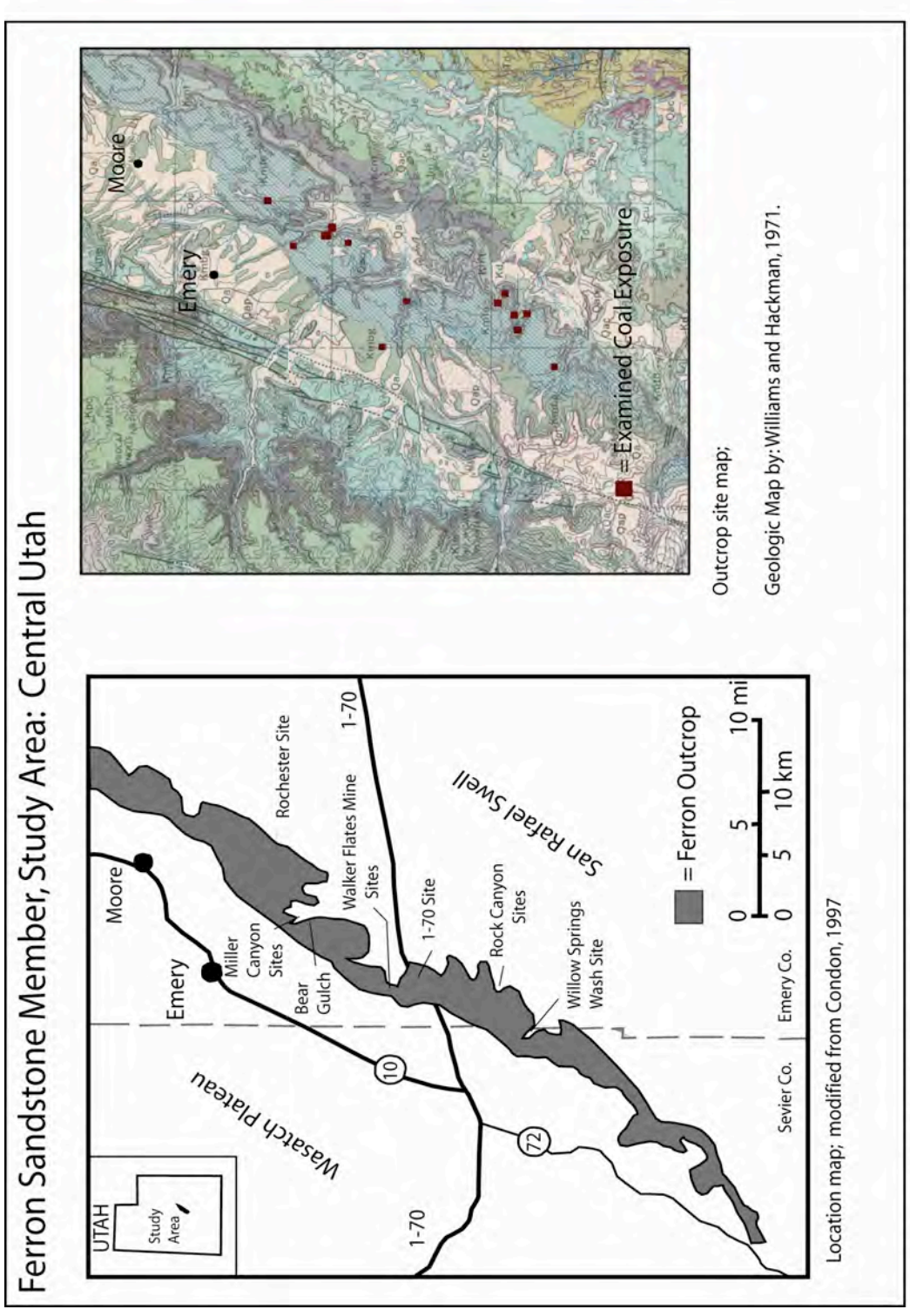

Fig. 2-1 Ferron Sandstone Member study area in central Utah. The Ferron outcrops are exposed in a northeast trending belt located to the east of the Wasatch Plateau and to the west of the San Rafael Swell

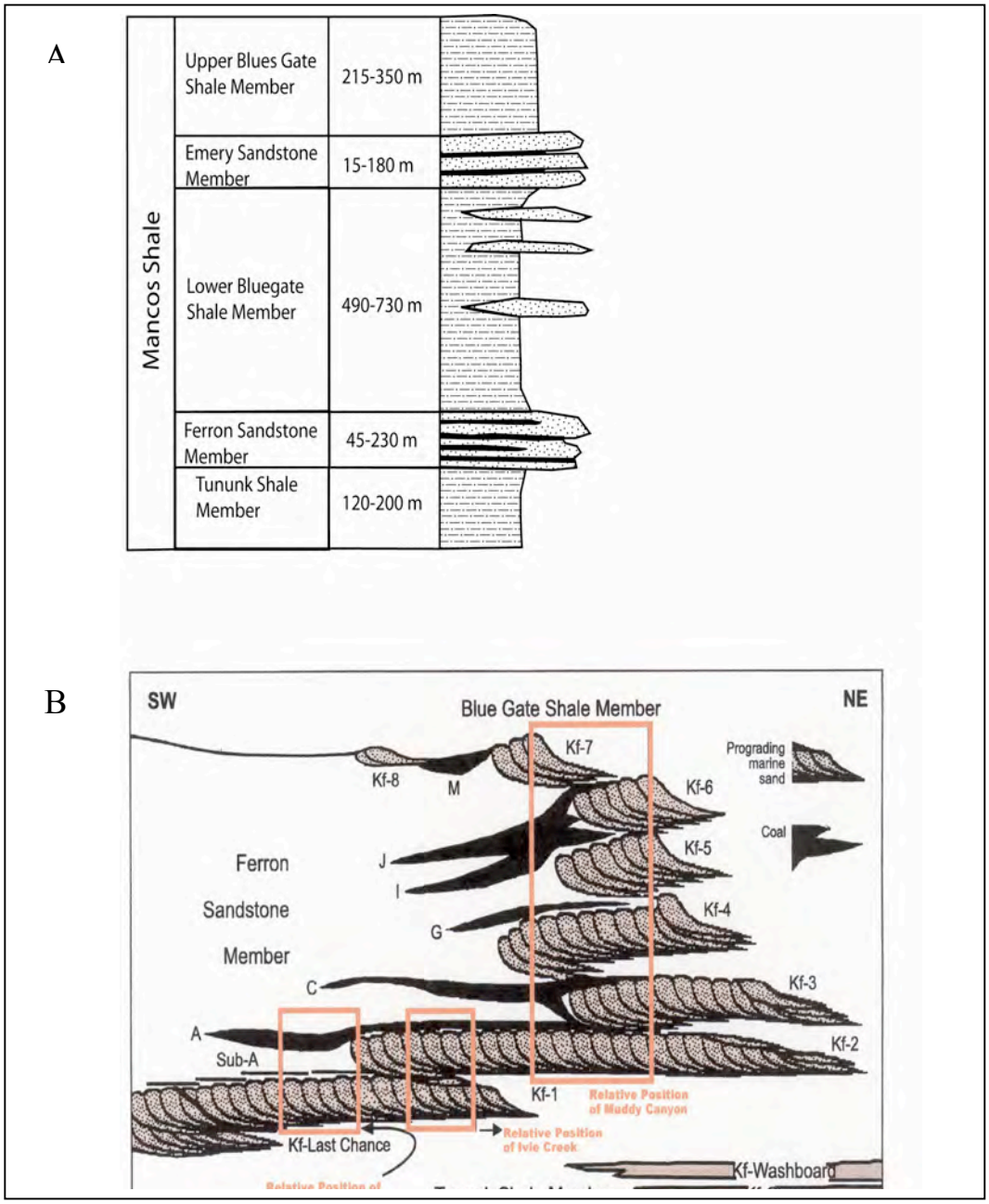

Fig. 2-2. The Ferron Sandstone stratigraphy. A. The Ferron Sandstone Member is located between thick shales of the Lower Bluegate and Tununk Shale Members of the Mancos Shale (modified from Garrison et al., 1997). B. A complex fluvial-deltaic architecture exists within the Ferron (below) (modified from Ryer, 1991; and Anderson et al., 1997.

Numerous authors (e.g., Hale and Van de Graph, 1964; Hale 1972; Cotter, 1975; Ryer, 1981; Gardner and Cross, 1994; Anderson et al., 1997; Garrison et al., 1997) have studied the stratigraphy and architecture of the fluvial-deltaic Ferron Sandstone. These studies have established that the Ferron Sandstone Member is composed of two primary delta lobes, the Vernal Delta and the Last Chance Delta (also referred to as the Upper Ferron). The Vernal Delta is interpreted as a relatively thin (55 to 90 m) storm and wave dominated shoreline/deltaic sequence that has a sediment source from the north (Ryer, 1981). The unexposed coals of the Ferron Sandstone in the Vernal Delta are the targeted source/reservoir rock of the Drunkards Wash and other Ferron play coalbed gas fields. Coal in the Vernal Delta occurs in 3 to 8 distinct seams (Garrison et al., 1997). The total coal thickness within the Drunkards Wash field ranges from 1.2 to 14.6 m, with an average thickness of 7.3 m (Garrison et al., 1997).

Hale (1972) named the exposed southern Ferron delta lobe the Last Chance Delta. The Last Chance Delta is younger (Ryer, 1981) than the Vernal Delta, and it is occasionally referred to as the Upper Ferron (see Garrison et al., 1997). With the uplift of the San Rafael Swell and tilting of the Ferron Sandstone, typical structural dip is now between 3 and 5º northwest (Condon, 1997), although the original depositional dip was toward the east-northeast (Ryer, 1981). Ryer (1981) recognized five major progradational cycles, or parasequences in the Last Chance Delta. These delta front sandstones are referred to as sandstones 1 to 5 (Ryer, 1981). Subsequent work by Gardner (1992, 1993), and Ryer (1991) led to the identification of two more stratigraphically higher delta cycles, named 6 and 7. Further studies interpreted the

lowest parasequence as being river dominated and changing from a proximal to distal facies in a northeastward direction (Utah Geological Survey, 1996). The younger parasequences are wave dominated shorefacies, distributary bars and channel sandstone beds (Utah Geological Survey, 1996). Recent studies have concluded that extensive coal zones occur at the top of parasequence sets within the Ferron Sandstone Member wedge unless coincident with a depositional sequence boundary (Garrison et al., 1997). Nomenclature for coal zones in the Upper Ferron was first developed by Lupton (1916), and retained by Ryer (1981) and Gardner (1993). They labeled coal and/or coal zones from the Ferron A Coal, C Coal, G Coal, I Coal, J Coal, and Ferron M Coal. The Ferron A Coal is the oldest coal and is found at the base of the Ferron Sandstone Member, and the Ferron M Coal is the youngest coal, near the top of the formation (Fig. 2-2b). We continue use of this nomenclature in our report.

We created a burial history plot of the Ferron Sandstone Member near Emery, Utah (Fig. 2-3). The burial history plot was created using the complete stratigraphic thickness drawn from several geologic maps that fall within our study area. In order to predict the appropriate deposition depth below water level where information was not available, we estimated an approximate depth based on stratigraphic features within each formation. The rate of sediment accumulation with this basin is a result of time and basin subsidence. On the plot, three curves are present. The upper most curve reflects the sea level at the time of deposition. Total subsidence is shown by the lowest curve and the tectonic subsidence curve in the center of the plots is calculated by removing the effects of compaction and isostatic response. In the basin modeling program we used, we

selected the parameters for this calculation that we concluded would best represent the actual conditions during basin development.

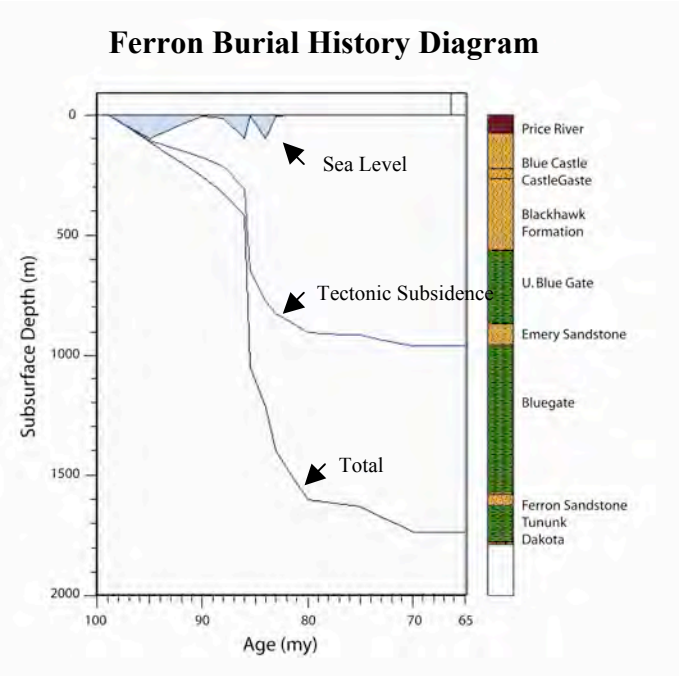

Fig. 2-3. Ferron burial history diagram. The Ferron Sandstone Member was buried to a depth of approximately 1625 m as a result of foreland subsidence and sediment input.

Our burial history plot indicates that foreland subsidence resulted in burial of the Ferron Member to a depth of approximately 1625 m below ground surface (Fig. 2-3). The Eocene Price River Formation marks the end of foreland subsidence and Ferron Sandstone Member burial, as later events were primarily erosional. Basin and Range extension, and the Laramide Colorado Plateau uplift unroofed this sequence (Lawton, 1986), leaving Ferron Sandstone Member coals buried to a depth between 550 and 1035 m (Lamarre and Burns, 1996) below the Drunkards Wash field. Isopach maps and vitrinite reflectance data (Montgomery et al., 2001) suggest that the Ferron Sandstone

Member was buried at least 1360 to 1500 m deeper in the Drunkards Wash area than it was near the town of Emery. The average R_0 value in Drunkards Wash is 0.7%, which corresponds to a high volatile B bituminous rank (Burns and Lamarre, 1997).

Fruitland Formation Geologic Setting

The San Juan basin in the east-central Colorado Plateau region is a giant coalbed play which has produced more than 7 tcf (trillion cubic feet) of gas (Ayers, 2002). Thick coals of the basal Fruitland Formation are the source of the gas as well as the target reservoir (Ayers, 2002). We examined coal in two outcrop locations and in three cores from the northern one-third of the basin (Fig. 2-4) in order to further our understanding of processes that affect coal cleating.

Similar to the Ferron Sandstone Member, the Fruitland Formation was deposited along the western margin of the Interior Cretaceous Seaway (Ayers, 2002). The Fruitland Formation consists of coastal-plain carbonceous shales, coals, mudstone, and sandstones deposited in a coastal plain setting (Tremain et al., 1991). Subsequent tectonic activity during the Laramide orogeny created both northeast- and southeast-directed shortening that resulted in the formation of the structurally asymmetrical San Juan basin (Fassett, 1985; Ridgley and Huffman, 1990).

The upper Cretaceous (Campanian) Fruitland Formation in the San Juan basin is more than 122 m thick in the northwest, but decreases in thickness until it disappears in the eastern part of the basin as a result of depositional thinning and erosion (Tremain et al., 1991). Throughout most of the basin, the Fruitland Formation is underlain by the Picture Cliffs Sandstone. The Kirtland Shale conformably overlies the Fruitland

Formation in the western two-thirds of the basin. The Fruitland Formation in the eastern third of the basin is unconformably overlain by the Tertiary Ojo Sandstone (Fasset et al., 1987).

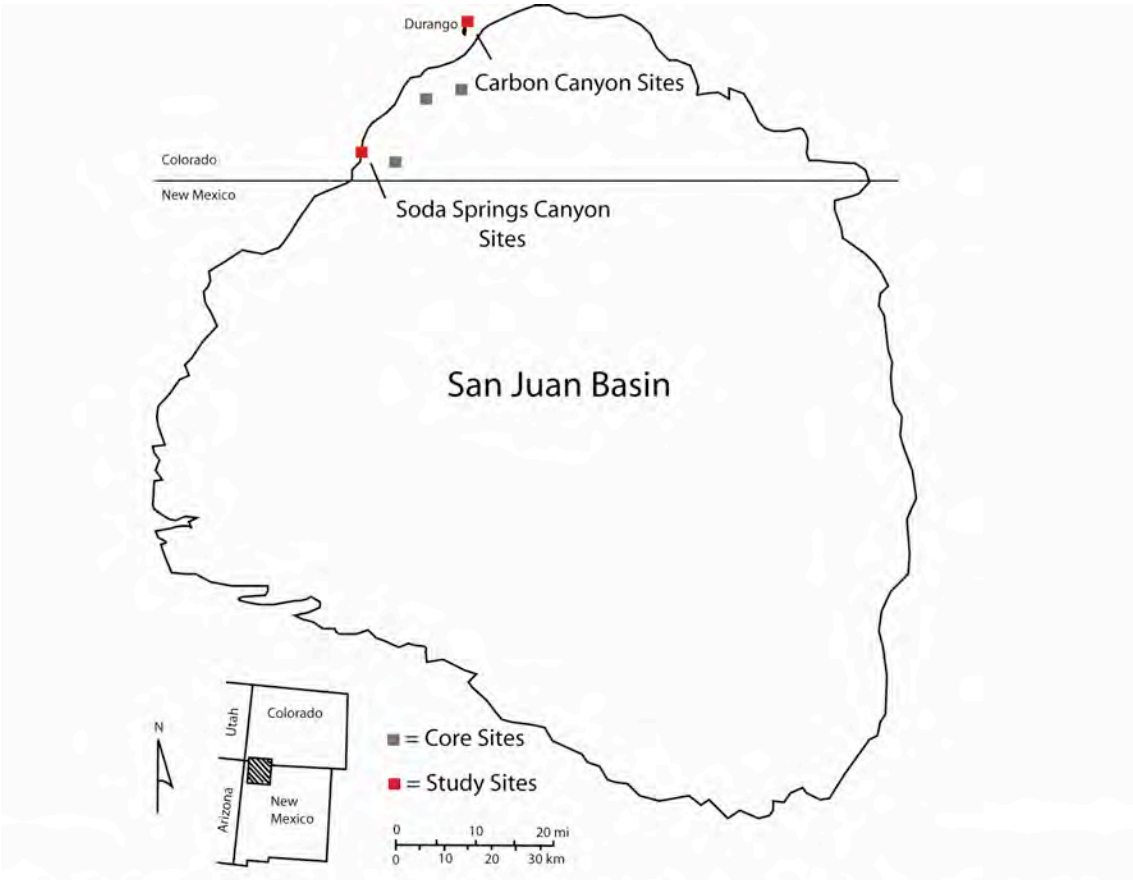

Fig. 2-4 Fruitland Formation location map. We examined Fruitland coal outcrops at two primary locations in the northern third of the San Juan Basin. Coal outcrops are exposed along the flanks of Hogback Monocline above.

Fruitland coal thickness is the greatest in the extensive, northwest trending belt of

backbarrier coals in the northern third of the basin (Ayers, 2002**)**. Coalbed methane wells within the basin commonly penetrate 6 to 12 coal beds of varying thicknesses (Ayer, 2002), with a total net coal thickness ranging up to 34 m (Ayers and Ambrose, 1990). Typical ash content in the basin ranges from 8% to 30%, and is commonly greater than 20% (Tremain et al., 1991). Coal ranges in rank from sub-bituminous B in the south to high-volatile A bituminous at the northern basin margins (Scott et al., 1990). In north-central parts of the basin, rank increases to low-volatile bituminous where coal reaches a depth of 1280 m **(**Scott et al., 1990**)**.

Definitions and Basic Concepts of Coal Composition and Deformation

Various terms have been used to describe the systematic fractures in coal, though generally they are still referred to by the old mining term: cleat (Dron, 1925). Cleat systems are open-mode, brittle fractures that form perpendicular to the least principal horizontal stress direction and parallel to the greatest principal horizontal stress direction (Engelder, 1985), similar to a "joint" in a rock. Cleats typically occur in two sets that are mutually perpendicular and also perpendicular to bedding (Laubauch et al., 1997). The dominant, through-going cleats forms first, and are referred to as "face cleats." The secondary cleat, or "butt cleat," is commonly nearly perpendicular to the face cleat. Butt cleats form later, and regularly terminate at the point of intersection with the dominate face cleat (Laubauch et al., 1997). Speculation and studies regarding the characteristics of cleats and their formation have received renewed attention, as coal cleats are a critical factor in coalbed methane recovery.

Over 95% of gas in coal is stored in micropores the coal matrix (Gray, 1987). These pores have been estimated to have diameters ranging from 0.5 to 1 nm (Van Krevelen, 1981), values so small that the coal matrix may have no effective permeability; hence, coal cleats are an essential element in coalbed methane recovery. Although some methane may occur as free gas in the coal cleat network, the majority of producible coalbed methane is adsorbed onto the cleat surfaces (Laubach et al., 1997). Producing coalbed methane is typically accomplished by pumping or removing water from the coalbed to lower the water pressure in the reservoir (Ayers, 2002**)**. As the pressure is sufficiently lowered, gas is desorbed from the cleat surface area, and possibly diffused through the adjacent coal matrix, where it flows in the form of free gas through the cleat conduits to the well bore. Permeability anisotropy is common in coalbed methane reservoirs as face cleat characteristics, specifically length, create an elliptical reservoir drainage pattern, with favorable drainage areas being parallel with face cleat orientation (Koenig, 1989). Coal cleats are critical to both water and gas production in this system. Good initial water production often indicates good reservoir porosity and permeability. Ideally, as water production slows, gas production increases. The graph of this relationship has been termed a "negative decline curve." Figure 2-5 is an example of a favorable negative decline curve from Drunkards Wash well #34, located in the southern portion of Area A, as discussed in chapter 3 of this thesis.

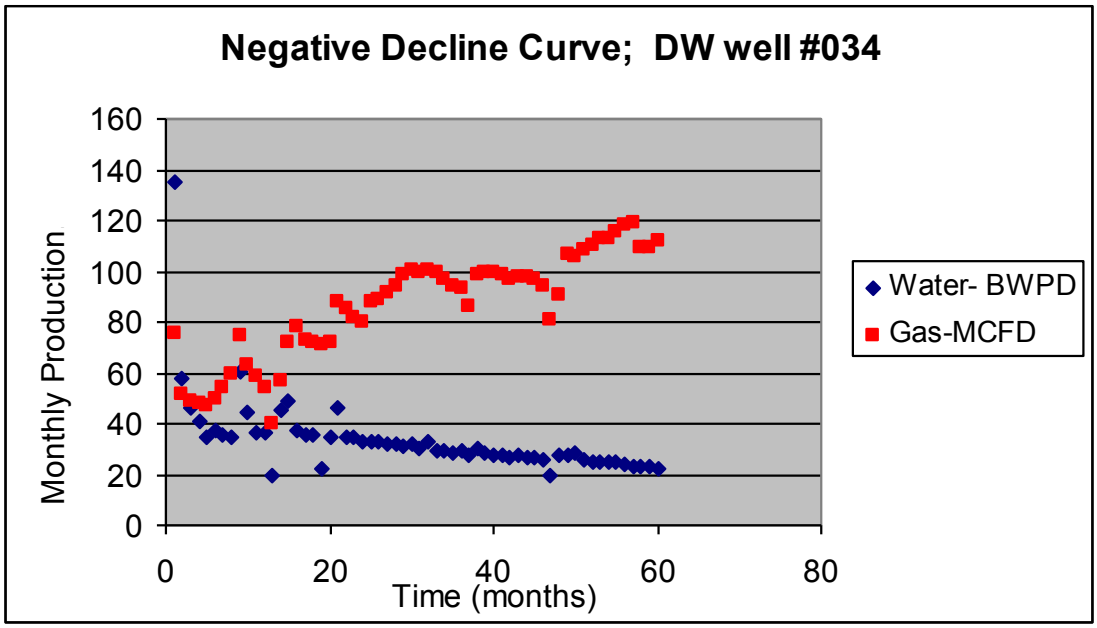

Fig. 2-5. Drunkards Wash well negative decline curve. In this ideal situation, reservoir pressure decreases as water is removed, and gas production increases.

Background Definitions

Numerous factors, including coal rank, coal composition, layer thickness, burial history, structural deformation, and coal age have been examined in attempt to understand coal cleat systems (Laubach et al., 1997). Because nomenclature used to describe coal characteristics is relatively specific to coal geology, and definitions often vary slightly between studies, this section provides some basic coal geology definitions, and the coal identification criteria we used in our study.

Coal Stratigraphy Nomenclature

There is a variety of unique terms used to describe coal stratigraphy. The term coal zone is used to describe a sequence of stratigraphy that includes all of the associated organic material within and adjacent to a coal bed. Whereas carbonaceous shale and

organic-rich mudstones are often interbedded with and adjacent to coal, we use the general term coal zone when referring to this entire sequence. A coal bed, is a more specific term used to describe a thickness of coal. Coal beds can be thick or thin, and may be composed of one or more lithotypes. A coal lithotype describes a thickness of coal that maintains a constant physical appearance, this is typically a result of consistent maceral composition within the lithotype.

Coal Rank

"Rank" in a qualitative sense indicates the position of coal in a more or less continuous series ranging from peat to anthracite. Quantitatively, coal rank is an assessment of the carbon content or volatile matter in coal (Evans and Pomeroy, 1966); the higher the carbon content, the higher the rank. During coalification, as the effects of overburden pressure and temperature transform peat into coal, the proportion of carbon matter increases, as hydrogen and oxygen are driven out of the organics (Evans and Pomeroy, 1966); hence, coals with the highest rank (anthracite) have been subjected to a longer or more extreme process than coals of lower ranks. An assessment of rank is also commonly determined based on the thermal maturity of coal. Thermal maturity of coal is determined by lab analysis of the optical properties of the coal maceral, vitrinite (Selley, 1998). This measure can be used to estimate the degree of coalification and hydrocarbon generation. The shininess, or reflective properties of vitrinite increases with maturity from peat to anthracite. This measure is commonly found in coal and petroleum geology literature, as the "vitrinite reflectance" (R_o) value. Figure 2-6 illustrates the relationship between coal rank and methane generation.

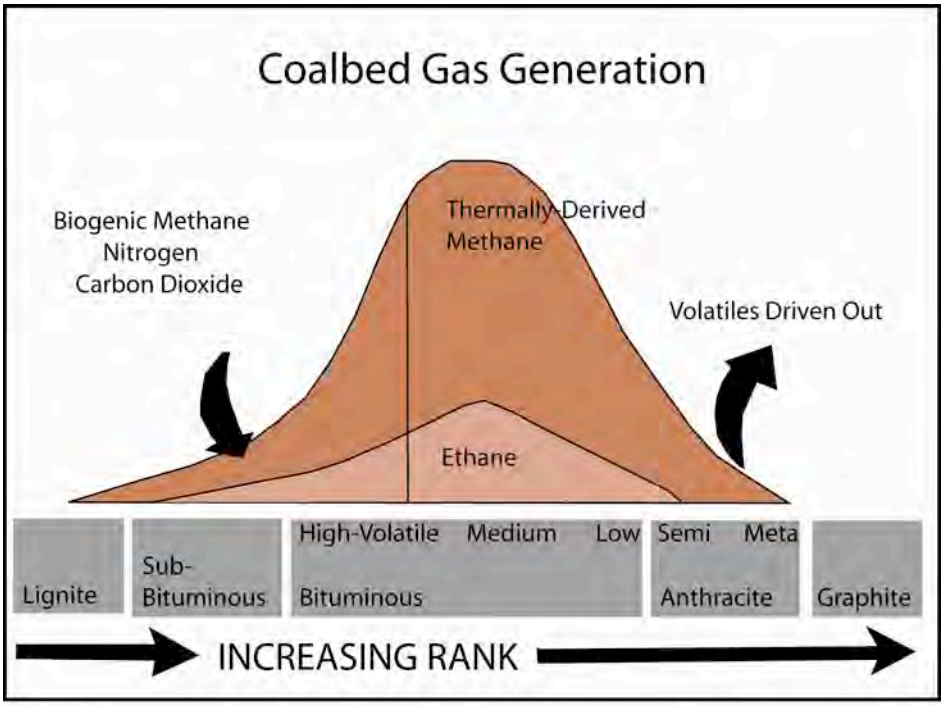

Fig. 2-6. Coalbed gas generation (modified from Lamarre, 2001). Coals within the Ferron Sandstone Member and Fruitland Formation range in rank between high volatile and low volatile bituminous.

Coal Composition

Maceral is the term used to describe the type organic matter in coal. Macerals are to coal as minerals are to igneous rocks. The maceral composition of coal affects numerous coal attributes, including appearance, strength and fracture characteristics, and the ability to generate hydrocarbons. Maceral composition of coal is determined in a laboratory by point counting. Coal samples are commonly crushed and adhered to glass with an epoxy, and polished before examination. There are many types of coal macerals. Upon determination of maceral composition, coal geologist can determine the coal type and characteristics far more accurately than any macroscopic outcrop examination.

Field Identification of Coal Composition

Whereas maceral composition analysis is relatively expensive and time consuming, coal research literature commonly discusses composition as based on some type of field identification. An evolution of field identification terms has taken place since the early work that often described coal as either bright or dull (Schopf, 1960). These terms quickly became obsolete and were replaced by the descriptive terms banded or non-banded coal (Schopf, 1960). The banded appearance seen in coal is due to compositional variances within coal created during coal deposition.. Due to the nature of coal deposition, banded coal is more abundant than non-banded (Schopf, 1960). Non-banded coal was the general term placed on a more homogeneous outcrop where compositional changes are not large enough to affect the physical appearance of the outcrop.

Stopes (1919) recognized four distinct bands types in bituminous coal that had differences in physical appearance and chemical properties, which she provisionally named vitrain, clarain, durain and fusain. These lithotype classifications have retained their usage from coal researchers as fundamental macroscopic compositional descriptive terms. In addition to the above descriptive terms, attrital coal, carbonaceous shale, and ash are common descriptors found in the literature. We continue the use of field description terms as set forth by Stopes (1919) and others. Defined below is a list of the primary compositional descriptive terms we use in our report.

Vitrain

Vitrain coal is derived from large organic fragments of ancient plants, such as woody trunks and bark that fall within the vitrinite maceral group. Vitrain commonly occurs in lenticles or bands of a few millimeters or greater in thickness. It is shiny black and vitreous in texture. Vitrain is macroscopically structureless and homogeneous (Stopes, 1919) (Fig. 2-7A). A lack of homogeneity is one of the fundamental characteristics of coal (Evans and Pomeroy, 1966), and coal outcrops almost always are composed of more than one coal type. In our research, we recognize the presence of vitrain and consider a coal bed to vitrain-rich if the dominant coal type is vitrain, and cleat characteristics are reflective of the above description.

Clarain

Clarain is bright, streaky or striated coal with a silky luster. It is not as uniformly brilliant and homogeneous as vitrain and lacks conchoidal fracture (Stopes, 1919). Clarain is the most common coal lithotype in both field areas. Clarain coal contains numerous maceral types as it derived from, leaves, stems, and smaller fragments of ancient plants. It is commonly weathered to a dull black color in outcrop, as the effects oxidation tend to affect clarain more than it affects vitrain (Fig. 2-7B).

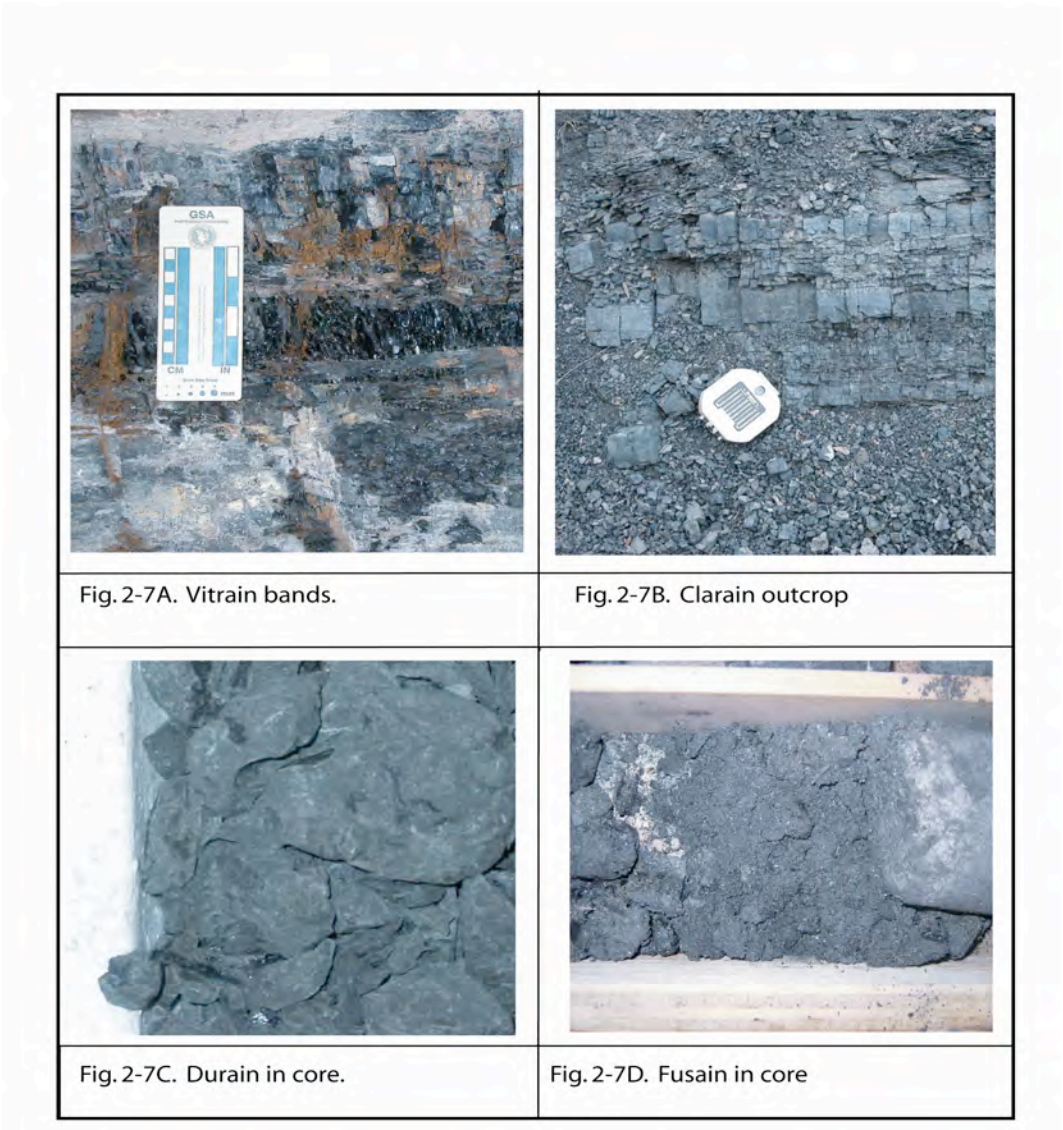

Fig. 2-7. Physical characteristics of coal. The physical appearance of coal can change dramatically as maceral composition varies. Examples of vitrain, clarain, durain and fusain are shown above.

Durain

Durain is a dull, hard compact coal. It ranges from grey to black. Durain occurs in thick and thin bands. Fractures in Durain form in irregular, non-uniform patterns (Fig. 2-7C) (Stopes, 1919). Our research focuses on cleated coal, and since durain is far less

abundant than vitrain and clarain in both field areas and contains no cleats, durain coal is rarely discussed in this report.

Fusain

Fusain is a fibrous, friable, dull charcoal-like material (Fig. 2-7D). It breaks down readily to fine dust which soils the hand, and is usually grayish-black in color (Stopes, 1919). It contains no cleats, and is only found in minor proportions in our field areas.

Carbonaceous Shale

Carbonaceous shale is a common coal composition term found in coalbed gas literature. The term carbonaceous shale is defined as a rock unit containing less than 50% carbon (University of Wyoming, 2004). Carbonaceous shale is dark grey to black in color and has a shaley texture. In both field areas, it is common to find carbonaceous shale adjacent to and interbedded among coal bands (Fig. 2-8). Although the industry has assigned a given carbon/ash ratio for labeling carbonaceous shale and assessing gas content, field identification of carbonaceous shale is widely used. Current expansion of "coalbed methane" resources commonly focuses on exploiting these shales.

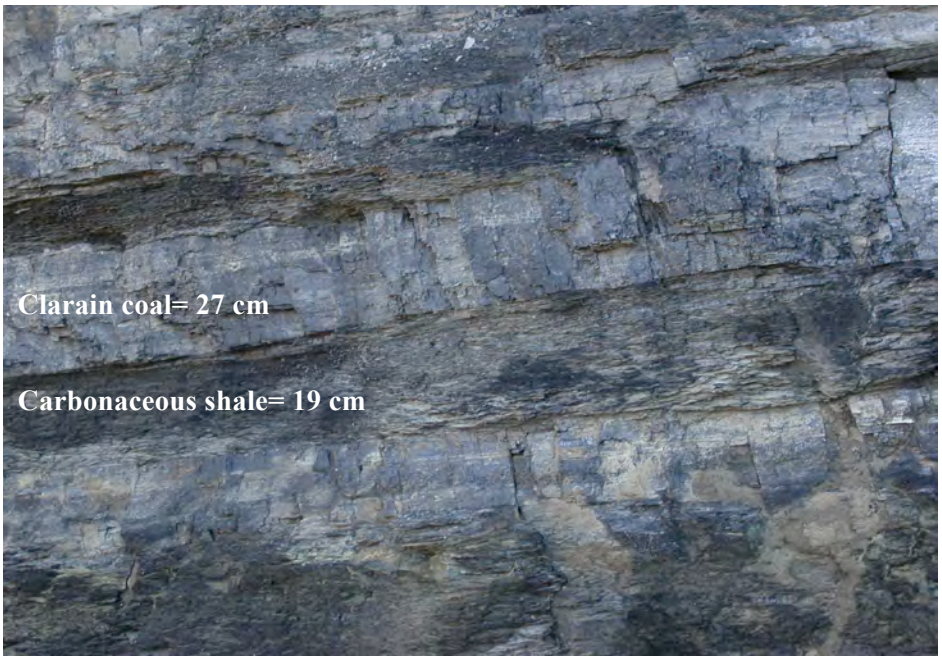

Fig. 2-8. Interbedded clarain coal and carbonaceous shale. This example is from the Fruitland Formation in Soda Springs Canyon, where clarain coal is interbedded with carbonaceous shale. Carbonacous shales are regularly found interbedd with coal throughout both field areas.

Organic-Rich Mudstones

We use the term organic-rich mudstone when referring to massive mudstone lacking shaley texture or cleats, but contains a significant visible quantity of organic debris. These mudstones, common in the Ferron field area, are typically found adjacent to coal beds, and are mentioned several times throughout this study.

Ash

The term ash is used to describe anything in coal that is not composed of carbon. Sand, silt, and mud are common ash in coal. Ash in coal often creates planes of weakness, resulting in a bed parting within the coal.

Previous Work on Coal Fracture Mechanics

Early laboratory analysis on cleats was largely performed in order to increase the safety and production in coal mines. With the recent interest in developing coalbed methane reservoirs, a revival in understanding coal fracture mechanics analysis has occurred. Due to many uncertainties and errors in early coal fracture tests, recent investigation has primarily shifted from the laboratory to the outcrop. Many testing apparatuses have been used in attempts to characterize cleat formation relative to applied stresses and orientation.

One laboratory test used to determining coal strength is the straight pull tests. Here, a sample of coal is cut into a rectangular shape, and attached between to pulling forces. With this method, fractures often begin to form from the vicinity of the grip instead from the intended site (Evans et al., 1966). This creates error in the test. If the slightest amount of bending is introduced into the sample during the test, a large amount of additional tension may be unintentionally added to the system (Evans et al., 1966).

The bending test is another test which has been used in coal cleat analysis. In this test, a thin rectangular portion of the coal sample is bent under the action of four parallel line loads until it breaks. The condition of the loading can be set up so that between the

two inner lines, the bending is constant. The maximum tension acting on the convex part of the sample can be measured and calculated (Evans et al., 1966).

Both the bending test and the straight pull test required manipulation of the initial shape of the sample, this fact has proved to be the disadvantage of these test types, causing test results to show higher tensile strength values than those obtained in conventional testing.

Often the tensile strength of a material is determined by applying a compressive load. It has been shown that even when compressive stresses are applied to a sample, the breakage appears to be essentially tensile in nature (Evans et al., 1966). The diametric compression test is one method that has been used to analyze coal fracture. In this test, a disc of coal is subjected to a directly opposite uniform load at the extremes of a diameter. Due to the nature of the setup, a uniform principal tensile stress acts at right angles to the diameter, and tensile failure is apparently induced (Evans et al., 1966). The disadvantage of this test is that the tensile stresses are associated with an orthogonal compressive stress, which increases from a minimum of three times the constant tensile stress. This combination of tensile and compressive stress results in the creation of a large shear stress in the sample. This fact creates some difficulty in determining that the fracturing observed is a failure of tension rather than shear stress (Evans et al., 1966).

Compressive strength tests often cause friable coal samples to shatter as strength is exceeded, leaving the sample too deformed to perform any useful analysis. A more solid sample may not shatter, but the fracture system may develop unpredictably and in inconsistent patterns. Biaxial and triaxial testing shows that both yield stress, and

fracture stress increase with increased confining pressure, but the amount varies from one coal to another (Evans et al., 1966).

Open mode fractures are thought to form near the surface in a truly tensional structure setting, or at depth as joints; however, the presence of cleats at depth caused some contention (Laubach et al., 1997). Numerous theories evolved over time that attempted to explain how open mode fractures could form at depths where the overburden pressure was large enough to make all stress directions essentially compressive. Pore pressure models developed by Hubbert and Rubey (1959) were used by Secor (1965) which showed that open-mode fractures could exist in a compressive setting if pore pressure was sufficiently high. Subsequent research shows that shrinkage occurs during coalification and devolatization (see Ting, 1977; Laubach et al., 1997), which reaches a maximum between vitrinite reflectance measurements between 0.3 and 0.5% (Burnham and Sweeney, 1989), and may be a more fundamental cause of cleat development. Further investigations indicate that cleat orientation is controlled by the tectonic stress field during coalification and can be use as a kinematic paleo-stress indicator (Laubach et al., 1997).

Numerous authors (e.g., Ting, 1977; Law, 1993) suggest that coal rank affects the development and/or density of cleats in coal. Cleats are absent or poorly developed in lignite, and appear to reach a maximum abundance at an approximate rank of low-volatile bituminous (Ting, 1977). Law (1993) estimates average face cleat spacing in lignites from approximately 22 to 0.2 cm in anthracites. A lack of systematic fractures in some anthracite implies that cleats anneal by repolymerization at high-rank (Levine, 1993), yet

some extremely high rank coal contains systematic fractures (Law, 1993). Coal rank differs moderately within and between our two field areas. Due to rank consistency in our study areas, we assume coal rank's influence on coal cleating to be relatively consistent, and focus our examinations on other cleat controlling factors.

The relationship between bed thickness and fracture spacing in coal-rich sequences has been examined by numerous authors. Spears and Caswell (1986), Grout (1991), Tremain et al. (1991), Close and Mavor (1991), and Law (1993) found that average cleat spacing is linearly proportional to coal lithotype-layer thickness (Laubach et al., 1997). In contrast, Daniels et al. (1996) found no relationship between cleat spacing and bed thickness. Laubach et al. (1997) suggested that comparisons of cleat spacing versus bed thickness typically cannot account for the range of cleat sizes found, and the apparent bed thickness/fracture spacing relationship may be an illusion.

Coal type and ash content have also been examined as factors which affect cleat spacing (e.g., Kendall and Briggs, 1933; Stach et al., 1982; Spears and Caswell, 1986; Tremain et al., 1991; Law, 1993). General conclusions indicate that bright coal lithotypes (vitrain), which contain smaller quantities of ash, have smaller cleat spacing than do dull lithotypes (durain) (Laubach et al., 1997).

Hucka et al. (1997) measured and determined the maceral composition and rank of six coalbeds within the Ferron Sandstone from the Emery East, Walker Flats, and Price quadrangles. Coal characterization data from Hucka et al. (1997) show that coals in the study area have a high inertinite content (16.45%) and a moderate to average vitrinite content (78.38%). The same coal samples range in rank from high-volatile bituminous A

to high-volatile bituminous C (Hucka et al., 1997). Composition commonly varies drastically within a single coalbed and we do not know the exact location on the outcrop from which coals sampled by Hucka were taken, we are unable to directly tie published composition data from Hucka et al. (1997) to coal cleat characteristics in specific Ferron coal type. Fruitland coals within the south-central San Juan Basin are composed of vitrinite (80%), liptinite (5.2%), and inertinite (14.1%) (Close et al., 1997). In the northern San Juan Basin, coal rank is high-volatile A bituminous, corresponding to vitrinite reflectance measurements of 0.78 % or higher (Kelso and Wicks, 1988; Scott et al., 1991).

Methods

Approximately 30 km south of the Drunkards Wash Field, in Emery and Sevier Counties, coalbeds of the Ferron Sandstone are exposed on natural cliff formations and in portals of old mine workings. In the summer of 2004, these Ferron coals of the Last Chance Delta, assumed to be a reservoir analog of the Ferron coals to the north, were carefully analyzed and evaluated in order to provide insight into the nature of coal cleat characteristics. Table 2-1 summarizes the locations and sites examined in this study.

During early fieldwork investigations, data was collected from 10 sites at eight different locations in the exposed Ferron Member of the Mancos Shale. At the outcrops, we recorded in situ cleat orientations, densities, measured a small stratigraphic column, collected a variety of digital photographs, and made a compilation of notes recorded in field notebooks. Appendix A is a summary sheet from the major initial sites. To insure

that no bias was introduced in the cleat orientation data set, we stretched measuring tapes along the center of the outcrop and measured the nearest cleat at each 10 cm interval using a Brunton compass. We measured a minimum of twenty orientations at each site to increase accuracy of the computed median cleat orientation. In the event that the outcrop length was short and the number of cleat orientations would not be satisfactory using the above method, we measured orientations along the measuring tape at 1/3 and 2/3 the height of the outcrop. Orientations were then entered into Allmendinger's (2002) stereonet program. Since the Ferron Sandstone bedding is nearly horizontal, typically less than 4º NW, in situ cleat orientations were plotted on the stereonets. Initially we collected average cleat densities at each site by counting the number of cleats per meter at several randomly selected points along the outcrop. A stratigraphic column for each site was created using measuring tapes, Jacob staff and level, and measuring weighted string lengths where cliff faces did not allow access for other methods. Densities and orientations of fractures in sedimentary beds adjacent to coal seams were carefully counted, measured, and evaluated to look for possible correlations with average cleat densities in the coals.

Table 2-1. Outcrop sites and locations. We examined coal fracture characteristics from 26 sites at 13 different locations in the Ferron and Fruitland Formation study areas.

Site	Location	Coal Zone	Coal Thick. (m)	Coal Type	Comments:
1	Bear Gulch	Ferron A/C	5.7	vitrain-rich	Exposure in old mine portal. Ferron A/C coals meet; good location.
2	Walker Flats Mine	Ferron M	1.6	clarain	Strip mine; clarain and carb-shale.
3	Walker Flats Mine	Ferron M	1.5	clarain	Fracture intersections; mechanical layers. Top of Ferron.
4	Miller Canyon	Ferron C	2	clarain/vitrain-rich	Mine portal closed off with cinder blocks. Tonstein layer.
5	Willow Springs Wash	Ferron A,C	0.25	clarain	Clarain and carb-shale. Fracture intersections; mechanical layers.
6	Live Earth Mine	Ferron G	2.4	ashy clarain	Coaly carb-shale. Small mechanical layers.
7	Miller Canyon	Ferron G	0.31	clarain	5 m carb-shale below coal. NE side of canyon. Fracture intersect.
8	Miller Canyon	Ferron G	0.56	clarain	SW canyon; fenced mine portals. Lots of carb shale.
9	I-70 Site	Ferron A	0.76	clarain	I-70 roadcut; lots of traffic. C coal also present.
10	Rochester Site	Ferron G	0.05	clarain	Near rock art panel. Thin coal; carb-shale. Fract. multiplication
11	Rock Canyon	Ferron A,C,G	3.2 total	All	Great place to view coal cleat characteristics. Kind of steep. Cliff
12	Rock Canyon	Ferron C	1.8	clarain	Mechanical layers; fracture intersections.
13	Rock Canyon	Ferron A	0.6	clarain	Mechanical layers; fracture intersections.
14	Rock Canyon	Ferron A	0.8	clarain	Mechanical layers; fracture intersections.
15	N. Plateau Rock C.	Ferron A	0.9	clarain	Exposure in arroyo. Mechanical layers.
16	S. Rock Canyon	Ferron C	0.7	clarain	On cliff front; S. Rock Canyon. Mechanical layers; fracture intersect.
17-21	Carbon Canyon	Fruitland	16.2	vitrain-rich	Large exposure of vitrain-rich coal. Clarain also present.
22	Durango, Co.	Menafee	8.68	vitrain-rich	Vitrain-rich coal and carb-shale. Mechanical layers. Large exposure
23-26	Soda Springs Canyon	Fruitland	4.5 exposed	clarain/carb-shale	Large exposure of clarain/carb-shale. Normal fault. Great site.

Site	Location	Lattitude	Longitude	Northing	Easting
1	Bear Gulch	N38°51.080'	W111°13.000'	4300093.76	481198.77
2	Walker Flats Mine	N38°49.278'	W111°17.337'	4296778.53	474886.90
3	Walker Flats Mine	N38°49.279'	W111°17.300'	4296780.12	474969.37
4	Miller Canyon	N38°52.510'	W111°13.031'	4302738.56	481160.22
5	Willow Springs Wash	N38°43.374'	W111°18.462'	4285864.81	473251.40
6	Live Earth Mine	N38°50.492'	W111°13.400'	4299007.68	480617.61
7	Miller Canyon	N38°52.646'	W111°13.024'	4302990.06	481170.94
8	Miller Canyon	N38°52.575'	W111°13.120'	4302859.08	481031.84
9	I-70 Site	N38°48.058'	W111°15.982'	4294516.18	476869.76
10	Rochester Site	N38°54.300'	W111°11.837'	4306045.16	482893.63
11	Rock Canyon	N38°44.020'	W111°17.252'	4287053.83	475008.25
12	Rock Canyon	N38°43.999'	W111°17.199'	4287014.75	475084.91
13	Rock Canyon	N38°44.013'	W111°17.157'	4287040.45	475145.83
14	Rock Canyon	N38°44.578'	W111°16.532'	4288082.59	476054.37
15	N. Plateau Rock C.	N38°44.616'	W111°16.523'	4288152.82	470607.62
16	S. Rock Canyon	N38°43.887'	W111°17.184'	4286807.55	475105.99
17-21	Carbon Canyon	N37°14.299'	W107°51.842'	4125716.00	778197.10
22	Durango, CO.	N37°15.385'	W107°52.452'	4127694.90	777228.50
23-26	Soda Springs Canyon	N37° 2.465'	W108° 5.717'	4103173.40	758348.10

After collecting the basic outcrop information listed above, we began to note some common factors affecting coal cleating. At this point, we returned to the study area to collect specific types of data at each outcrop. In addition to adding numerous sites at several new locations to our Ferron database, we extended our coal fracture research project to the thick coals found in the basal Fruitland Formation outcrops near Durango Colorado, and south into the San Juan Basin. We examined cleat characteristics as a function of coal composition and mechanical layer thicknesses. Cleat development within all coal lithotypes was examined. Thicknesses of mechanical layers within coal stratigraphy were measured with metric measuring tapes and recorded in field notebooks. Mechanical layer thickness often changes in a relatively short distance. Cleat densities within a given mechanical layer were counted over the entire distance that thickness remained constant, typically one meter or less. Cleat densities were counted perpendicular to face cleat orientation in order to get an accurate density count. Since coal exposures in the field areas are often found on cliff faces, measured string lengths were often nailed to the outcrop so that one person could easily perform the cleat density counts.

Our research also investigates joint continuations from adjacent sedimentary beds coal or coal zones. In order to study these regional joints as they break through varying lithologies with different internal strengths, we measured fracture attitudes, thicknesses of involved stratigraphic packages, and widths of the damaged sedimentary rocks. Numerous digital photographs of fracture intersections were taken at all appropriate sites.

Where joints multiplied as they crossed lithologies, scaled sketches were drawn in field notebooks to be referred to during data analysis.

We examined core from three shallow water-level monitoring wells in the northern vicinity of the San Juan Basin, and core from three wells in the Drunkards Wash Field. The Drunkards Wash core was laid out by staff members at the ConocoPhillips core facility in Bartlesville, Oklahoma. An operator in the northern San Juan Basin allowed us to examine 29 boxes of core acquired from depths between 92.7 and 225.6 m below ground surface from the three different wells at our research facility at Utah State University. During core analysis, we focused on the relationship between coal composition, coal thickness, adjacent sedimentary beds, and stratigraphic thickness affect on cleat density, as well as all fracture characteristics throughout the core.

Results

Composition Controls

We examined macroscopic compositional effects on coal cleating at each outcrop in our field areas and during core description. Throughout the Ferron Sandstone Member and in the Fruitland Formation, it is evident that coal composition largely controls cleat development and density. Variations in composition occur between and within nearly all coal outcrops. Cleat characteristics within a given lithotype tend to remain constant. Figure 2-9 illustrates how variations in coal compositions yield unique cleat characteristics. The four main coal lithotypes, as defined by Stopes (1919), all have unique cleating traits that can be identified through a thorough evaluation.

Vitrain Coal

Vitrain coal is composed of macerals within the vitrinite group. Vitrain commonly occurs in lenticles or bands of a few millimeters or greater in thickness. Pure vitrain coal only accounts for a small percentage of the total volume of coal in our field areas. Vitrain coals contain a very high density of face cleats that form perpendicular, or nearly perpendicular to bedding, and parallel to face cleat sets in adjacent coal lithotypes (Fig. 2-10). As is apparent in Figure 2-10, vitrain contains a high density of non-oriented conchoidal fractures, which creates the greatest connectivity between face cleats. Typical cleat spacing in vitrain from our field areas is less than 1.5 cm (Fig. 2-10). Due to the nature of coal bedding and outcrop orientations, top or bottom views at cleat connectivity and length is limited, and no quantitative analysis was performed; however, the high density of face cleats and conchoidal fractures likely results in cleat connectivity that is favorable for high coal permeability.

More commonly, vitrain occurs as smaller particles in a mix with other non-vitrinite macerals and not in pure lenticles or bands. If the composition is dominated by vitrain, and cleat characteristics are reflective of this, then the coal is classified as "vitrain-rich" coal. Vitrain-rich coal is very common in parts of the Upper Ferron and in the Fruitland Formation. Vitrain-rich coal, similar to pure vitrain, has a well developed face cleat set approximately perpendicular to bedding (Fig. 2-11), which is the fundamental source of fracture permeability. Face cleat spacing is slightly greater than spacing in pure vitrain; however, in comparison with other coal types, spacing is still very small. The median face cleat spacing in vitrain-rich coal from field and core

research is 1.85 cm (Table 2-2). We have found that face cleat density in this coal type is not controlled by layer thickness. Rather, macroscopic observations of vitrain-rich coal indicates that as vitrain content and homogeneity increases so does face cleat

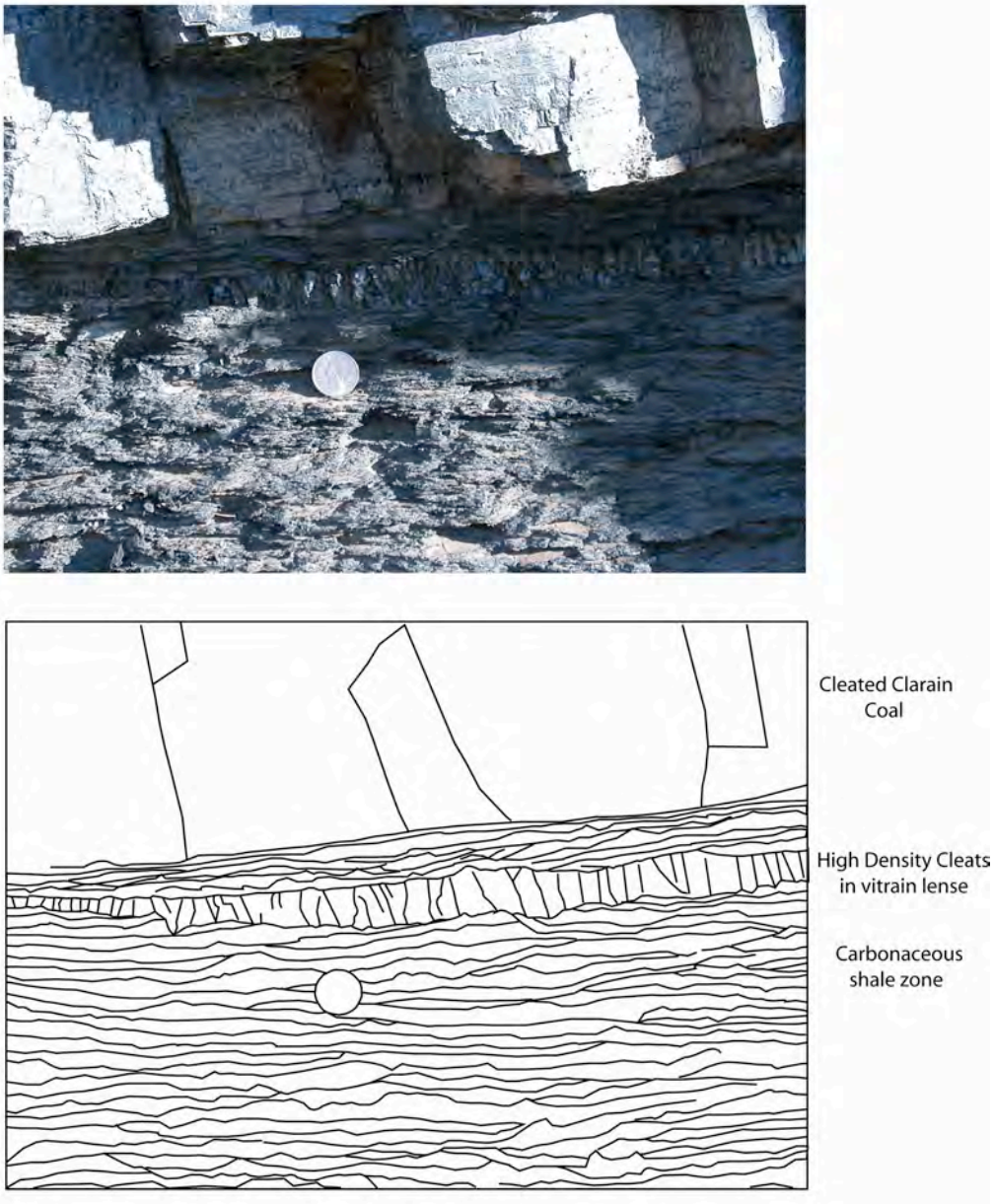

Fig. 2-9. Cleats as a function of coal composition. In this photograph of Fruitland coal, clarain, vitrain and carbonaceous shale are present. Note the cleat terminations upon intersection with the carbonaceous shale, as seen in the fracture overlay of the photograph.

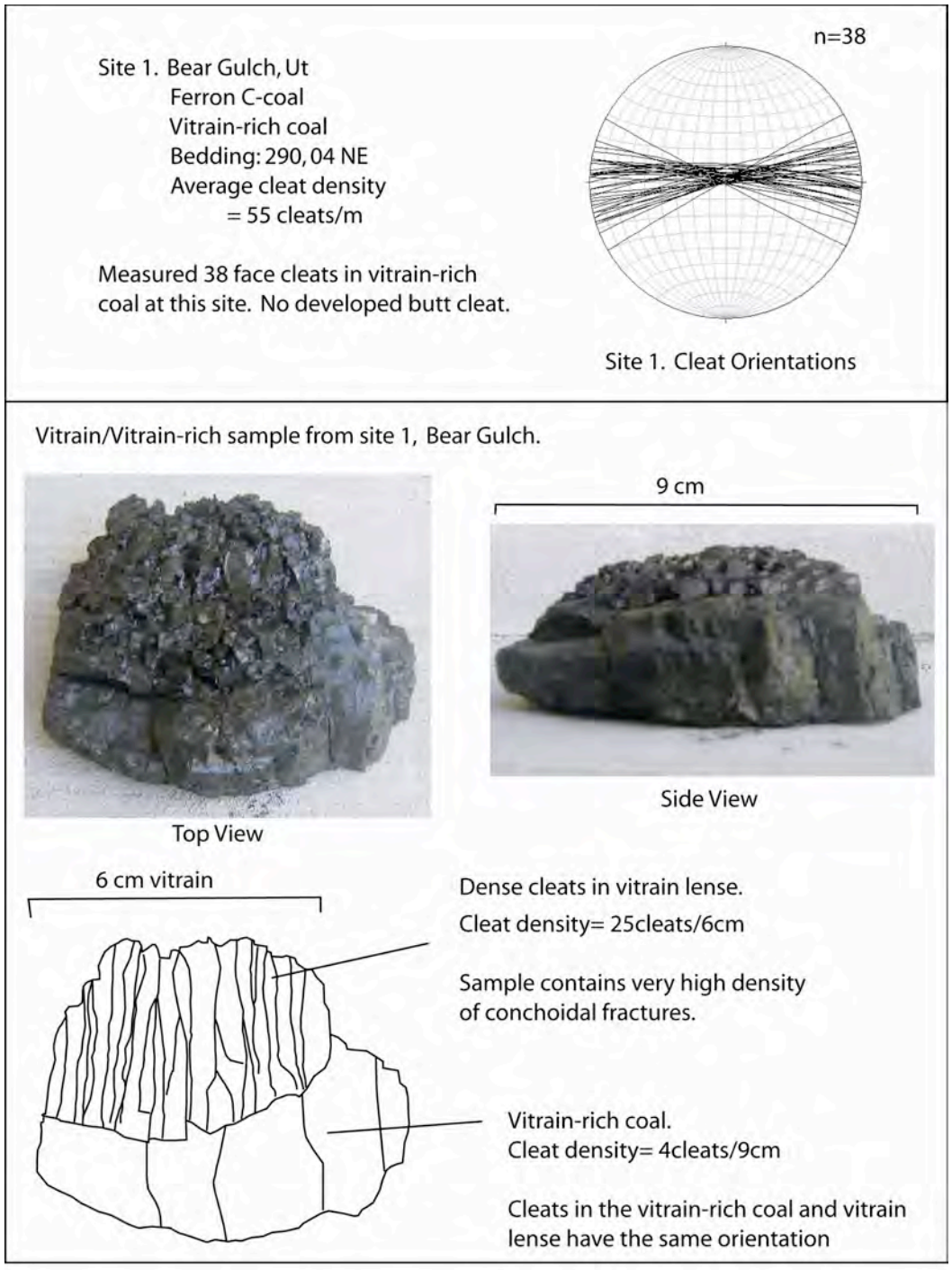

Fig. 2-10. Vitrain and vitrain-rich coal cleat characteristics. Vitrain coals contain a very high density of face cleats that form at, or near perpendicular to bedding, and parallel to face cleat sets in adjacent coal lithotypes. Typical cleat spacing in vitrain from our field areas is less than 1 cm.

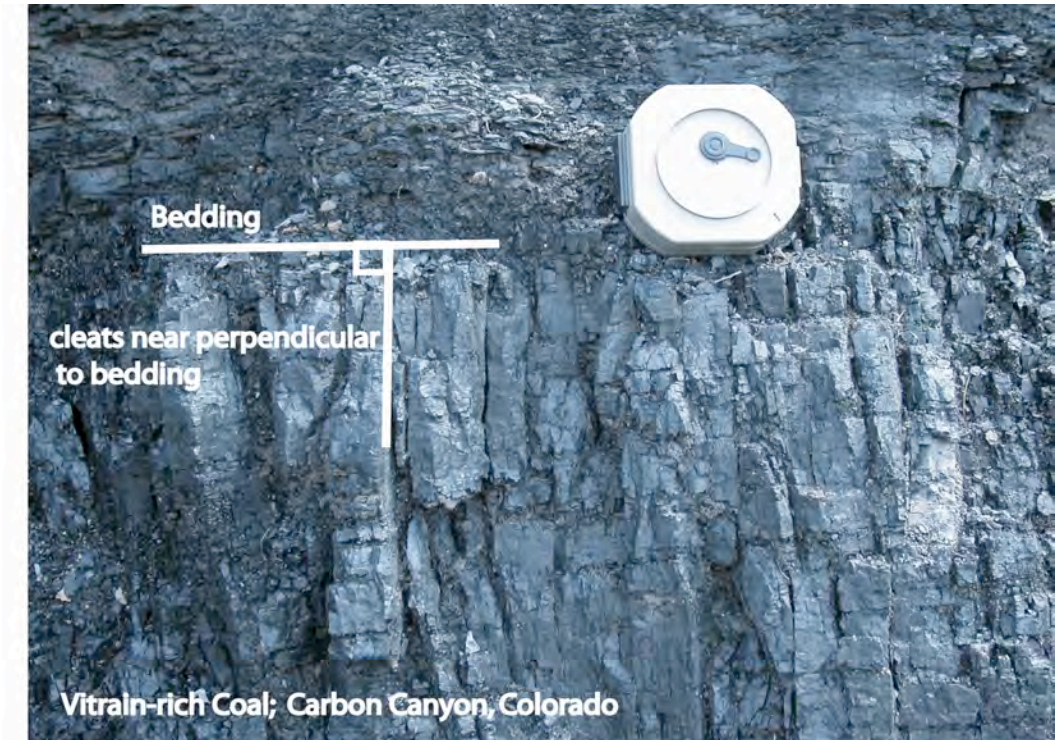

Fig. 2-11. Cleats in vitrain-rich coal. Face cleats in vitrain-rich coals form near perpendicular to bedding. No butt cleat set is formed. Conchoidal fracture is apparent on small vitrain grains.

Table 2-2. Vitrain-rich cleat spacing. Cleat spacing ranges between 1.11 and 3.33 cm. The median cleat spacing is 1.85 cm. Face cleats create the majority of fracture permeability in vitrain-rich coal.

Cleat Spacing in Vitrain-Rich Coal:

# Cleats	Measured Length (cm)	Cleat Spacing (cm)
64	100	1.56
46	100	2.17
12	20	1.67
30	50	1.67
21	50	2.38
5	9	1.80
20	33	1.65
16	33	2.06
18	33	1.83
43	100	2.33
9	10	1.11
8	15	1.88
15	50	3.33
6	8	1.33

Median Cleat Spacing = 1.85 cm.

density. This increased homogeneity also increases average cleat height, as fewer cleats are arrested at intersections of materials with different mechanical properties. In vitrain-rich coals, conchoidal fractures are apparent on individual vitrain grains, but provide a less effective means of face cleat connectivity than they do in pure vitrain coal.

Clarain Coal

Clarain coal is composed of numerous maceral types derived from leaves, stems, and smaller fragments of ancient plants (Stopes, 1919). It is commonly weathered to a dull black color in outcrop, as the effects of oxidation tend to affect clarain more than it affects vitrain (Stopes, 1919). Despite the differences in compositional makeup and appearance of clarain coal, we made no attempt to further divide and classify this attrital coal type during our research. Clarain coal is present and abundant in coal seams throughout the Ferron study area, and is the dominant coal type present in the Fruitland Formation at Soda Springs Canyon.

Clarain coal contains well-developed face and butt cleats found nearly perpendicular to bedding and mutually perpendicular to each other (Fig. 2-12B). Cleat surfaces are typically smooth, straight and roughly parallel to adjacent cleats (Fig. 2-12A and B). Due to the parallelism of the through-going face cleat set, face cleats are long compared to butt cleats (Fig. 2-13A). In some clarain coals, butt cleats can be nearly as prevalent as face cleats (Fig 2-13B). Butt cleats regularly terminate against face cleat surfaces, though it is not uncommon for a significant quantity of butt cleats to propagate through two or more face cleats (Fig. 2-13A). While no systematic cleat length data has been collected (Laubach et al., 1997), we suggest that cleats should be longer where

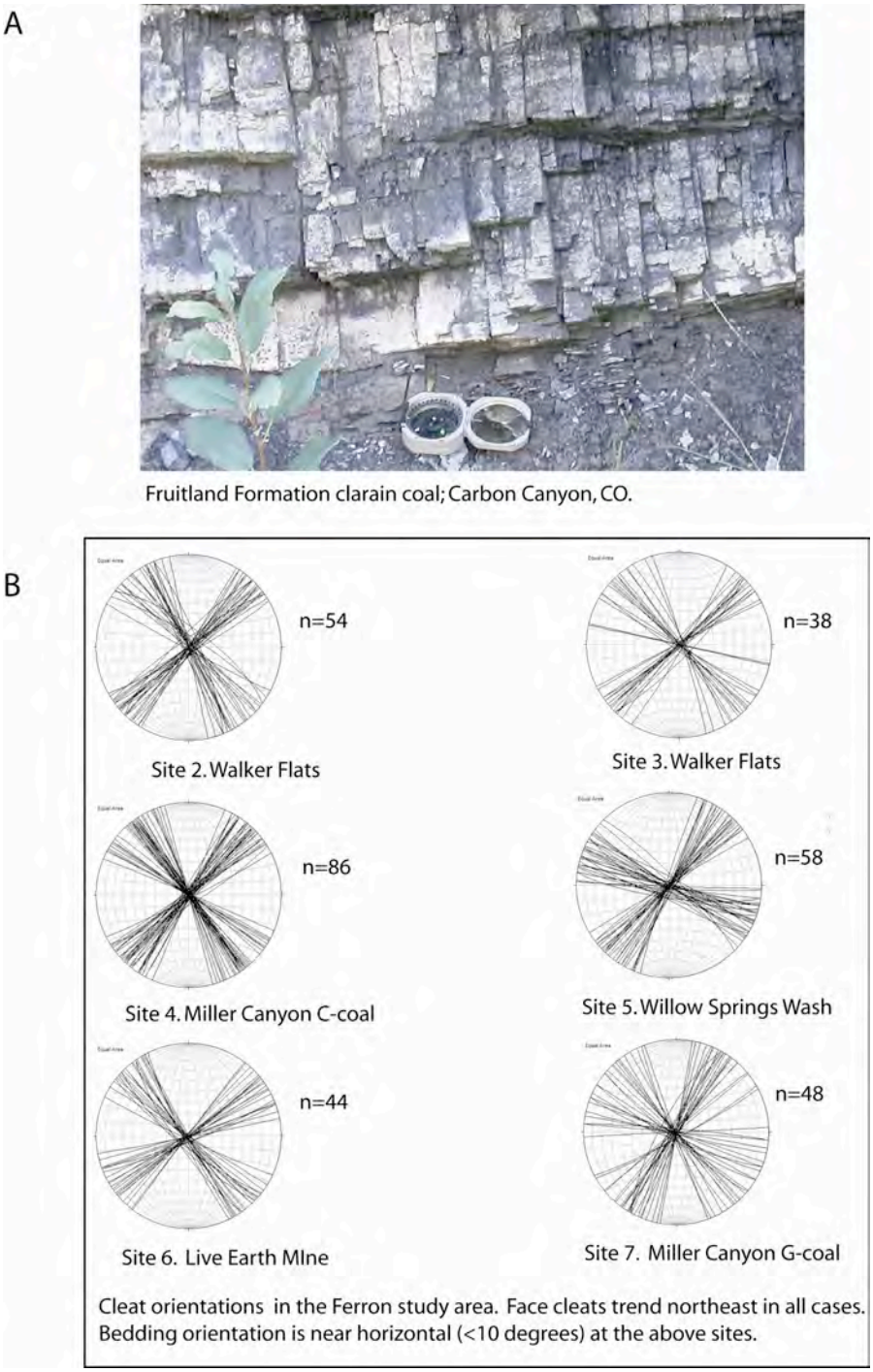

Fig. 2-12. Cleats in clarain coal. The photograph of clarain coal (A) is representative of clarain found in both the Ferron and Fruitland Formations. Face and butt cleats in clarain form at or near perpendicular to bedding, and mutually perpendicular to each other (A and B). The parallelism among cleats of the same set can be easily seen by the lack a variation in fractures when plotted on stereonets (B).

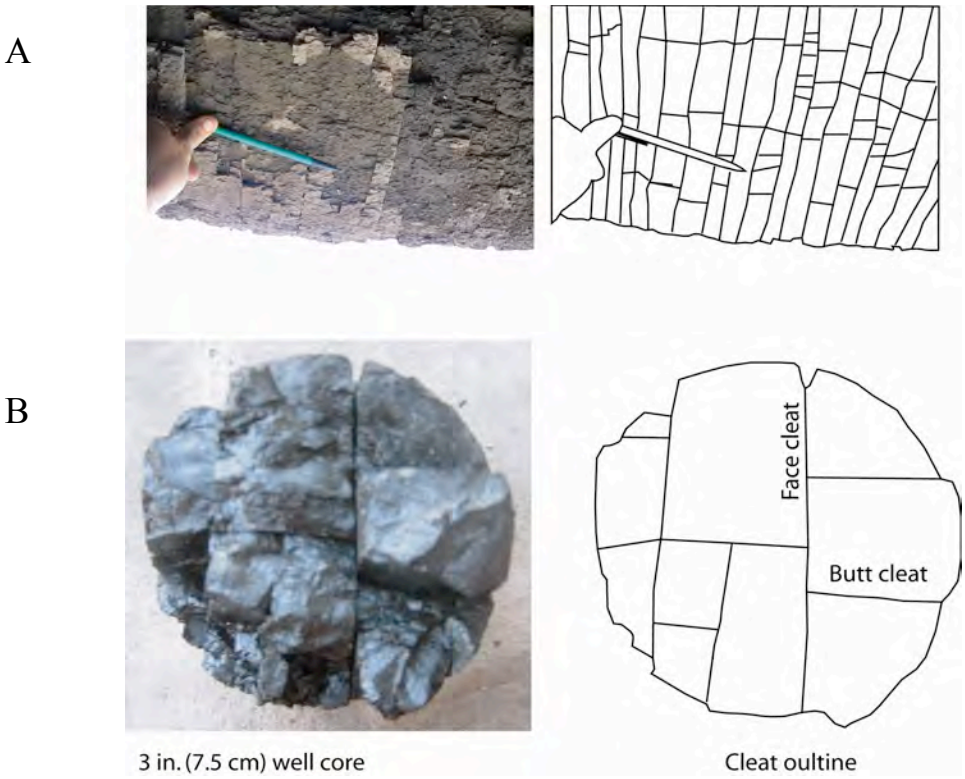

Fig. 2-13. Cleat length (A) and cleats in core (B). Looking up at the underside of a clarain bed it is clear that face cleats are long, and parallel to adjacent cleats (A). Cleat surfaces are typically smooth and straight. Butt cleats terminate against face cleats; however, it is not uncommon for a butt cleat to penetrate two or more face cleats (A). In this clarain coal interval of well core, butt cleats are nearly as prevalent face cleats. This near equal abundancy is present in several Ferron outcrops, making cleat set identification sometimes difficult.

spacing is greater. In coal where cleats are closely spaced, slight variations in cleat orientations increase the likelihood of face cleat intersection and/or termination. In bedding parallel views of clarain coals in our study areas, face cleat lengths commonly exceed outcrop length (Fig. 2-13A). Where face cleat spacing is small (< 2cm), we

noted that a significant quantity of cleats appear to bend or curve and terminate against adjacent face cleats.

From 64 fracture density counts at different locations from both field areas, we found face cleat densities ranging from 8 to 210 cleats/m in clarain coals (Tables 2-2 and 2-3). Where two-directional outcrop faces allowed density counts of both face and butt cleats, we noted that butt cleat density regularly increases as face cleat density increases. This can be seen in Figure 2-13B as face and butt cleats are present in nearly equal proportions. This relationship is also apparent in coal talus, as clarain coal is commonly found in cubic shapes within the debris. Layer thickness is the primary control on cleat density in clarain, and is discussed later in this paper.

Durain and Fusain Coal

Durain and fusain coals represent a small portion of the total coal in our field area. Both coal types lack any type of well developed cleat system (see Fig. 2-7). Their absence would increase the bulk permeability of the coal seam. Durain coals contain irregular fracture patterns. Fractures in durains do not display a strong, preferentially oriented trend. Although these fractures are oriented roughly perpendicular to bedding, the chaotic fracture trends prevent the systematic spacing and parallelism that is developed in a true cleat system. In core, durain coal is often broken down into small irregularly shaped chunks (Fig. 2-7C). Cleat systems in other coal lithotypes terminate upon intersection with durain.

Fusain is a friable coal lithotype that readily breaks down into charcoal-like powder. Fusain contains no systematic cleat system. Fusain layers are often very thin

(<1mm) in our field areas, and are commonly interbedded with other coal lithotypes. Fusain may occur in thicker bands, as an 8 cm layer is present in one San Juan Basin core. Fusain layers may create strength variations in coal, and can be found as bounding units to mechanical layers in both field areas. Unlike durain, whose physical characteristics would prohibit fluid or gas migration, the lack of coherence in fusain, may slow migration, but would not likely arrest it.

Carbonaceous Shale

Carbonaceous shales are very common in both field areas. In Soda Springs Canyon, Colorado, clarain coals of the Fruitland Formation are interbedded with carbonaceous-shales in nearly equal proportions (Fig. 2-8). Carb-shales are found in the Ferron Sandstone, interbedded among various coal lithotypes and adjacent to coal beds. In some Ferron outcrops, coal zones may be composed solely of carbonaceous shale due to locally high ash contents (e.g., Ferron G-coal). The distribution of carbonaceous shale among cleated coal lithotypes commonly defines mechanical and lithotype layer thickness, as coal cleats rarely penetrate the ductile shale. Carb-shales are formed as a result of high ash content which creates bed partings in coal. When bed parting density is sufficiently high (>1bp/cm), a shaley texture dominates the appearance of the coaly material. Carb-shales rarely contain face and butt cleats; however, we found cleated carb-shales at Site 3, Walker Flats Mine. The shaley partings in carbonaceous shale are commonly undulating and short, as the ash beds separate small, frequently lenticular-shaped coal material. Connectedness appears to very high, due to the high density of intersecting partings. Joints in sandstones and cleats in adjacent coal lithotypes regularly

terminate upon intersection with carbonaceous-shale layers (see *Joint Intersection* subsection of Results section). Tremain et al. (1991) found that cleats rarely cross interbedded shales, even when they are less than 1.25 cm thick. The inherent nature of carbonaceous shale creates strong permeability anisotropy, as potential fluid and gas migration is confined primarily to migration parallel to bedding within the shale partings. Furthermore, when interbedded with cleated clarain or vitrain coal, carb-shales create a confining layer that restricts vertical fluid or gas migration heights to the thickness of cleated coals between the shale.

Mechanical Layering and Effects on Cleat Spacing

We examined cleat density as a function of mechanical layer thickness. Similar to the definitions used by Underwood et al. (2003), we define a mechanical layer in coal as one or more stratigraphic units that exhibit fracture spacing independently of others. Fractures, or cleats, span the entire length of the mechanical layer, and terminate at bounding units, called "mechanical interfaces" by Gross et al. (1995). In our research, if 75% or more of the cleats terminate at confining bounding units, then we classify the bounded unit as a mechanical layer. Bounding units are commonly composed of thin ash (clay, silt, sand) layers, carb-shale layer, adjacent sedimentary beds, or adjacent coals of different compositions. Prior research that explains cleat spacing variations as a function of lithotype layer thickness (Spears and Caswell, 1986; Grout, 1991; Tremain et al., 1991; Close and Mavor, 1991; Law, 1993) to a large extent, agree with our results. For example, a band of clarain coal, lying between two beds of carb-shale that halt cleat propagation, is a mechanical and lithotype layer, and cleat spacing will vary as the clarain

thickness varies. The variations in cleat spacing observed by Laubach et al. (1997) can be addressed by observing the smaller order mechanical layer effects within the coal. We found that small mechanical differences in coal, even less than 1mm thick, can create bounding units that arrest cleat propagation, define mechanical layer thickness, and create cleat spacing variation within the clarain coal (Fig. 2-14). In clarain coal, thin bed partings often create mechanical interfaces that affect cleat density. Commonly, several mechanical layers may be juxtaposed within a single lithotype layer (Fig. 2-15). This juxtaposition of differing mechanical layer thicknesses creates a hierarchical effect among cleat systems. We were unable to establish any correlation of mechanical layer thickness with cleat spacing in vitrain or vitrain-rich coal.

We counted cleat densities in 64 mechanical layers of various thicknesses from clarain coals at 15 sites in the Ferron Sandstone Member and the Fruitland Formation (Tables 2-3 and 2-4). Face cleat densities range from 8 to 210 cleats/m and are exponentially related to thickness variations in mechanical layers ranging from 46 to 0.4 cm, respectively (Fig. 2-16). Very high correlation values of 0.8833 and 0.8117 verify this relationship between fracture spacing and mechanical layer thickness for the Ferron and Fruitland coals. Figure 2-16 illustrates that the density of cleats in both field areas correlates with mechanical layer thickness variations. Since these density counts were performed on attrital clarain coals of slightly different compositions and physical appearances from field areas with different stress histories, we suggest that the mechanical layering within coal stratigraphy is the primary control on cleat density in clarain coals.

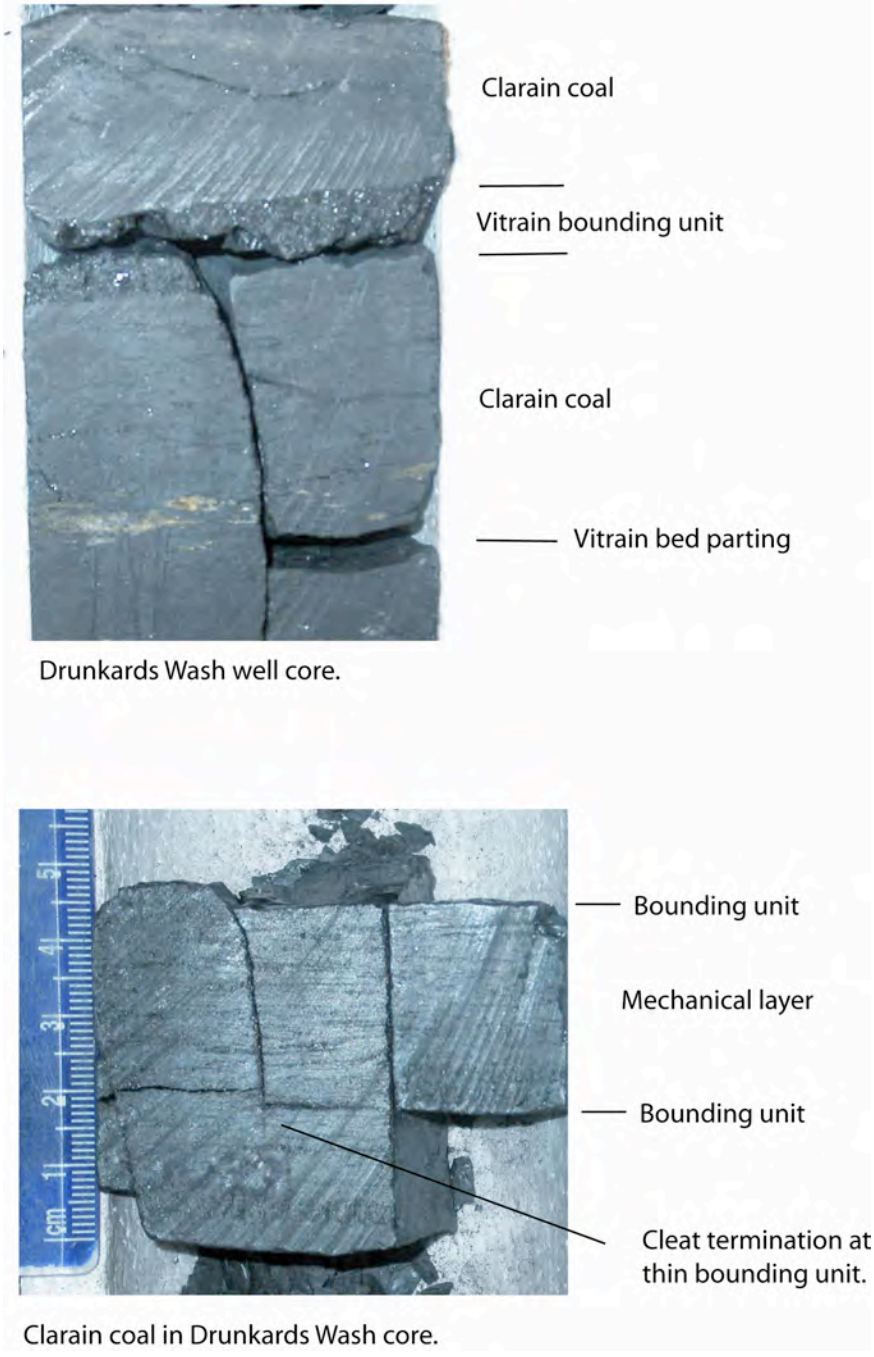

Fig. 2-14. Bounding units in coal. Bounding units can be created by large scale lithotype variations in outcrop or very small mechanical differences, such as bed parting, or thin coal lenses of different composition, as seen in these core photos. Bounding units define mechanical layer thickness and control cleat density in clarain coal.

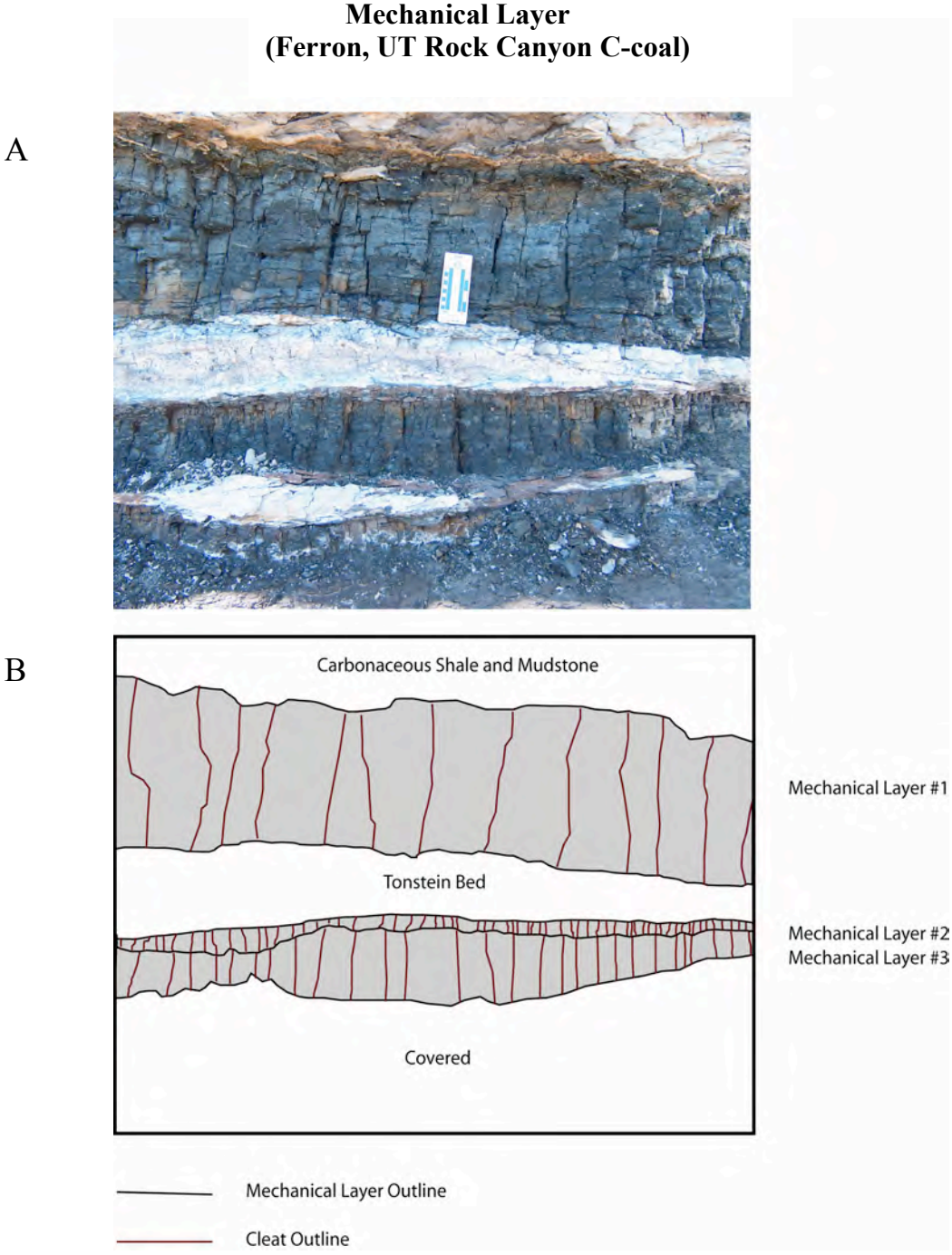

Fig. 2-15. Illustration of mechanical layers in coal. Mechanical layers control cleat density in clarain coal. From the fracture overlay (B) of the photograph (A) several mechanical layers are present within a relatively constant coal lithotype. The number and juxtaposition of mechanical layers commonly create cleat density variations in a coal bed. Note that cleats do not continue into non-coal beds.

Table 2-3. Ferron mechanical layers. Mechanical layer thickness varies laterally. We counted cleat densities in mechanical layer for a long as the thickness stayed constant (up to one meter).

Ferron Coals n=33				
Mechanical Layer	**Measured Density**	**Measured Length**	**Density**	**Location**
Thickness (cm)	Number Fracs.	(m)	#Fracs/m	
36	9	1	9	Site 15
15	20	1	20	Site 15
21	14	1	14	Site 15
8	38	1	38	Site 15
6	34	1	34	Site 15
9	27	1	27	Site 15
6	26	1	26	Willow Springs Wash
8	24	1	24	Willow Springs Wash
20	16	1	16	Willow Springs Wash
17	15	1	15	Walker Flat Mine
11	26	1	26	Walker Flat Mine
13	14	1	14	Rock Canyon
5	24	0.73	33	Rock Canyon
12.5	11	0.72	15	Rock Canyon
4	24	0.61	39	Rochester
2	31	0.45	69	Miller Canyon Site 4
4	11	0.29	38	Miller Canyon Site 4
2.5	16	0.35	46	Miller Canyon Site 4
1	13	0.16	81	Miller Canyon Site 4
11	8	0.34	24	Miller Canyon Site 4
8	15	0.56	27	Miller Canyon G-Mine
20	6	0.28	21	Miller Canyon G-Mine
5	10	0.36	28	Miller Canyon G-Mine
6	19	0.4	48	Miller Canyon G-Mine
25	9	0.5	18	Miller Canyon G-Mine
17	13	1	13	Miller Canyon G-Mine
24	8	1	8	Bear Gulch
1.5	39	0.33	118	Site 6 G-Coal Zone
0.4	21	0.1	210	Site 6 G-Coal Zone
13	6	0.5	12	Site 6 G-Coal Zone
11.5	15	0.5	30	Site 6 G-Coal Zone
12	23	1	23	Site 12
25	11	1	11	Site 14

Table 2-4. Mechanical layers in Fruitland Formation coal.

Fruitland n=31				
Mechanical Layer	**Measured Density**	**Measured Length**	**Density**	**Location**
Thickness (cm)	Number Fracs.	(m)	#Fracs/m	
45	9	1	9	Carbon Canyon 2
10	14	0.5	28	Carbon Canyon 2
5	13	0.33	39	Carbon Canyon 2
13	17	1	17	Carbon Canyon 2
20	8	0.5	16	Carbon Canyon 2
4.5	17	0.33	52	Carbon Canyon 2
7	11	0.5	22	Carbon Canyon 2
13	5	0.25	20	Carbon Canyon 2
46	7	0.5	14	Carbon Canyon 2
9	9	0.5	18	Carbon Canyon 2
4.5	8	0.5	16	Carbon Canyon 3
5	14	0.33	42	Carbon Canyon 3
5.5	9	0.33	27	Carbon Canyon 3
6.5	10	0.33	30	Carbon Canyon 4
3.5	21	0.33	64	Carbon Canyon 4
12	10	0.5	20	Carbon Canyon 4
6	14	0.5	28	Carbon Canyon 4
8.5	6	0.33	18	Carbon Canyon 4
14	10	0.5	20	Carbon Canyon 4
4	10	0.25	40	Carbon Canyon 4
3	7	0.2	35	Carbon Canyon 4
4	13	0.33	39	Carbon Canyon 4
14	7	0.5	14	Carbon Canyon 4
0.4	20	0.1	200	Carbon Canyon 4
13	10	0.5	20	Carbon Canyon 4
3	11	0.33	33	Carbon Canyon 4
46	5	0.5	10	Carbon Canyon 4
9	12	0.5	24	Menafee Coal
5	8	0.33	24	Menafee Coal
17	6	0.5	12	Menafee Coal
5.5	11	0.33	33	Menafee Coal

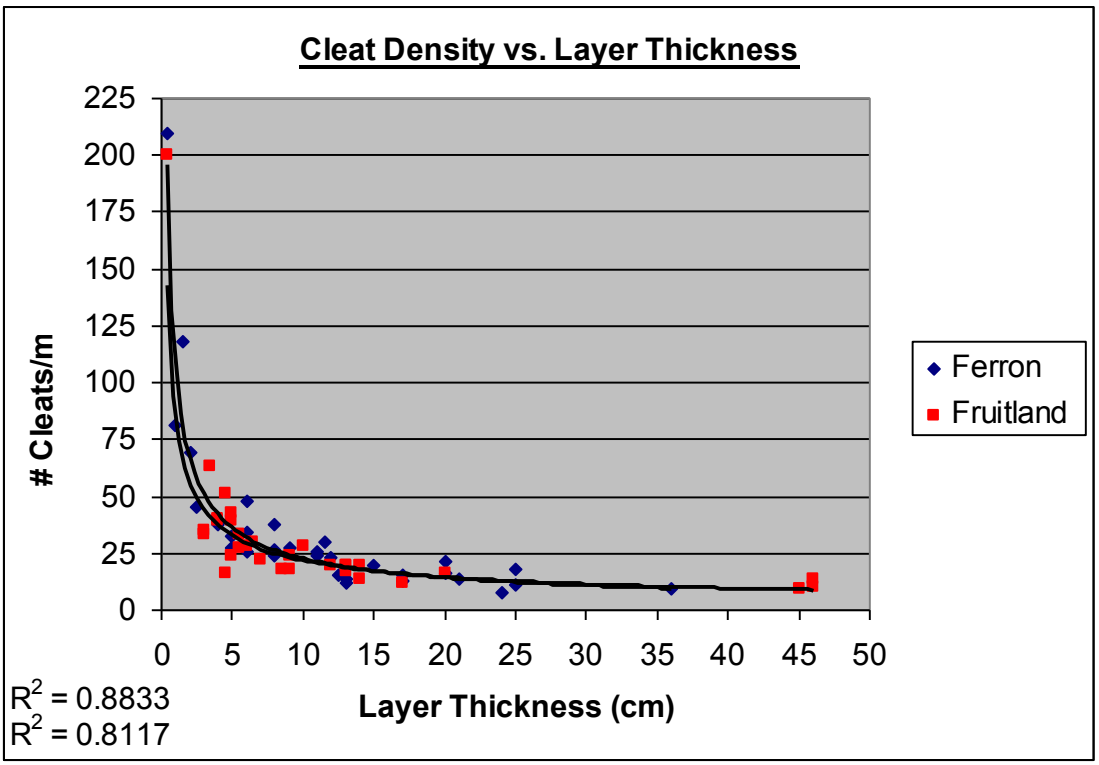

Fig. 2-16. Combined correlation graphs of mechanical layer thickness versus cleat density. The mechanical layer influence on cleat density extends beyond a single region. Clarain cleats in both field areas are present in nearly the same frequency as a result in mechanical layer thickness variations. Although there are undoubtedly minor compositional, rank, and stress history variations among sites, cleat density remains dependant on mechanical layer thickness. We suggest that mechanical layer thickness in clarain coal is the primary control on cleat density.

Sedimentary Joints in Coal Stratigraphy

Coals in the Ferron Sandstone and Fruitland Formation are commonly separated by and/or interbedded with carbonaceous shales, sandstones, siltstones, and mudstones. Differences in material strength between the rock types create interesting fracture characteristics at stratigraphic intersections. Numerous authors (e.g., Cook and Erdogan, 1972; Erdogan and Biricikoglu, 1973; Helgeson and Aydin, 1991; Rijken and Cooke, 2001) have suggested that rock fractures initiate in brittle layers and terminate in ductile

layers. Rock strength in coal stratigraphy varies from semi-ductile in carb-shales and mudstones, to brittle in sandstone and siltstones, to very brittle in coal. During our research, we found coal cleat systems never propagated into adjacent sandstones, siltstones or mudstone beds, and rarely cross even thin carbonaceous shale layers (Fig. 2-15). Stratigraphic joint intersections from sandstones into coal or carb-shale are not so easily defined. To investigate this issue, we examined cleat and joint characteristics in outcrops and in core where joints from adjacent sedimentary beds (primarily sandstones) intersect coal or coal zone stratigraphy. From this analysis, we found four primary reoccurring patterns at these intersections that we term 1) joint breakthrough, 2) joint weakening, 3) joint termination, and 4) joint multiplication.

We use the term "joint breakthrough" when a joint in a sandstone continues through one or more stratigraphic layers, including a coal bed (Fig. 2-17). Favorable conditions for this type of fracture intersection are commonly apparent at the Rock Canyon Site, in the Ferron Sandstone Member. From 22 joint intersections measured at Rock Canyon and various other sites in the Ferron study area, 9 of which fall under our classification of "joint breakthrough," we have established a minimum sandstone/coal thickness ratio of 4:1 for which it is common to have joint breakthrough (Table 2-5; Fig. 2-18). If the ratio is less than 4:1, joint termination or joint weakening become the dominant but not exclusive tendency. Breakthrough joints maintain a relatively constant orientation in all affected units. Cleat density in adjacent coals is unaffected by joint breakthrough, although cleat aperture may enlarge along the trend of the joint. Joint

breakthrough may instigate fluid or gas migration within the sedimentary beds involved, and may be beneficial or detrimental reservoir production depending on circumstances.

Fig. 2-17. Outcrop illustration of fracture intersection patterns. This photograph from the Rock Canyon, Utah site illustrates differences in fracture intersections with coal stratigraphy as a result of bed thickness relationships. Note sandstone joints breakthrough the coal bed where the overlying sandstone is thick compared to coal thickness. Where joints are present in the thin sandstones, joint continuation does not breakthrough the coal.

Table 2-5. Joint intersection types. These measurements are primarily from the Rock Canyon, Utah site where outcrop exposure is best suited for the study. Two anomalously high fracture ratios are highlighted in yellow. Note both are sandstone to carbonaceous shale fracture intersections. Further analysis may establish a better fracture breakthrough ratio in the ductile carbonaceous shale units.

Joint From Thickness (m)		Joint Into Thickness (m)		Stratigraphic Ratio	Joint Type
Sandstone	1.22	Coal	1.30	0.9:1	Joint Weakening
Sandstone	.45	Coal	1.07	0.4:1	Joint Weakening
Sandstone	1.19	Carb-shale	0.76	1.6:1	Joint Termination
Sandstone	1.30	Coal	1.07	1.2:1	Joint Weakening
Sandstone	2.44	Carb-shale	0.30	8.1:1	Joint Multiplication
Sandstone	3.05	Coal	0.24	12.7:1	Joint Breakthrough
Sandstone	0.24	Coal	0.61	0.4:1	Joint Termination
Sandstone	0.45	Carb-shale	0.24	1.9:1	Joint Multiplication
Sandstone	3.10	Carb-shale	1.07	2.9:1	Joint Multiplication
Sandstone	7.00	Carb-shale	0.76	9.2:1	Joint Breakthrough
Sandstone	7.00	Carb-shale	0.76	9.2:1	Joint Multiplication
Sandstone	4.10	Coal	0.98	4.2:1	Joint Breakthrough
Sandstone	5.89	Coal	1.13	5.2:1	Joint Breakthrough
Sandstone	1.20	Carb-shale	2.10	0.6:1	Joint Termination
Sandstone	5.33	Coal	0.39	13.7:1	Joint Breakthrough
Sandstone	6.50	Carb-shale	2.50	2.6:1	Joint Termination
Sandstone	3.00	Coal	0.80	3.8:1	Joint Breakthrough
Sandstone	1.00	Carb-shale	0.78	1.3:1	Joint Termination
Sandstone	2.99	Carb-shale	0.30	10.0:1	Joint Breakthrough
Sandstone	3.50	Carb-shale	1.62	2.2:1	Joint Weakening
Sandstone	5.97	Coal	1.10	5.4:1	Joint Breakthrough
Sandstone	3.70	Coal	1.00	3.7:1	Joint Breakthrough

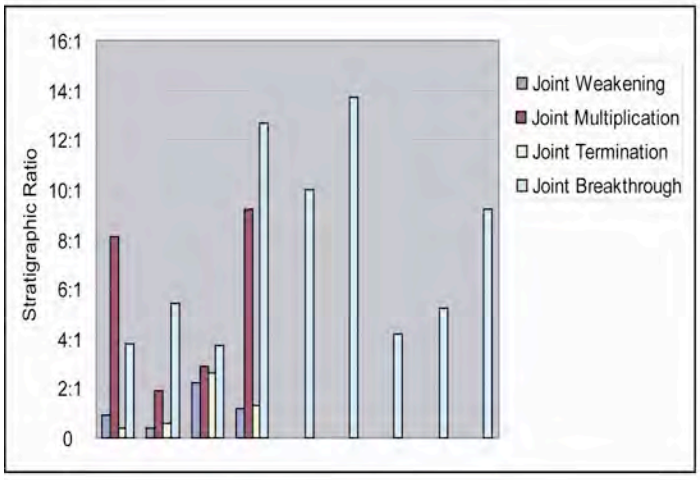

Fig. 2-18. Joint intersection graph. This graph illustrates data as shown on Table 2-4. Joints intersecting coal breakthrough the coal when the thickness ratio of the adjacent sandstone is greater than 4:1. Where fractures intersect carb-shale, the minimum fracture ratio established for joint breakthrough is exceeded in several cases.

If the sandstone to coal thickness ratio is < 4:1, then "joint weakening" may become the dominant pattern (Table 2-5). Joint weakening occurs when a joint in an adjacent sandstone intersects a coal bed but does not penetrate it (Fig. 2-19). Rather, the joint can be traced through a partial distance of the coal before becoming lost in the coal/shale. In the Ferron study area, carbonaceous shales and mudstones often lie between a coal layer and the nearest sandstone. Joints commonly weaken and often disappear within these ductile beds. For this reason "joint weakening" is the most common intersection style within the Upper Ferron. When a fracture breaks through the ductile beds surrounding the coal, it regularly weakens and fades out somewhere in the coal matrix.

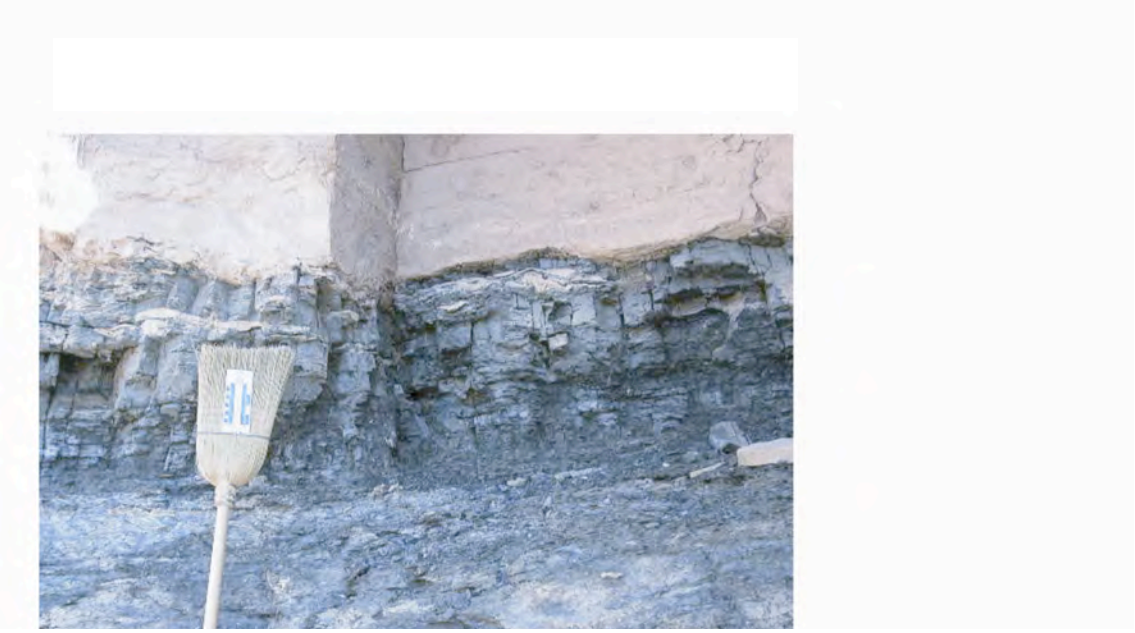

Fig. 2-19. Joint weakening. Joint weakening intersection patterns are commonly found in coal stratigraphy. A sandstone joint is present in the overlying lying, and weakens as it enters the coal. The fracture does not breakthrough into the underlying carbonaceous shale.

"Joint termination" is another primary joint intersection style. We apply this label to sandstone joints that do not continue into coal or coal zones. Joints in sandstone that are incorporated into a coalbed as a thin layer or lens commonly terminate upon intersection with adjacent coal**.** Joints may terminate upon intersection with cleated coal. Table 2-4 provides data showing that a sandstone joint 0.24 m tall, terminates upon intersection with coal. Sandstone joints regularly terminate at intersections with carb-shales or organic-rich mudstones (Fig 2-20 A and B). Carbonaceous shales and organic-rich mudstones are often found stratigraphically incorporated into a coal zone; hence the frequency of "joint termination" is often controlled the quantity of these ductile materials in the stratigraphy.

When a single sandstone joint appears to multiply upon intersection with another stratigraphic unit we classify the pattern as "joint multiplication." While joint multiplication can take place in cleated coals, they are hard to see in photos and illustrations. Figures 2-21, 2-22, and 2-23 show joint multiplication intersections in carb-shale and organic-rich mudstones. It is common for the joint multiplication to occur within the sandstone just prior to intersection with the organic-rich mudstones, carbonaceous shales or coal (Fig. 2-22). Joints maintain similar orientations in the sandstone and in organics where the multiple joints are typically found (Fig. 2-22). Where apparent multiplication has taken place, a fracture-damaged zone is created. From a "joint multiplication" examined in Willow Springs Wash, Utah, we measured our largest fracture-damaged zone of 1.7 m, perpendicular to joint orientation, within coal and carb-shale of the Ferron A-coal zone (Fig. 2-23). During our investigations, we

A

Sandstone joint termination at carbonaceous shale layer in the Ferron M-coal zone at Site 2., Walker Flats Mine.

B

Cleats terminate at carbonaceous shale layers. Soda Springs Canyon Site, Colorado.

Fig 2-20. Joint termination. Joints commonly terminate at ductile carbonaceous shale layers. The majority of cleats in adjacent coal also terminate at carb-shale layers. Photo A is from Walker Flats Mine site, Utah. Photo B is from Soda Springs Canyon site, Colorado.

A

B

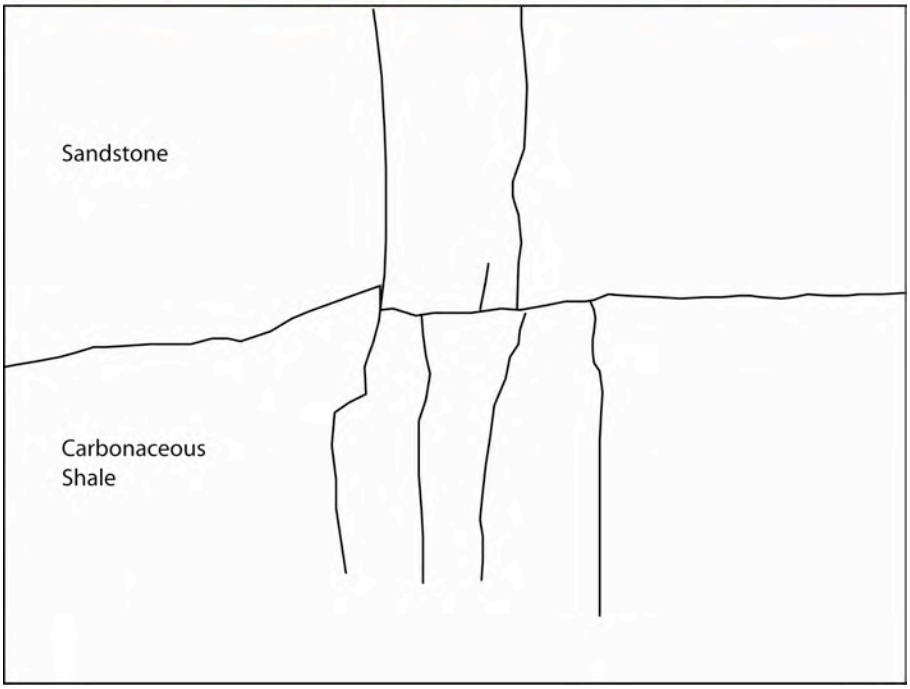

Fig. 2-21. Joint multiplication 1. When the sandstone to coal zone thickness ratio is less than 4:1, joint multiplication patterns may be present. Joints continuing into ductile carbonaceous shale units often multiply at stratigraphic intersections. This example is from the Ferron Rochester, Site 10, Utah.

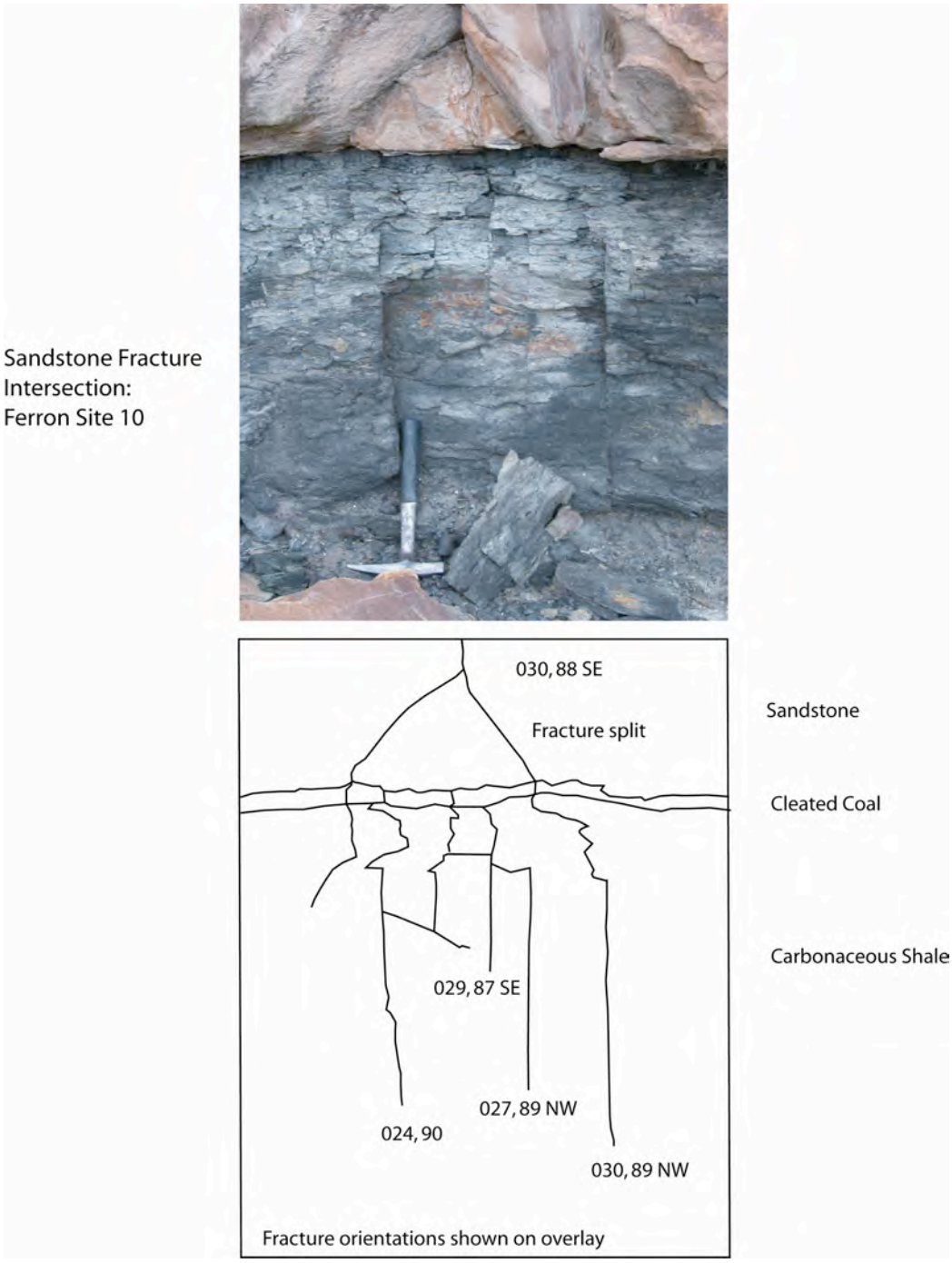

Fig. 2-22. Joint multiplication 2. A single joint in sandstone may split near the stratigraphic intersection with coal or carbonaceous shale. The sandstone joint (before the split) and the multiple joints in the coal zone share similar fracture orientations. Multiple joints in the carbonaceous shale commonly terminate within the ductile zone and are not present in underlying unit.

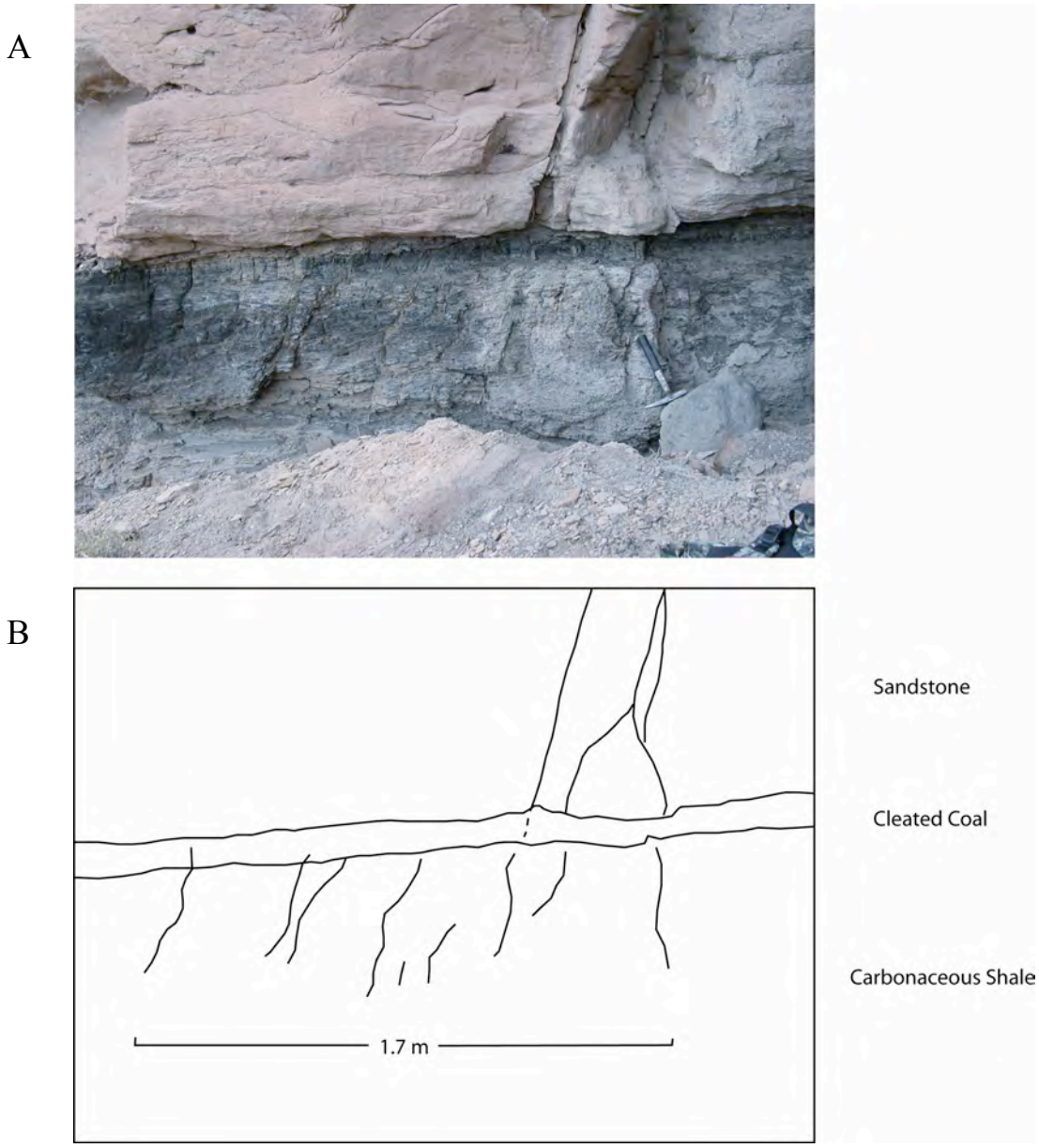

Fig. 2-23. Joint multiplication 3. Figure 2-23 B is and overlay of the photograph (A). Where multiple joints are found in a coal zone, as a result of a sandstone joint intersection, the fracture-damaged zone in the coal can be much greater than the fracture-damaged zone in the sandstone. In this joint multiplication intersection from the Ferron, Willow Springs Wash, Site 5, there is a 1.7 m fracture-damage zone as a result of joint propagation from the overlying sandstone.

noted that when joint multiplication happens in a ductile unit thicker than 2 m, then joint termination commonly takes place within the same unit. We also observed that when joint multiplication occurs in cleated coalbeds, joints can break through the coal, but rarely propagate into underlying units.

Joint Continuation and Sequence Stratigraphy

Joint continuation patterns as described herein can be predicted using a basic understanding of sequence stratigraphic and depositional framework systems. Sequence stratigraphy in a strict sense considers variations in sedimentation as a result of relative sea level rise and fall (Vail et al., 1977). Looking at the Ferron Sandstone Member in a "strict" sequence stratigraphic sense may oversimplify Ferron deposition, as we believe sediment input from the adjacent Sevier orogenic belt to be more or at least equally important to the overall lithologic packages deposited in the Ferron Sandstone. Nevertheless, the availability of great outcrop exposures of varying lithologies and thicknesses within the Ferron have proven to be a useful tool when examining predictable stratigraphic controls on joint continuation.

In fluvial-deltaic environment, sediments are deposited in a more or less continuous series ranging from offshore, to lower-middle-upper shoreface, to foreshore (beach), to lagoon, backswamps, or deserts. Lithologic features are often unique to a given depositional environment. Offshore sedimentary rocks are typically composed of fine-grained sediments although larger grained interbedded turbidite deposits can regularly be found. Sediment size increases up section until sands are the dominant sediments found in the system. Predictable lithologies are associated with each

depositional environment. These lithologies and package thicknesses can be identified using down-hole logs and seismic data. Using package thickness and lithology type, in conjunction with the joint continuation patterns described in this paper, a further understanding of reservoir connectivity and permeability may be attained.

Using the photograph shown in Figure 2-17, we provide an example of how stratigraphy affects regional joint continuation through coal zones. At Rock Canyon, the Ferron A-Coal is surrounded by sandstone. The underlying KF-1 sands grade from an offshore member of the Mancos Shale up to the first sandstones in the Ferron, which grade upwards into upper shoreface and foreshore sands. Due to the high quantity of sediment input in this deltaic environment, several channels are apparent in the sequence. A flooding surface is present at the top of the coal. The overlying sandstone of the KF-2 sequence is composed of cross-bedded shoreface and reworked delta channel sands. The flooding surface at the top of the coal has resulted in the deposition of a relatively thick sand directly atop the coal. The end result is that favorable conditions for "joint breakthrough" have been created and joints in the adjacent sandstone continue through the coal. Where the flooding surface is more extreme, and offshore shales and mudstones are deposited on top of the coal zone, a barrier between joints in the nearest overlying sandstone and the coal is established. In this case, joints from the adjacent sandstone would likely terminate in the shale, and the joints would not continue into the coal. Numerous lithologic combinations are created as a result of relative sea level rise, flooding surfaces, or sediment input. If these packages are identified correctly using any variety of methods, then reservoir joint characteristics could likely be predicted.

S*tructural Influences on Coal Cleats*

The majority of our research took place within the Upper Ferron Sandstone. Numerous folds and faults are present in the subsurface of the Ferron trend, but relatively few are exposed at the surface. In order to examine folding effects on coal cleating, we analyzed a small-scale fold within the Ferron M-Coal at the Walker Flats Mine site, Utah. Our research focus in the San Juan Basin primarily involved analyzing compositional, mechanical layer, and fault effects on cleat density; hence, no quantitative analysis of large-scale cleat density variations caused by the Hogback Monocline was performed.

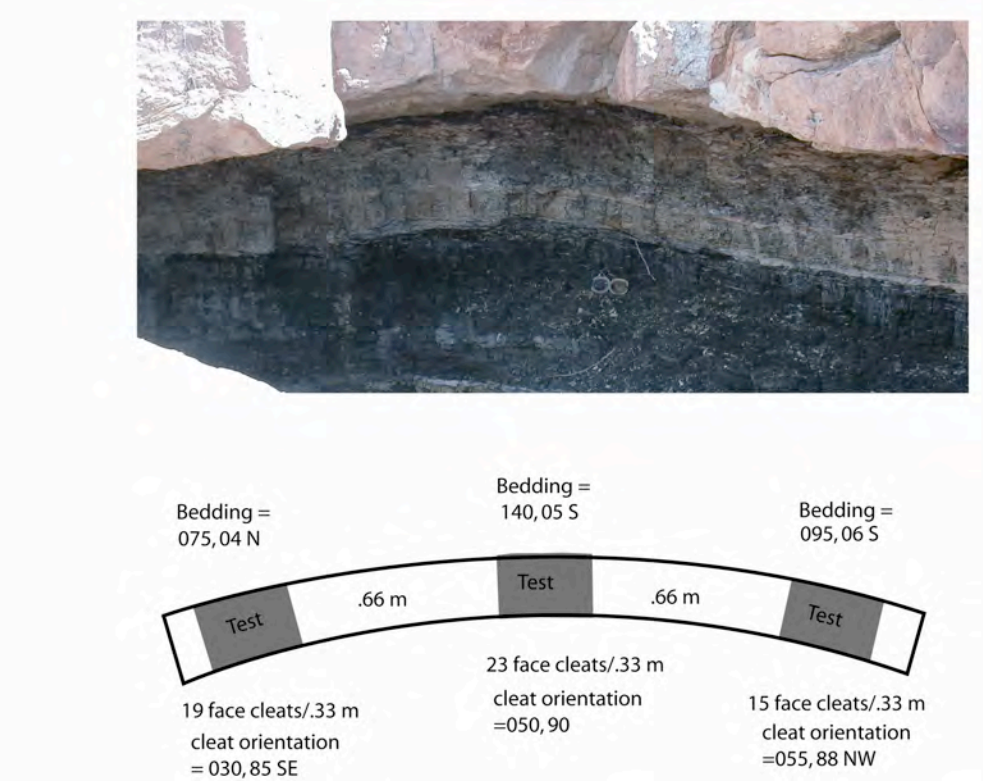

Fig. 2-24. Folding effects on cleat density. Cleat density near a fold hinge is enhanced as a result of increased tension during folding.

In the Ferron M-Coal at the Walker Flats Mine site, we analyzed coal cleat characteristics within a small, open anticline. Cleat density analysis in the field indicates that cleat density is enhanced along the hingeline of this fold (Fig. 2-24). Face cleat density from the left and right limbs is 19 cleats/.33 m, and 15 cleats/.33 m, respectively. Density along the hingeline is 23 cleats/.33 m (Fig. 2-24). No measurable cleat aperture variations were detected along this fold, and all cleats within the coalbed remained nearly perpendicular to bedding.

In the Soda Springs Canyon site, Colorado, a small normal fault cuts an alternating sequence of carb-shale and cleated, clarain coal in the Fruitland Formation (Fig. 2-25). This fault, oriented 127, 65 SW, has 21.6 cm of pure dip-slip offset. The orientation of the fault is nearly parallel to the average face cleat orientation in Soda Springs Canyon (132, 78 SW), and fault-induced fractures are nearly parallel to the fault trace (Fig. 2-25B and C). We performed scan-line density counts across the fault in several coal and carb-shale beds, and found that a fault-induced damage zone extends up to 20 cm perpendicular to fault strike into the footwall and hanging wall blocks. Within the damage zone, cleat density is 2 to 3 times greater than cleat density in areas unaffected by the fault. Cleat height is increased within the damage zone, as numerous cleats propagated beyond their expected termination points, and may cross several coal lithotypes (Fig. 2-25C). No observable butt cleat density increase is apparent in the vicinity of the damage zone. The amount of offset on the Soda Springs Canyon fault is roughly equal to the layer thicknesses of the interbedded lithotypes at this site, creating a

high percentage of lateral juxtaposition of cleated coal with carb-shales across the fault (Fig. 2-25D).

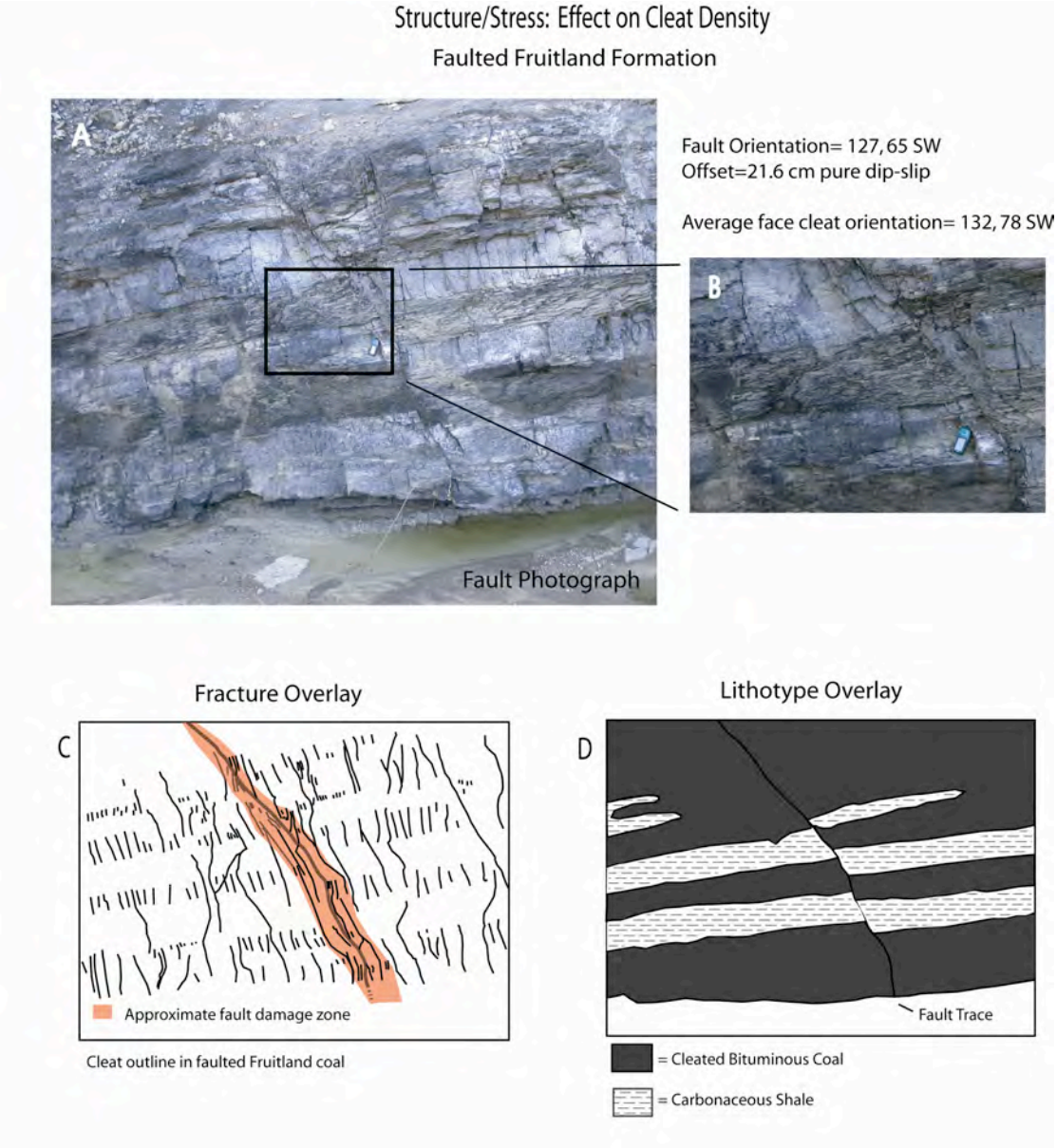

Fig. 2-25. Effects of faulting on coal. This normal fault (A) is in the Fruitland Formation at the Soda Springs Canyon site, CO. Near the fault, cleat density may be 2 to 3 times greater than cleat density outside the fault-damage zone (C). In this case the fault damage zone extends up to 20 cm perpendicular to fault. In this vicinity, cleats are aligned parallel to the fault orientation (B). Lithotype thickness and fault offset are roughly equal at this site, creating a large amount of lateral juxtaposition across the fault (D).

Discussion

Previous work suggests that cleat orientations are controlled by the tectonic stress field during coalification and can be used as kinematic paleo-stress indicators (Laubach et al., 1997). Orientation similarities among fault strike and face cleats at the Soda Springs Canyon site, and rock joints and face cleat orientations (Fig. 2-26) as seen in the Ferron sites, suggest that the fault and the joints were developed under the same stress conditions as the cleats. Furthermore, consistency in face cleat orientations along the length of the

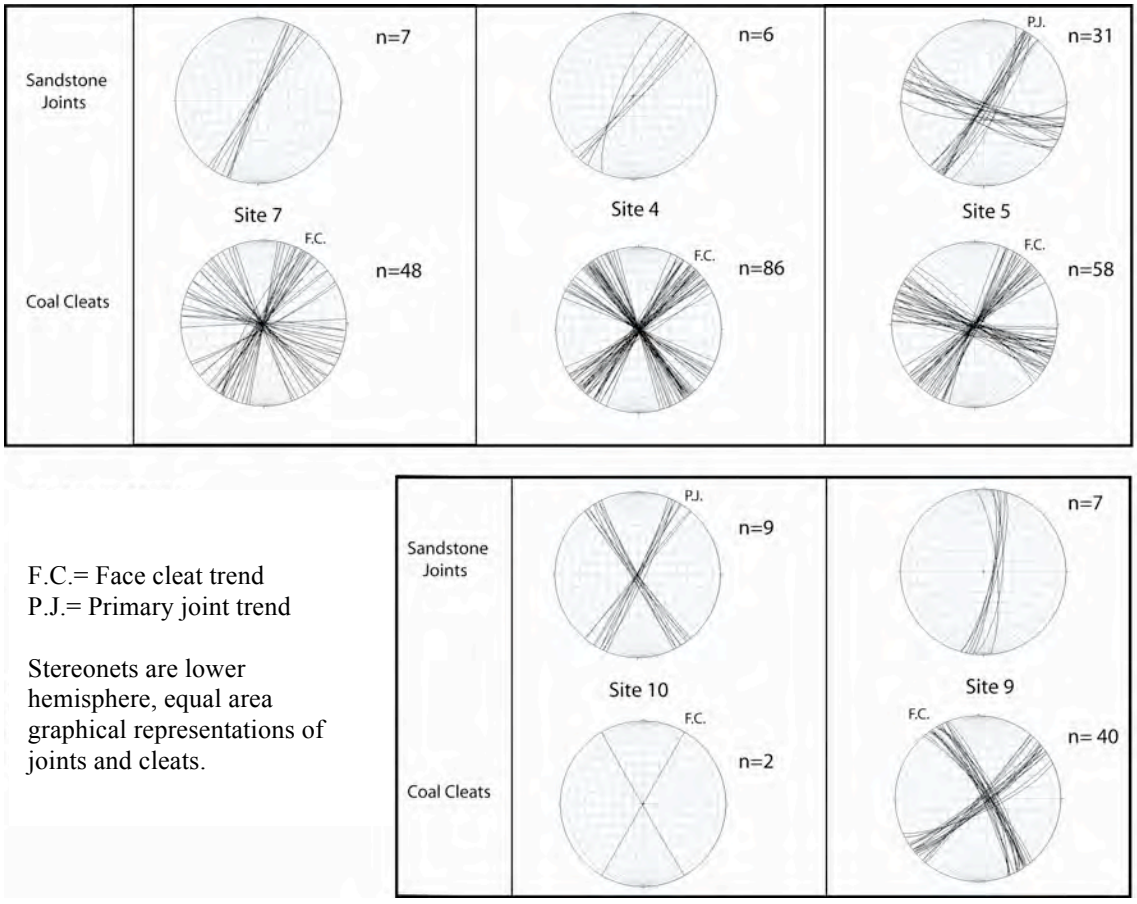

Fig. 2-26. Sandstone joint and coal cleat trends. Face cleats and primary joints from coal and sandstone in the Ferron Sandstone Member are oriented near parallel to each other.

Ferron trend, as measured by ourselves and Hucka (1991), likely indicates that cleats are oriented as a result of a regional-scale stress. Conversely, understanding the stress history of coalbed methane reservoir coals can lead to accurate prediction of cleat orientation and structural complexities within the gas field. Cleat spacing varies as a result of composition, mechanical layer thickness, and proximity to structural deformation. We suggest that having a knowledge of cleat orientations and the factors affecting cleat density within the coal will result in more efficient and profitable well placement.

Coal composition is a primary control on the type and density of cleats present. If coal compositional trends can be established and/or predicted within a coalbed methane field and cleat orientations can estimated from the paleo-stress history, then it may be possible to identify high and low permeability zones as a result of understanding how composition affects cleat types and densities. Vitrain and vitrain-rich coals contain the highest density of face cleats. Although a butt cleat set is rarely formed in these coal lithotypes, connectivity of the face cleats can be very high due to the conchoidal fractures and by the common intersections of the closely spaced face cleats. High bed-scale permeability in vitrain and vitrain-rich coals would result in effective dewatering and high potential methane production. Clarain coals contain face and butt cleat sets by which their density is controlled by mechanical layer thickness. In most cases, mechanical layer thicknesses and cleat spacing decrease as ash content increases, therefore we suggest that clarain coals with reasonably high ash contents are more permeable than low-ash clarains. When ash content increases to the point where

carbonaceous shales form, gas and fluid migration is confined primarily to a bedding parallel direction and is likely low due to compression normal to bedding caused by the overburden. If conditions could be created, or naturally exist, that overcome the effects of the lithostatic pressure and bed partings could be opened, favorable fluid/gas flow conditions could be found within carb-shales. Until recently, carb-shales have been largely overlooked for their potential as, and effects on, coalbed methane reservoirs.

If thin coal beds are overlain by a thick sandstone, we suggest that regional joints likely continue through the coal seam. Understanding whether joints in adjacent sedimentary beds continue into coal or coal zones can yield valuable insight into the vertical connectivity and fluid/gas migration paths within coal reservoirs**.** Where regional joints are present in a high density within a coal zone, migration conduits created by these joints may allow for degasification of coals. Conversely, water from adjacent formations may enter the coal zone and ultimately affect gas and water production rates. In the Ferron Sandstone Member coal in Drunkards Wash, thin coalbed gas reservoirs (less than a meter) are commonly perforated, and stimulated. Predicting fracture intersection systems within a coal reservoir may prove useful when designing fracture stimulation techniques. Commonly, gel, water, or air may be used to induce fractures in coal. If these media are intercepted by joints in the target interval, then fracture stimulation may be less effective than planned. Where regional joints continue into, through, or multiply in coal stratigraphy, the induced fracture medium is more likely to be intercepted.

Both faults and folds affect cleat characteristics in coal. If the orientations of these structures can be identified through sub-surface imaging, or at least predicted with

an understanding of the field's paleo-stress history, then application of structural cleat density variations as described in this paper should result in higher reservoir production and efficiency. We suggest that permeability near a fold hinge is enhanced due to an increase in cleat density. In addition to having increased permeability, anticlinal folds create structural hydrocarbon traps, in which favorable methane quantities may be found. Fault influences on reservoir producibility may be beneficial or detrimental. Coal permeability is increased in a fault-parallel direction due to increased face cleat density and height within the damage zone. Permeability across a fault may be drastically decreased as a result of lateral juxtaposition. Lateral juxtaposition can create compartmentalization and decrease methane production perpendicular to fault strike if present in a coalbed methane reservoir. Critical placement of wells along fault strike may yield favorable production results.

Conclusions

As coalbed fields reach initial well capacity, many operators continue exploration and development along the reservoir edges, or attempt to decrease well spacing in the initially high productivity areas in attempt remove as much gas as possible. Successful continued development within established coalbed methane fields will require a knowledge of coal cleat systems and fractures within the reservoir and adjacent beds in order to place new wells in high permeability zones, and to avoid inter-well linkage as well spacing decreases.

We suggest that a knowledge of cleat characteristics, as described in this report, can be used in conjunction with various types of down-hole data to estimate reservoir permeability. Furthermore, outcrop investigation of a coal reservoir analog yields critical information that can lead to increased coalbed methane production and efficiency. We have identified several factors that directly affect coal cleating:

- Coal composition is a primary control on the development and spacing of coal cleats. Each coal lithotype exhibits unique cleat characteristics that may be affected by maceral composition and ash content.
- Mechanical layer thickness controls cleat density in clarain coals. Bounding units typically arrest cleat propagation at lithotype contacts and at mechanical interfaces within clarain. Higher densities of bounding units create thinner mechanical layers. As mechanical layer thickness decreases, cleat density increases.
- Cleat density is affected by proximity to structural components such as folds and faults. In folded coal, cleat density is increased near the fold hinge-line. Where faults cut coal stratigraphy, there is in an increase in density and heights of coal cleats parallel to fault strike. Cleat connectivity and/or permeability may be altered beneficially or detrimentally by structural features.

Our research and analysis of the Ferron and Fruitland coals provide valuable insight concerning coal cleat characteristics that will aid in successful development and efficient exploitation strategies within the CBM fields.

References

Allmendiger, R. M., 2002, Stereonet for Windows V.1.1, Based on Steronet for Macintosh: Computer program; free version for non-commercial use.

Anderson, P.B., T.C., Chidsey, Jr., and T.A. Ryer, 1997, Fluvial deltaic sedimentation and stratigraphy of the Ferron Sandstone, Brigham Young University Geology Studies, v. 42, part II, p. 135-154.

Ayers, W.B, Jr., 2002, Coalbed gas systems, resources, and production and a review of contrasting cases from the San Juan and Powder River basins: American Association of Petroleum Geologists Bulletin, v. 86, p. 1853-1890.

Ayers, W.B., Jr., and W.A. Ambrose, 1990, Geologic controls on coalbed methane occurrence, Fruitland Formation, San Juan Basin, *in* W.B. Ayers, Jr., and other eds., Geologic evaluation of critical production parameters for coalbed methane resources, part 1-San Juan basin: Gas Research Institute, Annual Report. GRI-90/0014.1 (August 1988-July 1989), p. 9-72.

Burnham, A.K., and J.J. Sweeney, 1989, A chemical model of vitrinite maturation and reflectance: Geochem Cosmochim, Acta 53, p. 2649-2657.

Burns, T.D., and R.A. Lamarre, 1997, Drunkards Wash Project: coalbed methane production from Ferron coals in east-central Utah: Proceedings of the International Coalbed Methane Symposium, University of Alabama, Tuscaloosa, paper 9707, p. 507-520.

Close, J.C., and M.J. Mavor, 1991, Influence of coal composition and rank on fracture development in Fruitland coal gas reservoirs of San Juan Basin, Coalbed Methane, Rocky Mountain Association of Geologists Guidebook, p. 109-121.

Close, J.C., S. Woolverton, and K. Swainson, 1997, Non-fairway, underpressured Fruitland coal resource characterization study, southern San Juan basin, New Mexico: University of Alabama College of Continuing Studies, *in* Proceeding of the 1997 International Coalbed Methane Symposium, p. 23-32.

Condon, S.M., 1997, Preliminary results of coal cleat studies, upper Cretaceous Ferron Sandstone Member of the Mancos Shale, Emery and Sevier Counties, Utah, *in* J.C. Close, TA. Casey, eds., Natural Fracture Systems in the southern Rockies, Four Corners Geological Society Proceedings, p. 85-96.

Cook, T.S., and F. Erdogan, 1972, Stresses in bonded material with a crack perpendicular to the interface: International Journal of Engineering Science, v. 10, p. 677-697.

Cotter, E., 1975, Late Cretaceous sedimentation in a low energy coastal zone: The Ferron Sandstone of Utah: Journal of Sediment Petrology, v. 45, p. 669-685.

Daniels, E.J., S. Marshak, and S.P. Altaner, 1996, Use of clay mineral alteration processes to define syntectonic permeability of joints in Pennsylvanian anthracite coal: Tectonophysics, v. 263, p. 123-136.

Dron, R.W., 1925, Notes on cleats in the Scottish coalfield: Transactions of the Institute of Mining and Engineering, v. 70, p. 115-117.

Engelder, J.T., 1985, Loading paths to joint propagation during a tectonic cycle: An example from the Appalachian Plateau: USA: Journal of Structural Geology v. **7**, p. 45-476.

Erdogan, F., and V. Biricikoglu, 1973, Two bonded half planes with a crack going through the interface: International Journal of Engineering Science, v. 11, p. 745-766.

Evans, I., and C. D. Pomeroy, 1966, The Strength, Fracture, and Workability of Coal: Pergamon Press, New York, 277 p.

Fassett, J. E., 1985, Early Tertiary peleogeography and paleotectonis of the San Juan basin area, New Mexico and Colorado, *in* R.M. Flores, and S.S. Kaplan, eds., Cenozoic Paleogeography of the West-Central United States: Rocky Mountain Section of the Society of Exploration Paleontologists and Mineralogists, p. 317-334.

Fassett, J. E., S. G. Lucas, and F.M. O'Neil, 1987, Dinosaurs, pollen and spores, and the age of the Ojo Alamo Sandstone, Sand Juan Basin, New Mexico: U.S. Geological Survey Special Paper 501-D, p. D90-D94.

Gardner, M.H., 1992, Sequence stratigraphy of the Ferron Sandstone, East-Central Utah, *in* N. Tyler, M.D. Barton, and R.S. Fisher, eds., Architecture and permeability structure of fluvial-deltaic sandstones, east-central Utah: The University of Texas at Austin, Bureau of Economic Geology Guidebook, p. 1-12.

Gardner, M.H., 1993, Sequence stratigraphy of the Ferron Sandstone (Turonian) of East-Central Utah Ph.D. dissertation, Colorado School of Mines, Golden, 406 p.

Gardner, M.H., and T.A. Cross, 1994, Middle Cretaceous paleogeography of Utah, *in*: M.V. Caputo, JA. Peterson, and K.J. Franczyk, eds., Mesozoic systems of the Rocky Mountain region, USA: Rocky Mountain Section SEPM, p.471-503.

Garrison, J.R., Jr., T.C.V. Van Den Bergh, C. Barker, and D.E. Tabet, 1997,

Depositional sequence stratigraphy and architecture of the Cretaceous Ferron Sandstone: Implication for coalbed methane resources-A field excursion: Brigham Young University Geology Studies, v. 42, part II, p. 155-200.

Gray, L., 1987, Reservoir engineering in coal seams: Part 1- The physical process of gas storage and movement in coal seams: SPERE, pp. 28-34.

Gross, M.R., M.P. Fischer, T. Engelder, and R.J. Greenfield, 1995, Factors controlling joint spacing in interbedded sedimentary rocks: Interpreting numerical models with field observations from the Monterey Formation, USA, *in* M.S. Ameen, ed., Fractography: Fracture topography as a tool in fracture mechanics and stress analysis: Geological Society of America Special Publication 92, p. 215-233.

Grout, M.A., 1991, Cleat in coalbeds of southeast Piceance Basin, Colorado- correlation with regional and local fracture sets in associated clastic rocks, *in* S. Schwochow, D.K. Murray, and M.F. Fahy, eds., Coalbed methane of Western North America, Rocky Mountain Association of Geologists, p. 35-47.

Hale, L.A., 1972, Depositional history of the Ferron Formation, central Utah, *in* J.L. Baer, and E. Callaghan, eds., Plateau-Basin and range transition zone: Utah Geological Association Guidebook, p. 115-138.

Hale, L.A., and F.R. Van de Graph, 1964, Cretaceous stratigraphy and facies patterns-northeastern Utah and adjacent areas: Intermountain Association of Petroleum Geologists 13th Annual Field Conference Guidebook, p. 115-138

Helgeson, D.E., and A. Aydin, 1991, Characteristics of joint propagation across layer interfaces in sedimentary rocks: Journal of Structural Geology, v. 13, no. 8, p. 897-911.

Hubbert, M.K., W.W. Rubey, 1959, Mechanics of fluid filled porous solids and its application to overthrust faulting: Geological Society of America Bulletin, v. 70. p. 115-166.

Hucka, B., 1991, Analysis and regional implication of cleat and joint systems in selected coal seams, Carbon, Emery, Sanpete, Sevier, and Summit Counties, Utah: Utah Geological Survey Special Study 74, 47 p.

Hucka, B., S.N. Sommer, and D.E. Tabet, 1997, Petrographic and Physical characteristics of Utah Coals: Utah Geological Survey, Circular 94.

Kelso, B.S., and D.E. Wicks, 1988, A geologic analysis of the Fruitland Formation coal and coal-bed methane resources of the San Juan Basin, southwestern Colorado and northwestern New Mexico, *in* J.E. Fasset, ed., Geology and coal-

bed methane resources of the northern San Juan Basin, Colorado and New Mexico: Rocky Mountain Association of Geologists Guidebook, p. 69-79.

Kendall, P.F., and H. Briggs, 1933, The formation of rock joints and the cleat of coal: Proceedings of the Royal Society of Edinburgh, v. 53, p. 164-187.

Koenig, R.A., 1989, Hydrologic characterization of coal seams for optimal dewatering and methane drainage: Quarterly Review of Methane from Coal Seams Technology, v. 35, p. 30-31.

Lamarre, R.A., and T.D. Burns, 1996, Drunkards Wash Unit: Coalbed Methane Production from Ferron coals in east-central Utah: 1996 American Association of Petroleum Geologists, Rocky Mountain Section Meeting-Billings, Montana: American Association of Petroleum Geologists Bulletin, p. 80.

Lamarre, R.A., 2001, The Ferron Play: A giant coalbed methane field in east-central Utah: IPAMS Coalbed Methane Symposium, October 16, 2001.

Laubach, S.E, R.A. Marrett, J.E. Olsen, and A.R. Scott, 1997, Characteristics and origins of coal cleat: A review: International Journal of Coal Geology, v. 35, p. 175-207.

Laubach, S.E., and C.M. Tremain, 1991, Regional coal fracture patterns and coalbed methane development, *in*: J.C. Roegiers ed., Proceedings of the 32nd U.S. Symposium of Rock Mechanics, Dalkenia, Rotterdam, p. 851-859.

Law, B.E., 1993, The relationship between coal rank and cleat spacing: Implications for the prediction of permeability in coal: 1993 International Coalbed Methane Symposium Proceedings, University of Alabama, Tuscaloosa 2, 435-441.

Lawton, T.F., 1986, fluvial systems in the Upper Cretaceous Mesaverde Group and Paleocene North Horn Formation, central Utah: A record of transition from thin-skinned to thick-skinned deformation in the foreland region, *in* J.A. Peterson, ed., Paleotectonics and sedimentation in the Rocky Mountain region, AAPG Memoir 41, p. 423-442.

Levine, J. R., 1993, Coalification: The evolution of coal as a source rock and reservoir rock for oil and gas: American Association of Petroleum Studies in Geology, v. 38, p. 39-77.

Lupton, C.T., 1916, Geology and coal resources of Castle Valley in Carbon, Emery, and Sevier Counties, Utah: U.S. Geological Survey Bulletin, v. 628, 88 p.

Montgomery, S.L., D.E. Tabet, and C.E. Barker, 2001, Upper Cretaceous Ferron Sandstone: Major coalbed methane play in central Utah: American Association of Petroleum Geologists Bulletin, v. 85, p. 199-219.

Ridgely, J.L., and A.C. Huffman, Jr., 1990, Basin ananlysis study of the San Juan Basin Colorado and New Mexico, *in* L.M.H. Carter, ed., USGS research on energy resources, 1990 program and abstracts--Sixth V.E. McKelvey Forum on Mineral and Energy Resources: USGS Circular 1060, p. 68-69.

Rijken, P., and M.L. Cooke, 2001, Role of shale thickness on vertical connectivity of fractures; application of crack bridging theory in the Austin Chalk, Texas: Tectonophysics, v. 337, p. 117-133.

Ryer, T.A., 1981, Deltaic coals of the Ferron Sandstone Member of the Mancos Shale: Predictive model for Cretaceous coal-bearing strata of the western interior: American Association of Petroleum Geologists Bulletin, v. 65, p. 2323-2340.

Ryer, T.A., 1991, Stratigraphic, facies, and depositonal history of the Ferron Sandstone Member near Emery, Utah, *in* T.C. Chidsey Jr., ed., Geology of east-central Utah: Utah Geological Association Publication 19, p. 45-54.

Schopf, J. M., 1960, Field descriptions and sampling of coal beds: Contributions to general geology: Geological Survey Bulletin, v. 111-B, p. 28-32.

Scott, A.R., W.R. Kaiser, and W.B. Ayers, Jr., 1990, Thermal maturity of Fruitland coal and composition and origin of gases in the Fruitland Formation, San Juan Basin, *in* W.B. Ayers, Jr., and other eds., Geologic and hydrologic controls on the occurrence and producibility of coalbed methane, Fruitland Formation, San Juan Basin: Gas Research Institute, Topical Report. GRI-91/0072 (August 1987-July 1990), p. 241-243.

Scott, A. R., W.R. Kaiser, and W.B. Ayers, Jr., 1991, Composition, distribution, and origin of Fruitland Formation and Picture Cliffs Sandstone gases, San Juan Basin, Colorado and New Mexico, *in* S.D., Schwochow, D.K. Murray, and M.F. Fahy, eds., Caolbed methane of western North America: Rocky Mountain Association of Geologists, 336 p.

Scott, A. R., W.R. Kaiser, and R. Tyler, 1996, Development and evaluation of basin-scale coalbed methane producibility model; San Juan, Sand Wash, and Piceance Basins, Rocky Mountain Foreland, *in* R. Tyler, A.R. Scott, W.R. Kaiser, H.S. Nance, R.G. McMurry, C.M. Tremain, and M.J. Mavor, eds., Geologic and hydrologic controls critical to coalbed methane producibility and resource assessment: Williams Fork Formation, Piceance Basin, Northwest Colorado: The University of Texas at Austin, Bureau of Economic Geology, topical report

prepared for the Gas Research Institute, GRI-95/0532, p. 310-407.

Secor, D.T., 1965, Role of fluid pressure in jointing: American Journal of Science, v. 263. p. 633-646.

Selley, R.C., 1998, Elements of petroleum geology; second edition: San Diego, Academic Press, p. 213-214.

Spears, D.A., and S.A.Caswell, 1986, Mineral matter in coals: cleat minerals and their origin in some coals from the English Midlands: International Journal of Coal Geology, v. 6, p. 107-125.

Stach, B., M.T.H. Mackowsky, M. Teichmueller, G.H. Tayor, D.R. Chandrin, 1982, Coal petrology, Berlin, Gebruder Borntracger, pp. 5-86.

Stopes, M. C., 1919, On the four visible ingredients in banded bituminous coal: Proceedings of the Royal Society., v. 90 B, 470 p.

Ting, F.T.C., 1977, Origin and spacing of cleats in coal beds: Journal of Pressure Vessel Technology, v. 99, p. 624-626.

Tremain, C.M., S.E. Laubach, and N.H. Whitehead, 1991, Coal fracture (cleat) patterns in Upper Cretaceous Fruitland Formation, San Juan Basin, Colorado and New Mexico: Implications for exploration and development, *in* S. Schwochow, D.K. Murray, M.F. Fahy, eds., Coalbed methane of Western North America, Rocky Mountain Association of Geologists, p 49-59.

Underwood, C.A., M.L. Cooke, J.A. Simo, and M.A. Muldoon, 2003, Stratigraphic controls on vertical fracture patterns in Silurian dolomite, northeastern Wisconsin: American Association of Petroleum Geologists Bulletin, v. 87, pp.121-142.

Utah Geological Survey, 1996, Ferron Sandstone project moves to reservoir simulation stage: Utah Geological Survey, Petroleum News, May, p. 2-5.

University of Wyoming, 2004. Website definitions. http://www.nasc.uwyo.edu/coal/library/lookup

Vail, P.R., R.M. Mitcham, Jr., R.G. Todd, J.M. Widmier, S. Thompson, III, J.B. Sangree, J.N. Bubb, and W. Hatlelid, 1977, Seismic stratighraphy and global changes of sea level, *in* C.E. Payton, ed., Seismic stratigraphy- Applications to hydrocarbon exploration, AAPG memoir 26, p. 49-212.

Van Krevelen, D.W., 1981, Coal, Amsterdam, Elsevier, 514 p.

Williams, P. E., and R.J. Hackman, 1971, Geology of the Salina Quadrangle, Utah. U.S. Geological Survey Miscellaneous Investigation Series Map, I-591-A.

CHAPTER 3

CONTROLS ON METHANE PRODUCTION FROM TWO AREAS IN THE DRUNKARDS WASH FIELD, CENTRAL-UTAH[1]

Abstract

We use our knowledge of coalbed reservoirs and coal cleat characteristics in conjunction with data supplied by ConocoPhillips to examine production variations in two portions of the Drunkards Wash Field, near Price, Utah. A portion of the field, Area B, is one of the oldest areas in the field and has high production. Area A is younger and production is less favorable.

Our analyses indicate that gas production has no direct correlation to coal thickness, clean coal percentage, or coal plus carbonaceous shale thickness. Gas production and water production do show weak correlation, which is reflective reservoir permeability influence on production. From our analysis we suggest that the presence of small-displacement faults in Area B has increased reservoir permeability and ultimately increased methane production in this vicinity. In Area A, where current methane production is low, we suggest that larger faults intersecting thinner coal beds has had a detrimental effect on the coalbed methane production.

---

[1]Coauthored by Jason Kneedy and James P. Evans

Introduction

Production of coalbed methane (CBM) from the Rocky Mountain region is one of the most important new concepts in developing new sources of natural gas in the United States (Montgomery et al., 2001; Ayers, 2002). Recent drilling near Price, Utah (Fig. 3-1A), in the Upper Cretaceous Ferron Sandstone Member of the Mancos Shale, has resulted in one of the most successful plays of this kind (Anderson et al., 2003). Drunkards Wash is the largest gas field in Utah, and is the 18th largest natural gas field in the U.S. (Energy Information Administration, 2004), with 2003 total gas production reaching 79,210,724 MCF (thousand cubic feet) (Utah Oil, Gas and Mining, 2004). Estimated ultimate recoveries in Drunkards Wash range from 1.5-4.0 tcf (trillion cubic feet) (Montgomery et al., 2001).

Methane production in the Ferron trend began in the early 1990's by River Gas Co. and Texaco. In 2000, Chevron-Texaco and Phillips Petroleum acquired a major portion of the Drunkards Wash field and began drilling a large number of wells to exploit the methane. Anadarko, Dominion and Marathon have junior interests to exploit methane in Drunkards Wash. As of December 2003, 549 CBM wells were in production operated by ConocoPhillips (487 wells), Anadarko Petroleum (45 wells) and Marathon (17 wells) (Naranjo and Tabet, 2004) .

Due to the rapid expansion of the field, coalbed methane wells were commonly spaced using "simple" models that did not take into consideration the structure or the

stratigraphy within the coalbed reservoir. As Drunkards Wash reaches its initial well capacity, as designated by the 160-acre spacing agreement, more thought is put into well

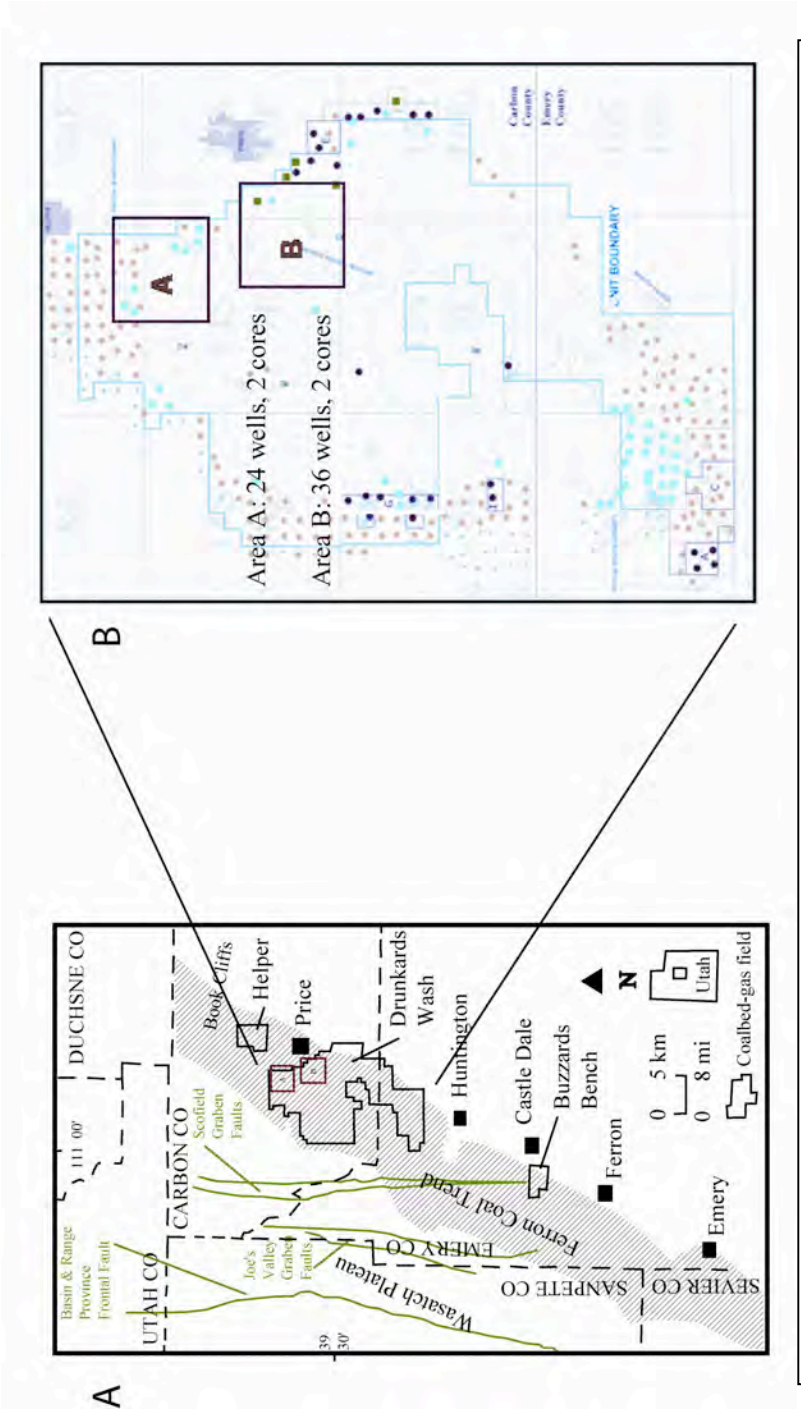

Fig. 3-1. Drunkards Wash location map (modified from Montgomery et al., 2001). The Drunkards Wash gas field is located in central Utah, near the town of Price (A). Within Drunkards Wash (B), Area B is one of the oldest parts of the field and has high gas production rates; Area A is younger and production is less than expected.

location. ConocoPhillips has identified two areas within the Drunkards Wash field that contain different production characteristics (Fig. 3-1 B). Area B is one of the oldest and most productive areas in the field. Area A is younger and methane production is relatively low. Faults are present in both areas. Using the ConocoPhillips data set for the two areas, applying our understanding of coal and coalbed reservoir characteristics, as determined from analysis of the Fruitland Formation and Upper Ferron reservoir analogs (Chapter 2 of this thesis), and using statistical analysis of production, we investigate the differences between the two areas in attempt to identify likely factors that result in low production in area A.

Background Information

Coalbed gas fields in the Ferron play are located along the western flank on the San Rafael Swell of central Utah, in which CBM is produced from within the Ferron Sandstone Member of the Mancos Shale (Ryer, 1981; Anderson et al., 1997; Lamarre, 2001; Montgomery et al., 2001). The Ferron Sandstone Member was deposited in a fluvial-deltaic environment during Turonian-Conacian (Late Cretaceous) time (Anderson et al., 1997). During this time, sediments eroding from the Sevier thrust system to the west/northwest were deposited into the foreland basin, which also accommodated the western margin of the Cretaceous Interior Seaway (Gardner, 1992). This resulted in a series of stacked, transgressive-regressive cycles (Anderson et al., 1997), which are apparent in the form of interbedded sandstones and coals in the Ferron Member.

Coals in the Ferron Sandstone in Drunkards Wash occur in 3 to 8 distinct seams (Garrison et al., 1997). The total coal thickness within the field ranges from 4 to 48 ft, with an average thickness of 24 ft; typical well depths range between 1800 to3400 ft (Lamarre and Burns, 1996). Coal permeability ranges from 5 to 20 md in Drunkards Wash (Montgomery et al., 2001). The average R_0 value in Drunkards Wash is 0.7%, which corresponds to a high volatile B bituminous rank (Burns and Lamarre, 1997; Lamarre, 2001). Coalbed gases of biogenic origin are common in coals of the Rocky Mountain region (Scott, 1993). Biogenic gases result from degradation of coals and wet gases by ground water introduced anaerobic bacteria. Thermogenic gases are a result of thermal maturation of coals, causing coals kerogens to be transformed into hydrocarbons. Isotope analysis of the Ferron coals imply a mixing of biogenic and thermogenic gases (Burns and Lamarre, 1997).

Field Information

Productive wells in the Drunkards Wash field average more than 500 MCF/day of gas, and after several years, typically continue to show negative declines (Anderson et al., 2003). Figure 3-2 is an example of a favorable negative decline curve from Drunkards Wash well #34. In this ideal case, water production decreases and gas production increases. In the major production area of Drunkards Wash, the first 33 producing wells averaged 974 MCF of gas and 85 bbl (barrels) of water per day after five years of continuous production (Anderson et al., 2003). Water pumped from the Drunkards Wash, Helper, Buzzards Bench, and other Ferron fields is disposed of by injection into the

Navajo Sandstone, which is at a depth below surface between 7000 to 13000 feet. Water pressure in the reservoir is monitored at each gas well. After the pressure in the reservoir is sufficiently low enough, gas diffuses from cleat surfaces and adjacent coal matrix and makes it way to the well bore in the form of free gas. From the well bore, gas is piped to an aimine facility within the field where it is pressurized, purified and sold to the pipeline company. Water pumped from the well may contain a small quantity of gas that is separated at the well site and also piped to the aimine facility. Typical gas from the field contains 6 to 7% CO_2 (Anderson et al., 2003). The majority of the CO_2 is separated from the methane and released into the atmosphere. A small percentage of the CO_2 is collected at the aimine facilities and trucked off to be used for carbonation in soda.

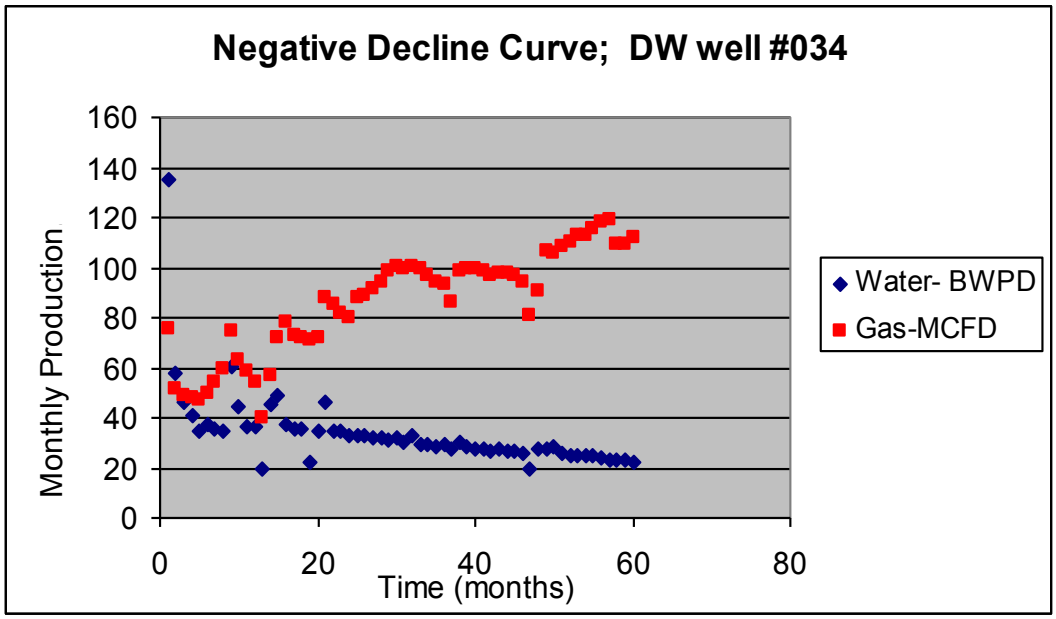

Fig. 3-2. Negative decline curve. On the graph, water rates are reported in BWPD (barrels water per day), and gas rates in MCFD (thousand cubic feet per day). In this ideal situation, reservoir pressure decreases as water is removed, and gas production increases. High initial water production may indicate good reservoir permeability. If permeability is too high and water quantities exceed pumping ability, gas production may not increase.

ConocoPhillips Data Set

ConocoPhillips provided a variety of data for methane production wells within Areas A and B of Drunkards Wash. The data set includes: Ferron Sandstone structure contour maps (Fig. 3-3A and B), and monthly gas and water production data for 24 wells

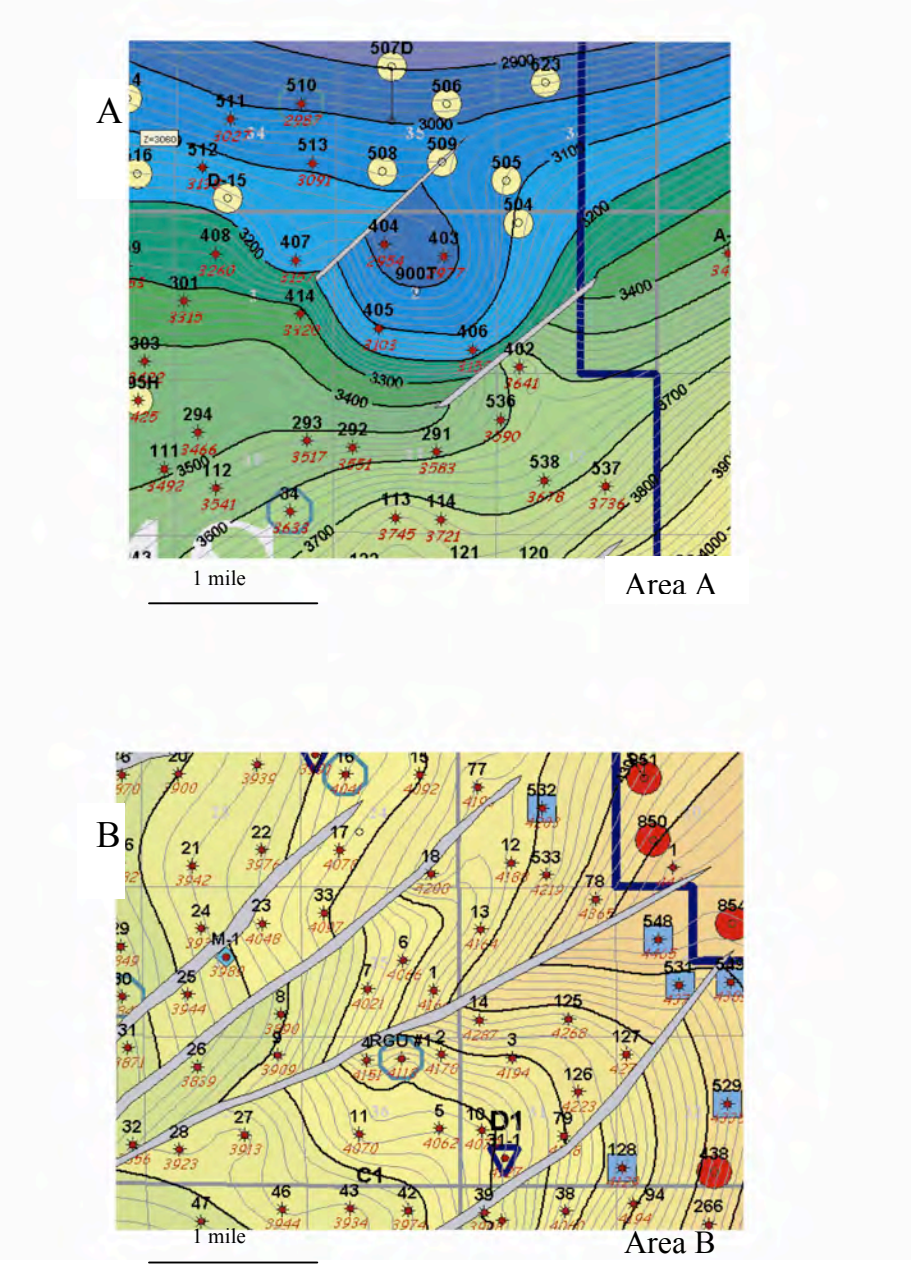

Fig. 3-3. Ferron Sandstone Member structure contour maps. ConocoPhillips provide these structure contour maps of the Ferron Sandstone for Area A (A) and Area B (B) of Drunkards Wash field.

in Area A and 36 wells in Area B (Appendix B). The data set also included core photos and gas content data for wells 510 and 636 (well 510 is in Area A and well 636 is near Area A), and a variety of down-hole logs for the data within the areas. Coal thickness, depth to the top of the Ferron Sandstone, and percent clean coal had been picked and calculated by ConocoPhillips, and was supplied to us in spreadsheet form (Appendix B). We examined core from three wells within Drunkards Wash at the Bartlesville, Oklahoma, Phillips Research Center. Unfortunately, a combined total of only a few feet of coal was present in the core, as the rest had been removed for various testing procedures.

Analyzing Production Data

Since it takes time to lower the hydrostatic pressure in the reservoir enough to produce gas, well age can affect methane production and our ability to examine production data of different ages. We tested the data set to verify that the age difference did not create an apparent production difference. The median age of wells in Area A is 25 months, and the median age of wells in Area B is 118 months. We performed several two-tailed Mann-Whitney U tests on the data, including a test on the current production and a test on all the wells at their one-year production rates (Fig. 3-4). Tests shown on Figure 3-4 verify that Area A has significantly lower production history. We concluded that age does not account for the production difference; hence, there must be some geologic explanation.

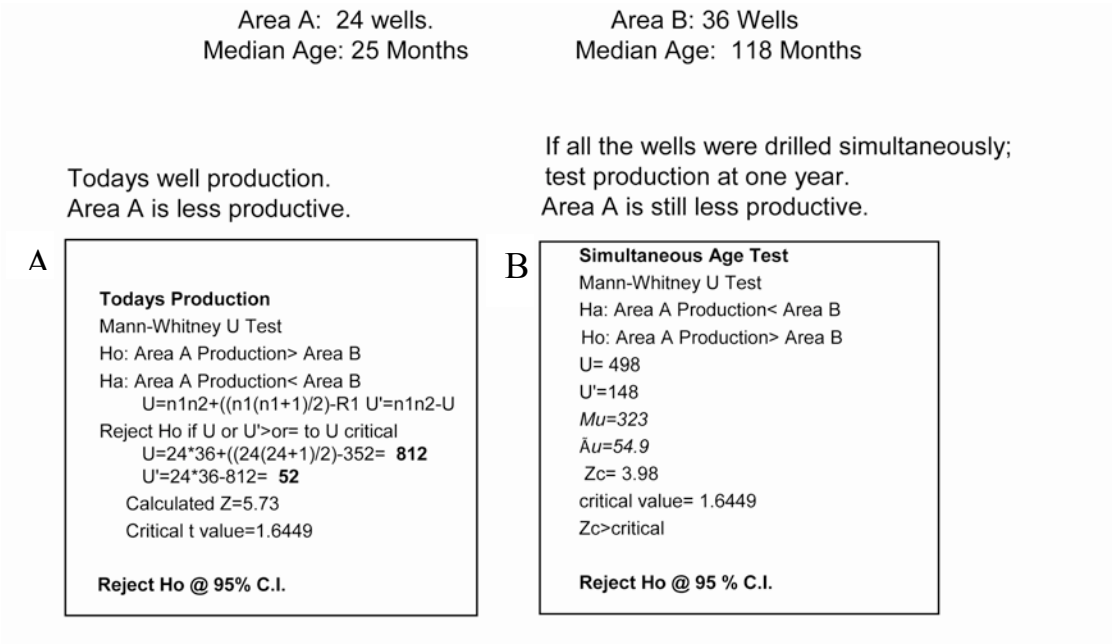

Fig. 3-4. Mann-Whitney U tests. Production tests at the current production rates (A), and at one year production rates (B) verify that Area A production is significantly less than production in Area B. These tests suggest that age difference does not account for production differences between the two areas.

The data provided by ConocoPhillips gives the average daily production rates for both gas and water, every month, for the life of the well. In order to determine a valid production number that can be plotted and/or mapped, the average daily production data for each month was summed and then divided that cumulative average by the age of the well in months (cumulative daily average per month/months on line, see example below). We use this cumulative average number in production maps and correlation graphs of both water and gas data in order to identify any possible trends present in the field.

Well 533 gas production; average production MCFD (million cubic feet per day).										
Month MCFD 1	2	3	4	5	6	7	8	Cum	# mo	Cumulative-average MCFD
49.20	104.32	128.06	181.53	300.03	308.30	294.19	288.84	1654.48	8	206.81

Contour maps of gas and water production, coal thickness, coal plus carbonaceous shale thickness, and percentage of clean coal in both areas were created in the program Rockware. After evaluating the maps created using different contour calculations techniques, we determined that inverse distance and kriging provide the most believable results. In order to show variations in contour options, we provide these two contour options for each variable mapped within this report.

We created cross sections through both portions of the field by hand, and with the program Smart Section, using the log data provided by ConocoPhillips. Using these cross sections and our geologic interpretation, we hand drew and digitized one structure contour maps for both Area A and Area B.

Synthesis of Drunkards Wash Field Data

Area B

Our structure contour map shows that the Ferron Sandstone Member of the Mancos Shale strikes roughly north and dips less than 4º west (Fig. 3-5B). The Ferron Sandstone is at its highest elevation in the northeastern portion of the area, where the top of the Ferron Sandstone reaches 4,465 feet above sea level (asl). In the southwestern portion of Area B, the top of the Ferron Sandstone's lowest point is 3,836 feet asl. ConocoPhillips' isopach map indicates that several faults are present in Area B that trend northeast/southwest (Fig. 3-5B). We agree that several faults are present in Area B; however, our fault placement is slightly different than that mapped by ConocoPhillips. We provide two types of cross sections to support our structure contour map interpretations. Figure 3-6 and 3-7 are two lines of sections running roughly

A

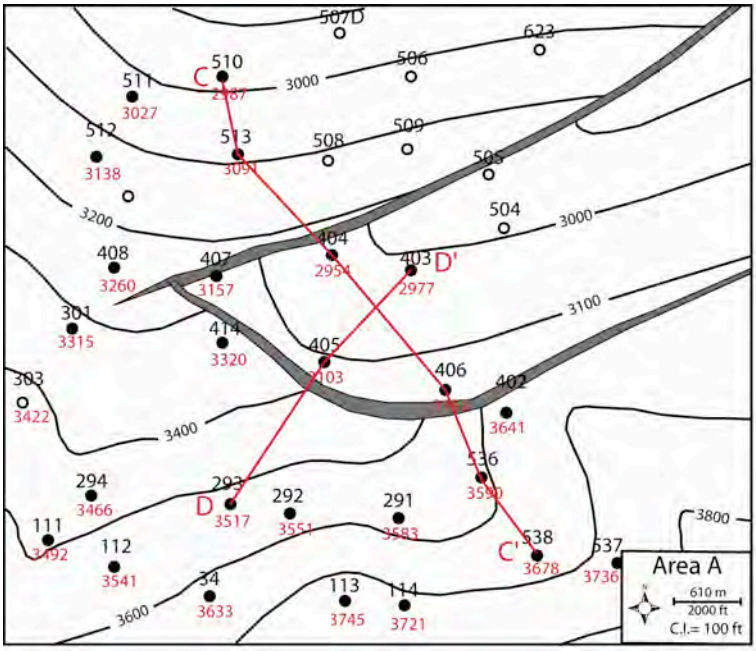

B

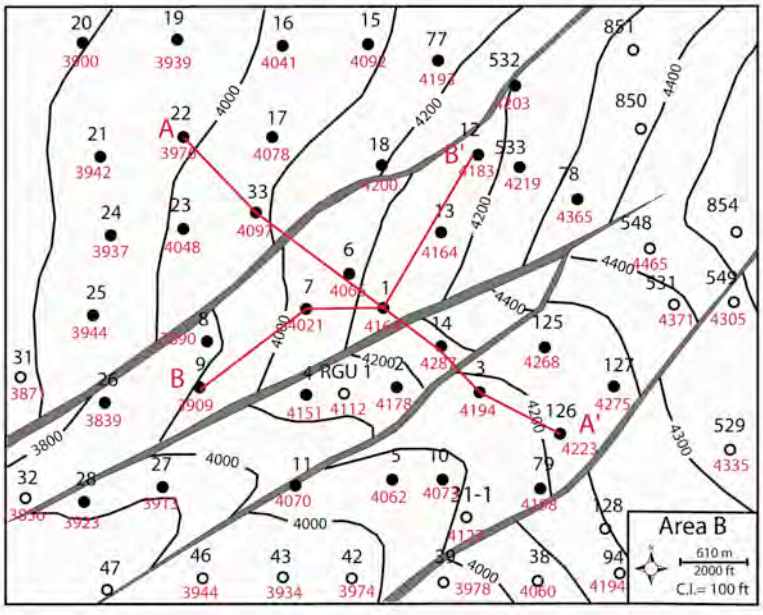

Fig. 3-5. Structure contour maps of the Ferron Sandstone Member. We created structure contour maps for Area A (A) and Area B (B) in Drunkards Wash. Our maps differ from those provided by ConocoPhillips, although we agree that several faults are present in both areas. Cross section lines are shown and labeled in red in their perspective positions and are examined in the following figures.

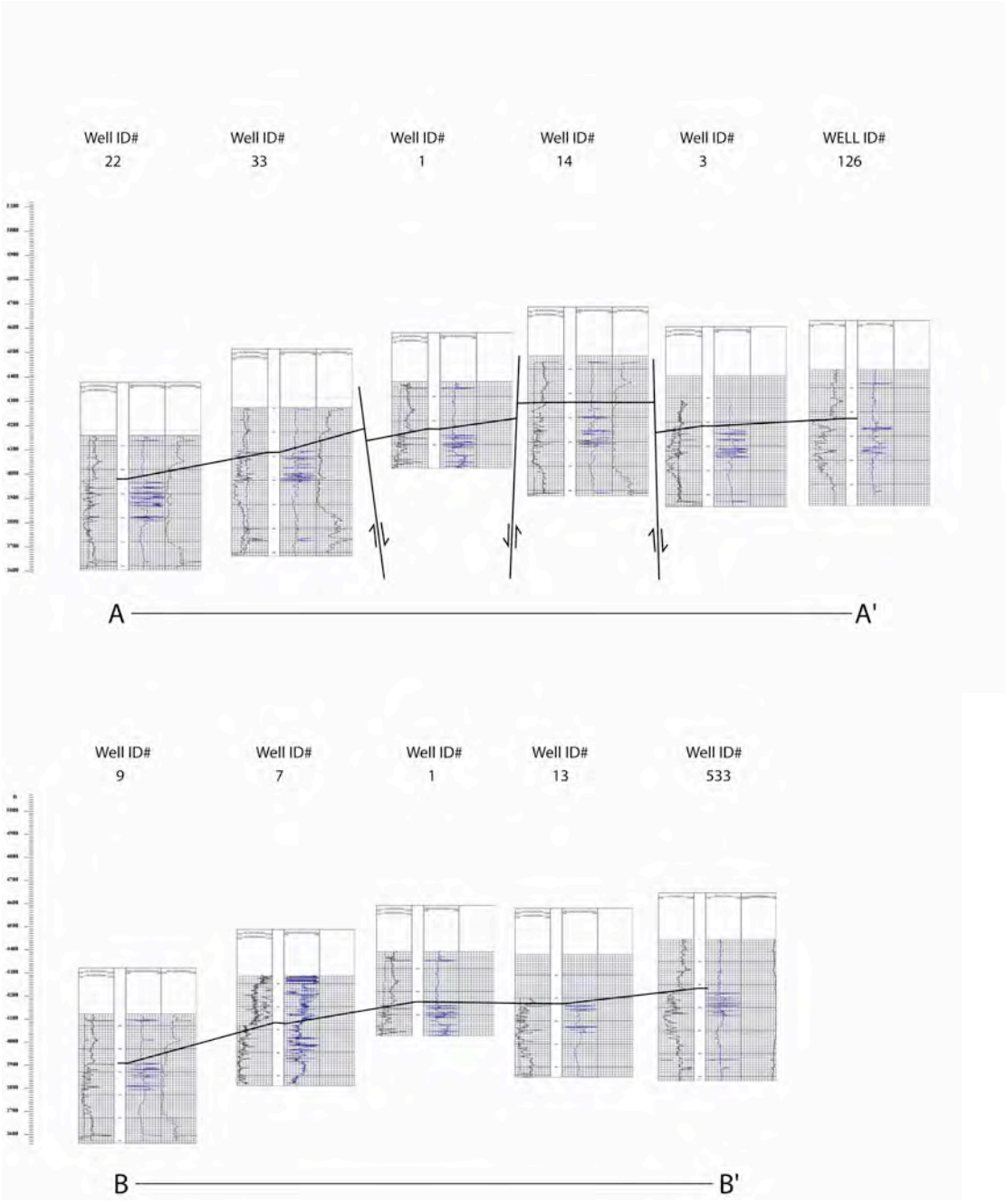

Fig. 3-6. Area B log cross sections. The log cross sections are structurally hung from the top of the Ferron Sandtone pick and correspond to the lines identified on figure 3-5. On the well logs, the gamma ray curve is in the left track, the bulk density curve (color blue) is in the center track, and conductivity is on the right track. Fault orientations as depicted on this cross section are interpretive, although we feel relatively confident of their location.

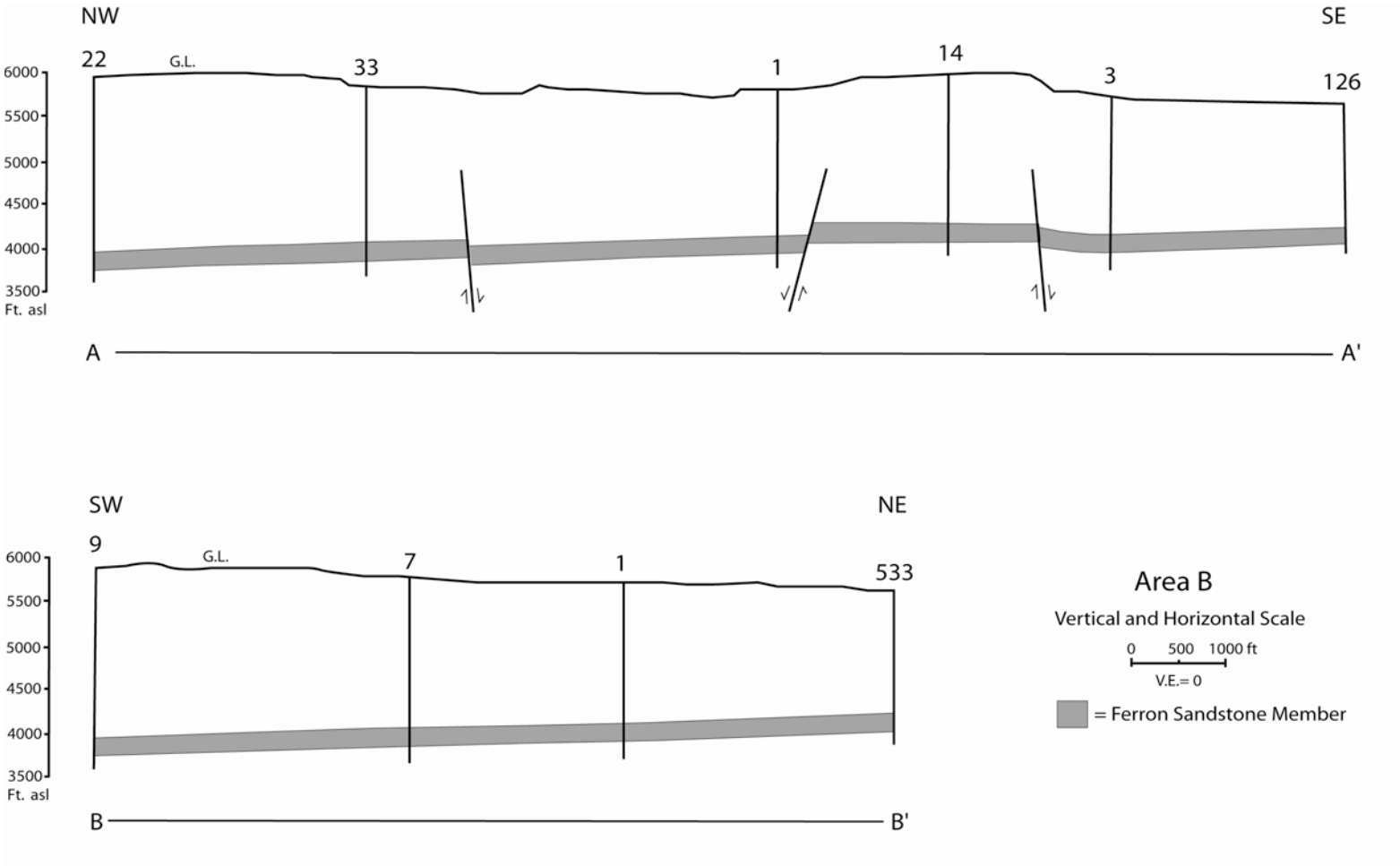

Fig 3-7. Area B cross sections. Cross section lines A-A’ and B-B’ contain no vertical exaggeration. Line A-A’ is placed perpendicular to fault trends, and line B-B’ is parallel to the fault trends.

perpendicular to each other through Area B. The cross sections display a section of the wireline log through the Ferron. The wells logs are structurally hung from the top of the Ferron Sandstone Member. To better visualize the magnitude of the faults apparent on the log cross sections (Fig. 3-6), we created cross sections with no vertical exaggeration through the same lines (Fig. 3-7). Faults in Area B are normal faults. A maximum throw of 150 ft is present as a result of the offset on both of the northern most faults. From the results of our outcrop studies (see Chapter 2 of this thesis), we suggest that face cleats in coal are often oriented parallel to the normal fault trend, and thus permeability may be enhanced in the direction of the fault trend.

Figure 3-8A and B shows that the average daily gas production in Area B ranges from 65 to 1705 MCFD (thousand cubic feet per day) (ConocoPhillips, pers. comm., 2003). Several wells with anomalously high production are present in the western portion of Area B. These wells are located outside the apparent fault-affected zone. High production in these wells could be a result of better completion techniques, or may be reflective of coal with better permeability or gas content. These highly productive wells are drilled in the structurally lowest portion of the Ferron in Area B. In the fault affected portion of Area B, two, vague northeast, high production trends can be seen (Figure. 3-8A and B). These trends are parallel to the normal faults mapped on our structure contour map. Both high production trends are located on up-thrown fault blocks.

Figures 3-9A and B are contour maps created from the average water production data.

A

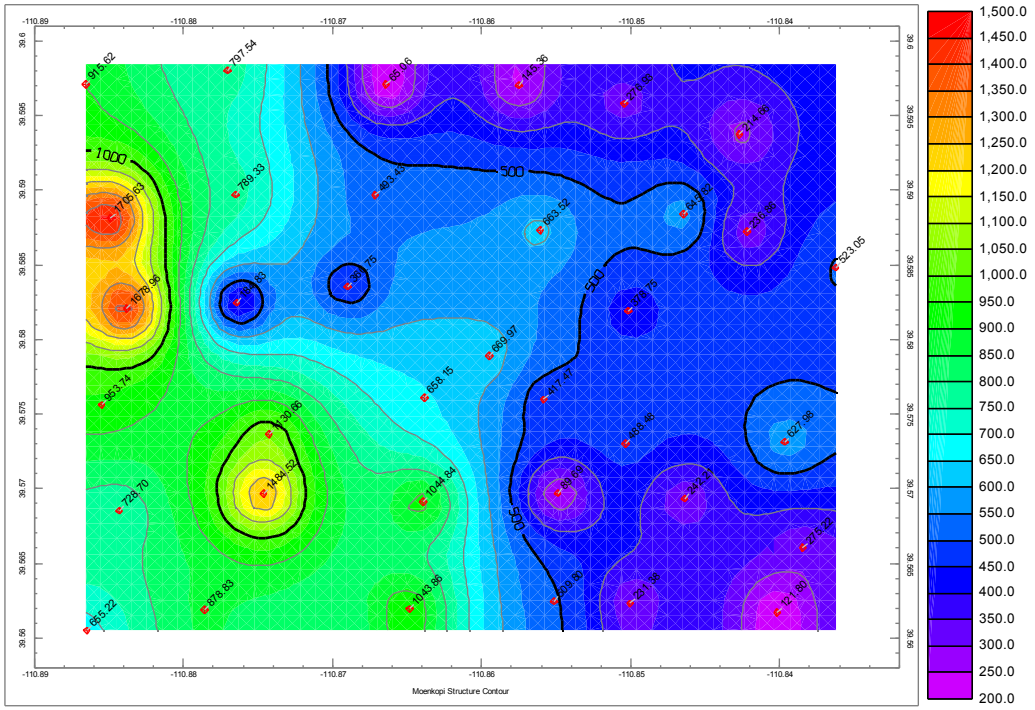

B

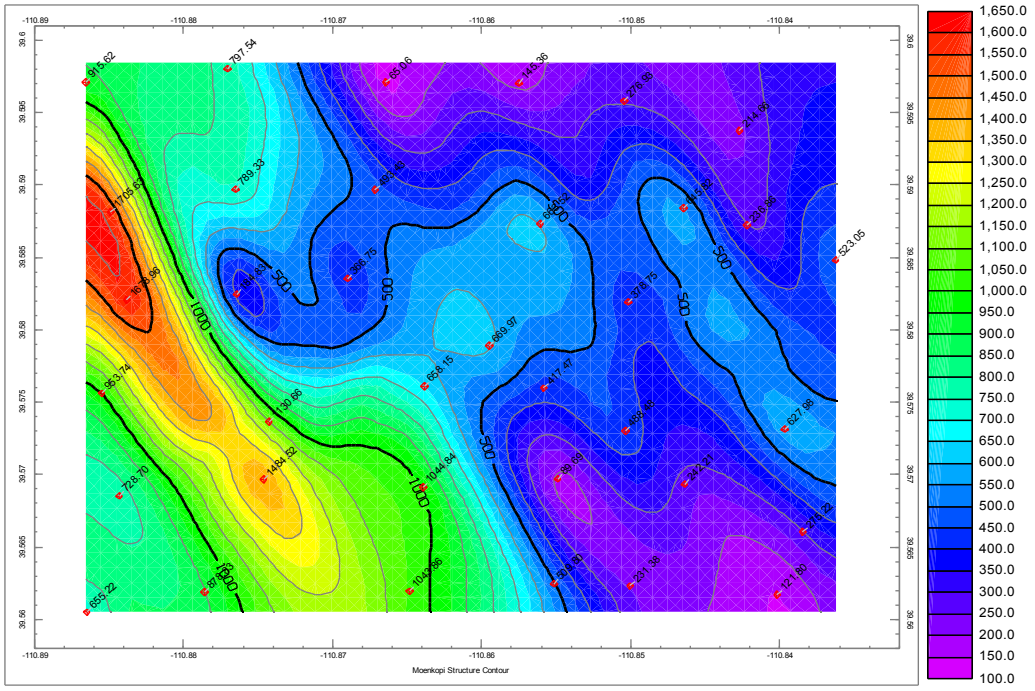

Fig. 3-8. Contour maps of gas production, Area B. (A) Inverse distance calculation. (B) Kriging calculation. In both of these contour maps there is a high production trend running northwest/southeast near the western edge of the area. Small scale northeast/southwest trends are apparent in the central region of Area B.

A

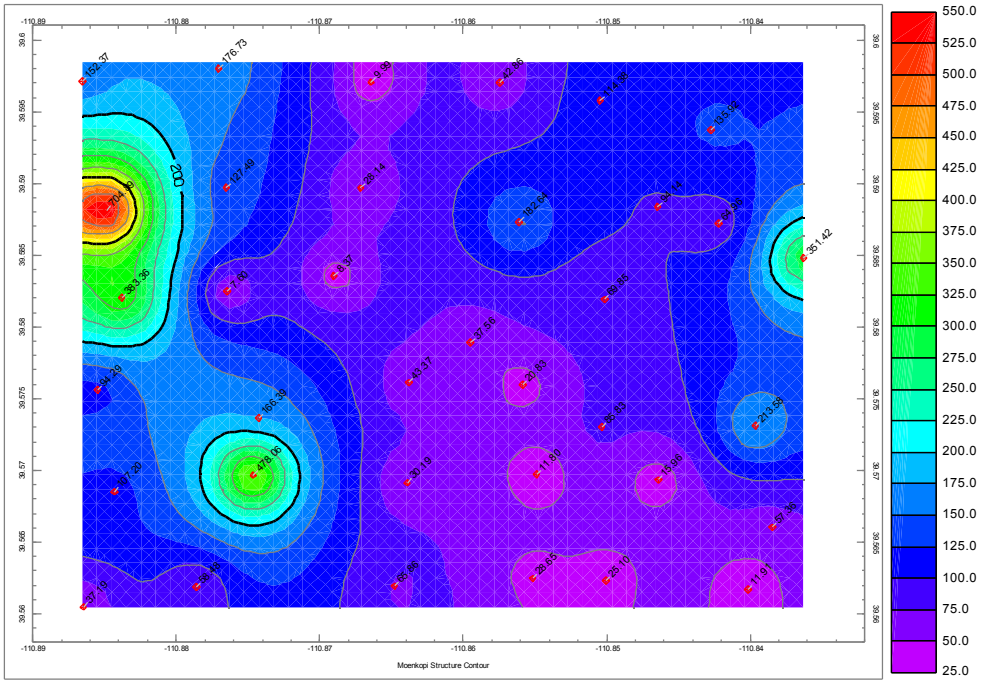

B

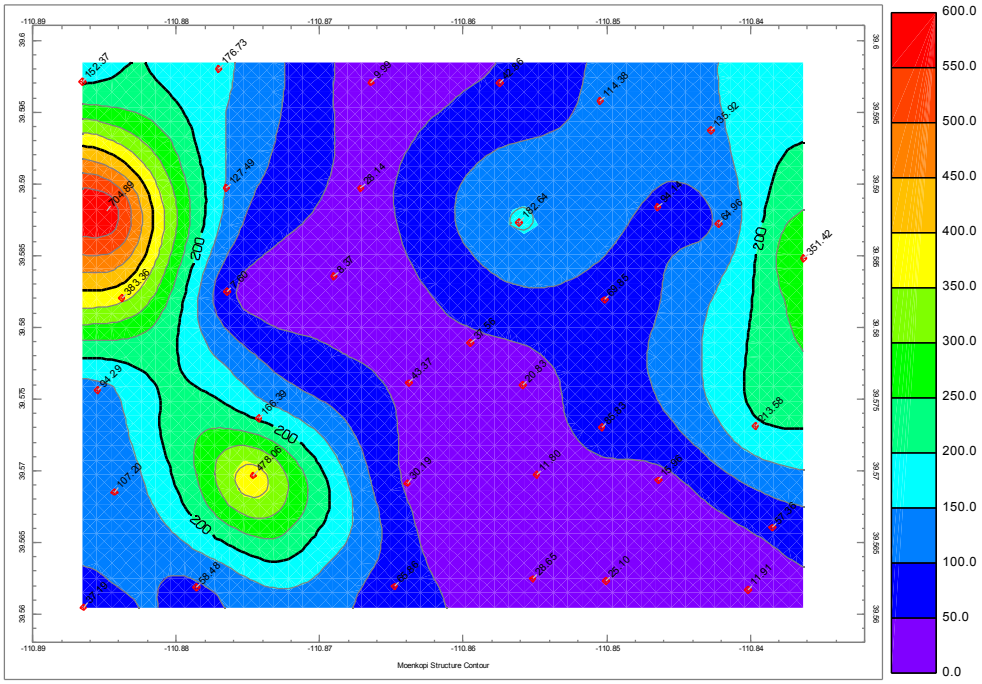

Fig. 3-9. Contour maps of water production; Area B. (A) Inverse distance calculation. (B) Kriging calculation. There is a high productivity northwest/southeast trend along the western edge of the area, similar to the gas production. A parallel low water production trend extends across the central portion of Area B.

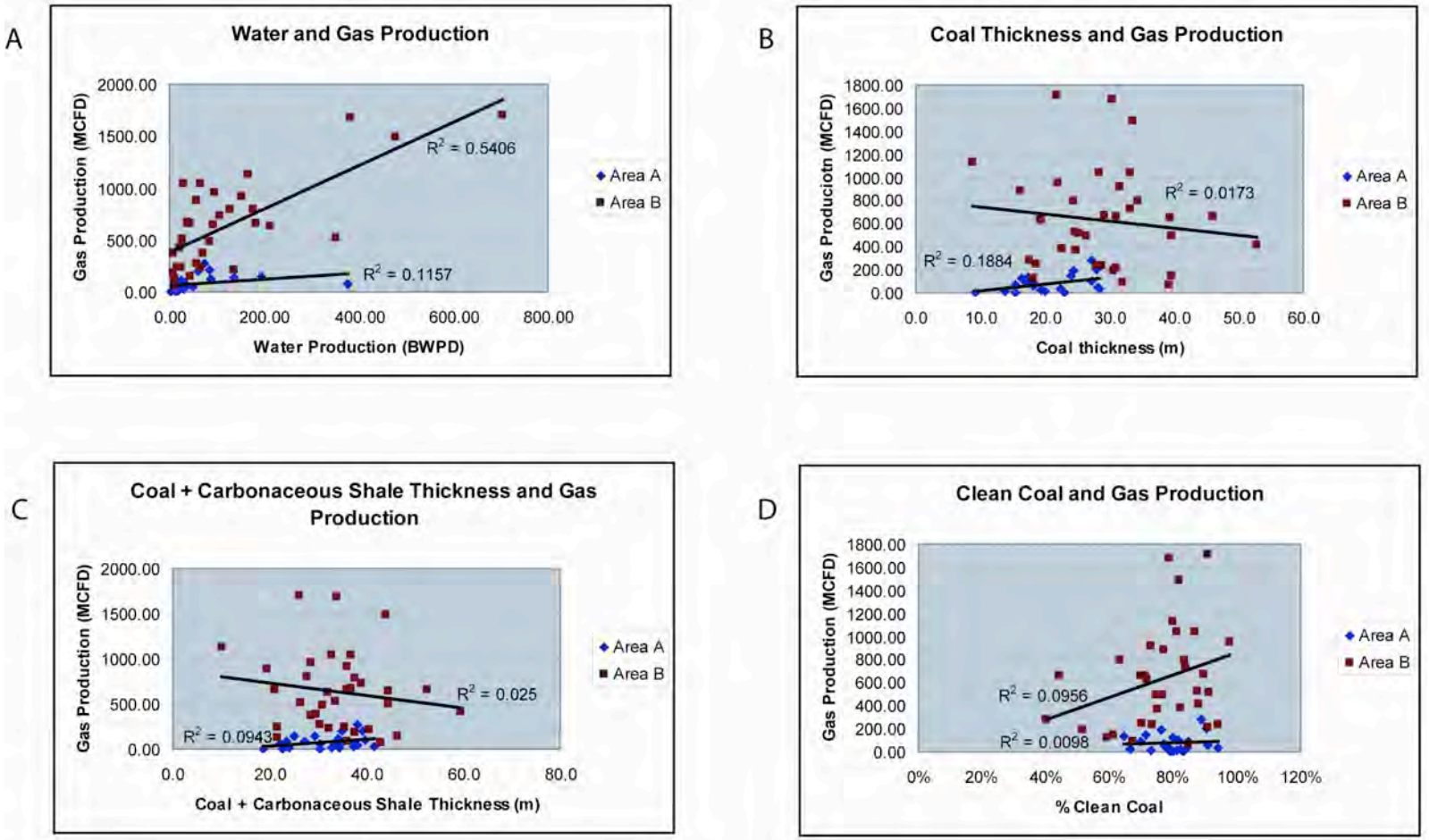

Fig. 3-10. Factors potentially effecting production. Water (A), coal thickness (B), coal plus carbonaceous shale thickness (C), and clean coal percentage (D) versus gas production for Area A and B are compared in graphs in the above figures. Water production and gas production in Area B share the only moderate correlation of the factors examined.

These maps closely resemble the gas production maps (Fig. 3-8A and B), as similar trends are apparent on both. In wells with high gas production, high water production is likely, as shown by the maps. Water and gas production have a R^2 correlation value of 0.54 (Fig. 3-10A). This correlation between water production and gas production has the highest correlation of the factors we tested.

In Area B, total coal thickness ranges between 8.8 and 52.8 feet (2.7-16.1 m) (ConocoPhillips, pers. comm., 2003). Contour maps of coal thickness indicate that it is the greatest in a north/south trend located in the upper two-thirds and central area of the maps (Fig. 3-11A and B). There is no obvious correlation between coal thickness and gas production upon first examination of these maps. Figure 3-10B verifies that there is no correlation between coal thickness and gas production, with a negative correlation of R^2=0.02.

Carbonaceous shale ranges in thickness from 1.1 to 13.0 feet (.36 to 4.0 m) in Area B (ConocoPhillips, pers. comm., 2003). Figures 3-12A and B are contour maps of the coal plus carbonaceous shale thickness. These maps are very similar to coal thickness maps, and again show no correlation to gas production (Fig. 3-10C).

The ConocoPhillips data set had coal lithology broken down into several coal types, with the respective lithotype thickness listed for each well. ConocoPhillips geologists suggested that there may be a correlation between the percent “clean coal” and gas production. We used their lithotype classification to create contour maps of the percent clean coal (Fig. 3-13A and B). “Clean coal” comprises between 67.2 and 94.1% of the coal stratigraphy in Area B (ConocoPhillips, pers. comm., 2003). The contour

A

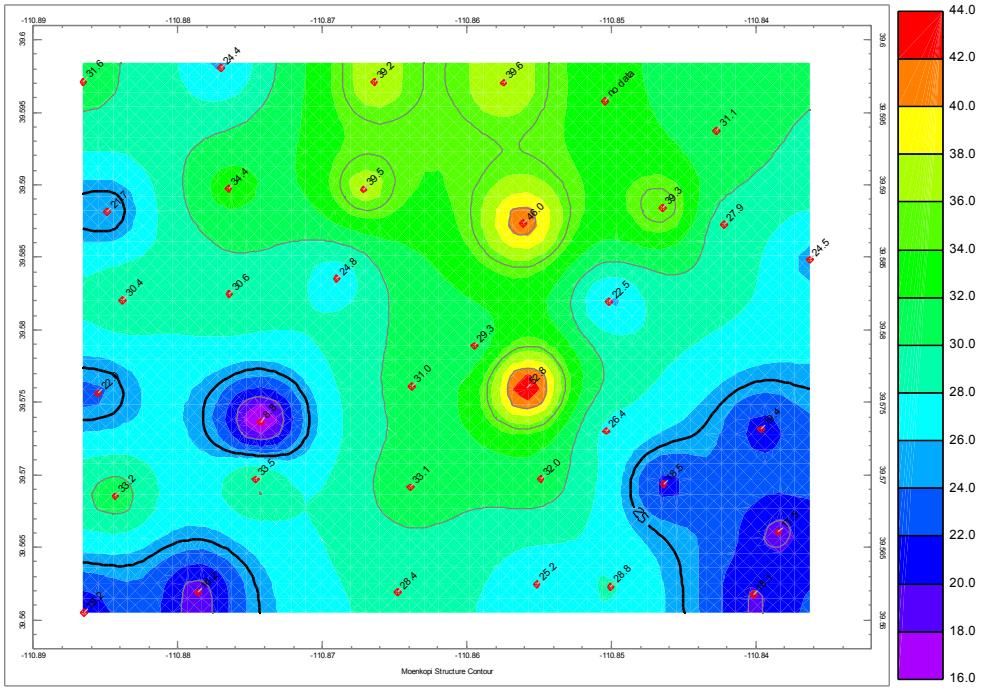

B

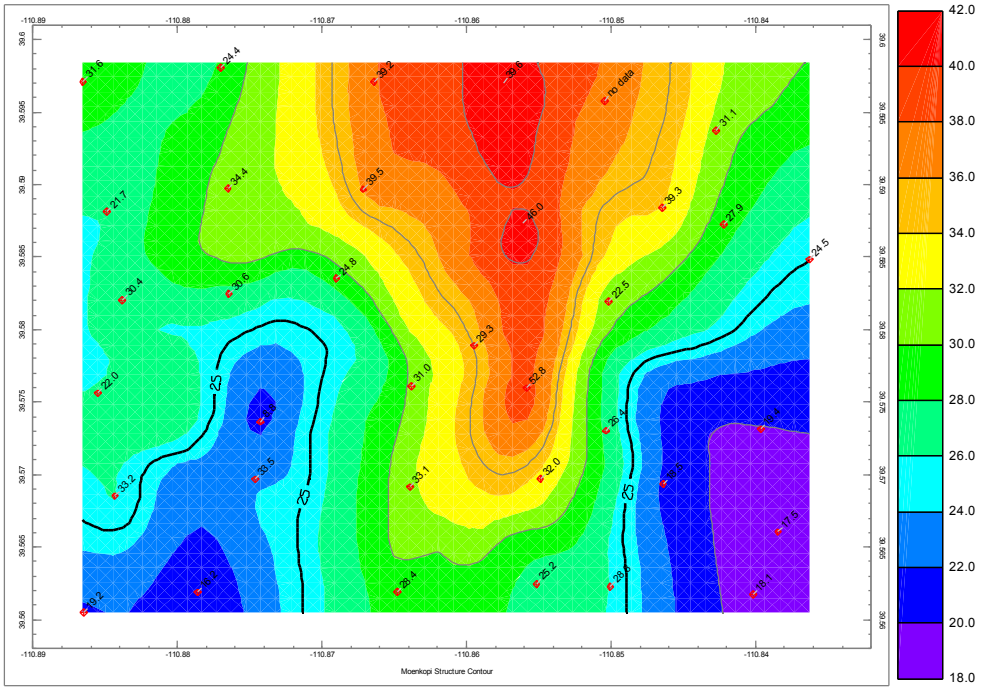

Fig. 3-11. Area B coal thickness. (A) Inverse distance calculation. (B) Kriging calculation. Coal thickness is greatest in a north/south trending belt located in the upper two-thirds and central portions of Area B.

A

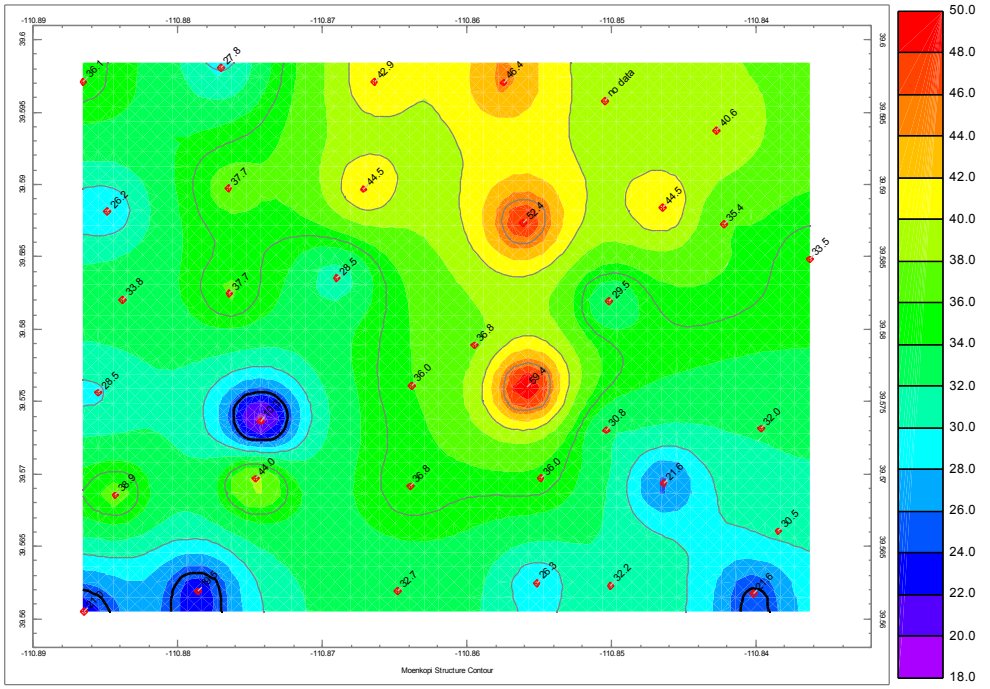

B

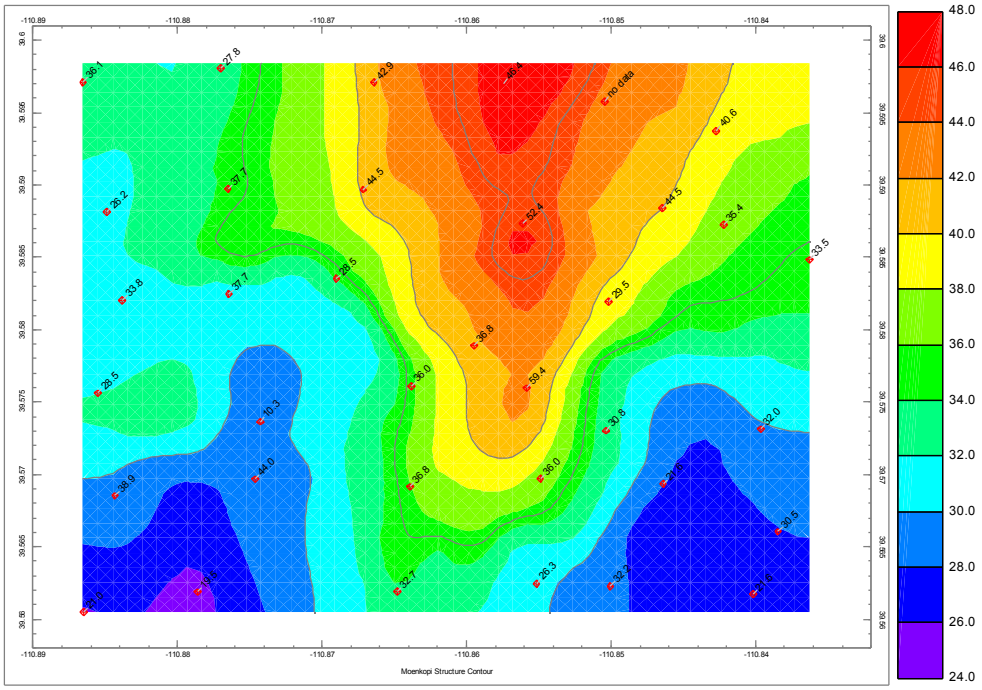

Fig. 3-12. Area B coal plus carbonaceous shale thickness. (A) Inverse distance calculation. (B) Kriging calculation. These contour maps look very similar to coal thickness maps. The thickest section of carbonaceous shale plus coal is located in the north-central portion of Area B.

A

B

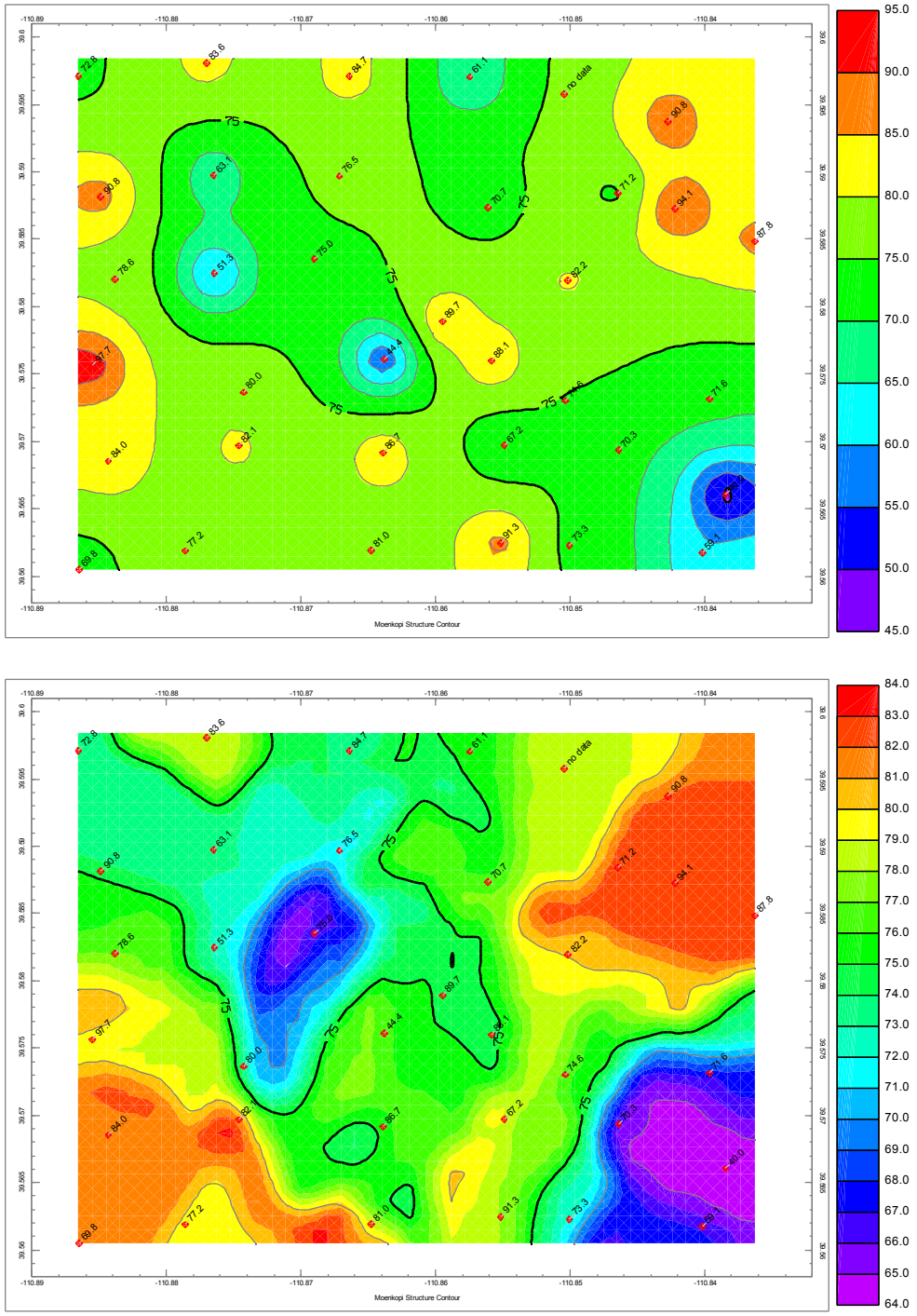

Fig. 3-13. Area B percent clean coal. (A) Inverse distance. (B) Kriging calculation. These maps show that areas in the northeast and southwest portions of Area B contain the highest percentage of clean coal.

maps indicate that the highest percentages of clean coal occur in the southwest and northeast portions of Area B. For this area, there is no graphical correlation between gas production and percent clean coal, as the R^2 value is only 0.096 (Fig. 3-10D).

Area A

We created log cross sections (Fig. 3-14) and 1:1 cross sections (Fig.3-15) in order to aid in our interpretation and creation of the structure contour map for Area A (Fig. 3-5A). There is no well control present in the northeast section of Area A. As a result of this, fault placement, lengths, and structural elevations are interpretive. We have mapped two major faults in Area A (Fig. 3-5A). The northern most fault has offset Ferron Sandstone stratigraphy by 220 ft. The southernmost fault has offsets up to 600 ft. This offset is 4 times greater than the largest fault offset in Area B. Structure contour maps indicate that the Ferron Sandstone Member of the Mancos Shale in Area A strikes roughly west/southwest and dips north/northwest 5º or less, although some variations occur as a result of fault related folding. The Ferron ranges in elevation from 2,987 to 3,745 feet (910 to1,142 m) asl, with the highest elevations being located in the south/southeast portions of the area. Ferron depths below ground surface range from 1,986 to 3,020 feet (605 to 921 m).

We contoured the gas production ratio using directional weighting and kriging contouring calculations techniques (Fig. 3-16A and B). The average production in Area A is only equal to 12% of the average production in Area B. In Area A the gas production ratio ranges from 2.85 to 277.4 MCFD (ConocoPhillips, pers. comm., 2003).

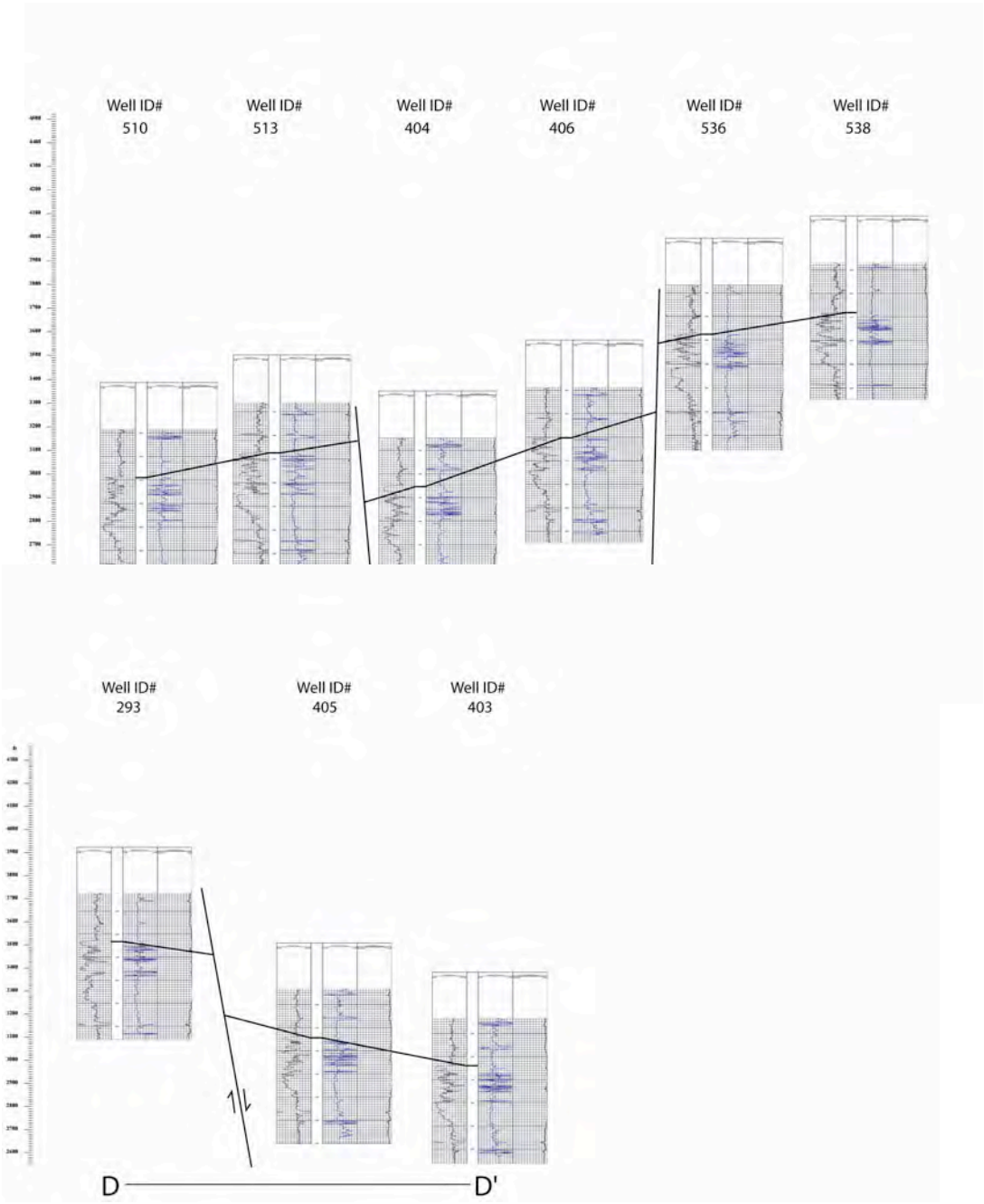

Fig. 3-14. Log cross sections; Area A. These cross sections are structurally hung from the top of the Ferron Sandstone. The location of line C-C' and D-D' are shown on figure 3-5A. Two faults with relatively large amounts offset are present in Area A.

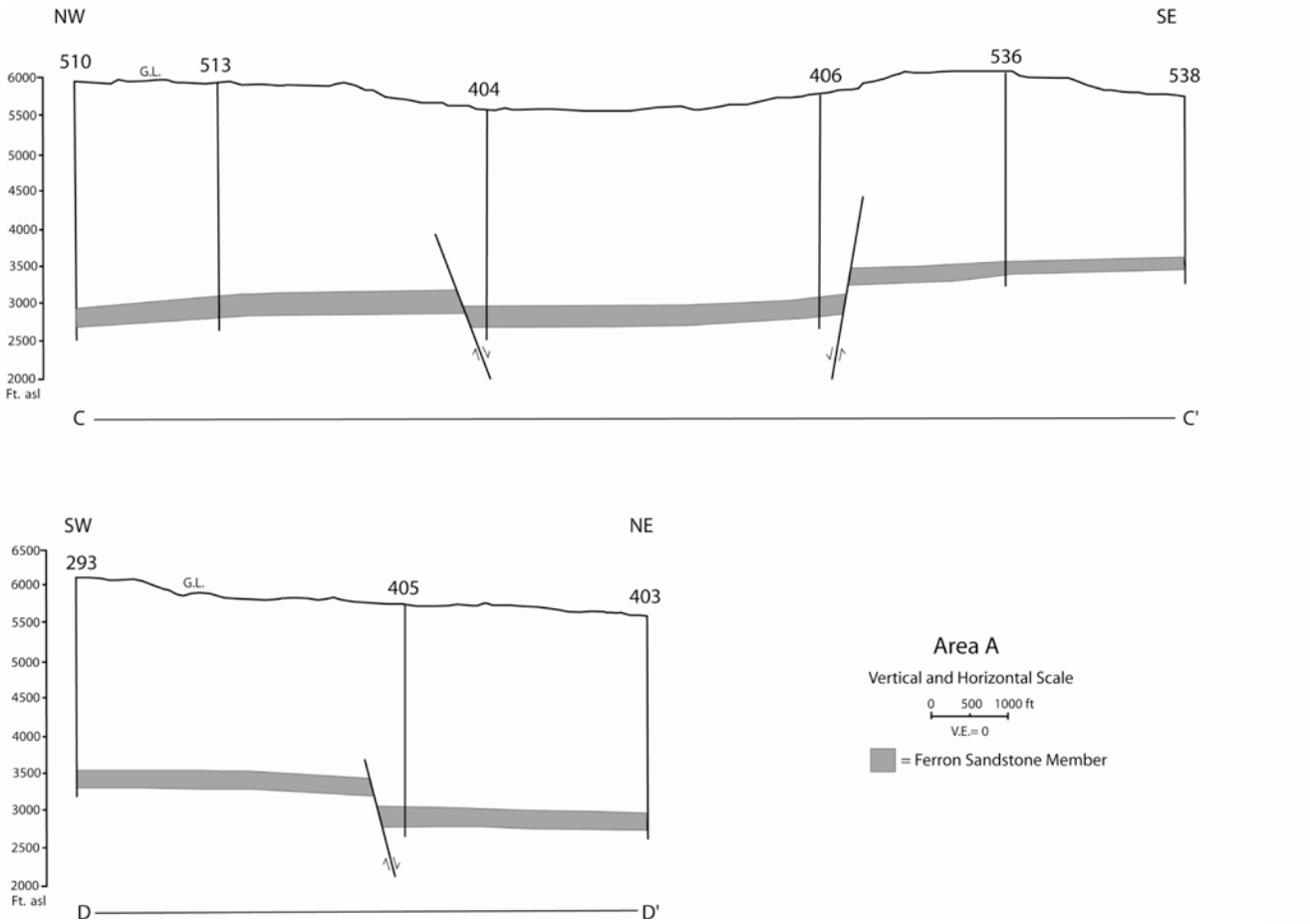

Fig. 3-15. Area A cross sections. Cross sections C-C' and D-D' run near perpendicular to each other in Area A (Fig. 3-5A). Two faults are present in Area A, creating lateral juxtaposition of the Ferron Sandstone Member coals. No vertical exaggeration is present in the cross sections.

A

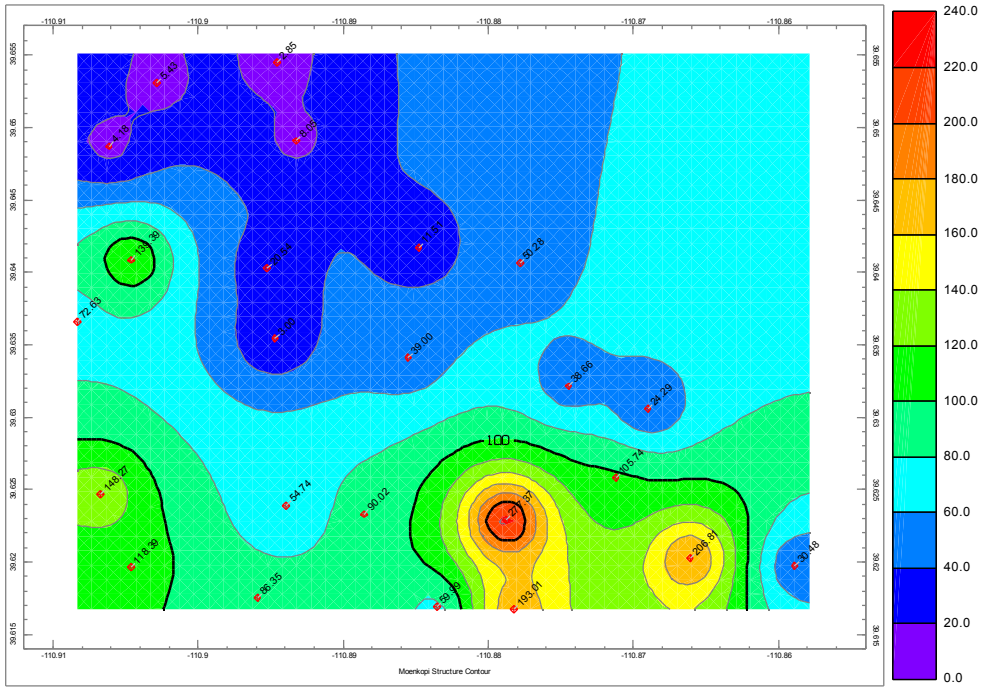

B

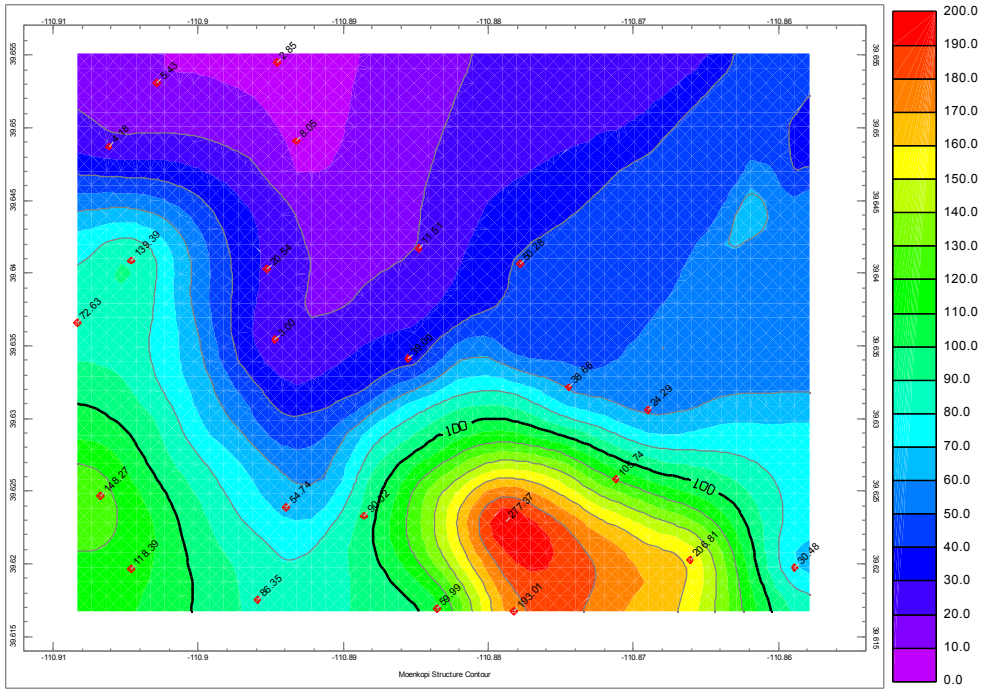

Fig. 3-16. Contour maps of gas production, Area A. (A) Inverse distance calculation. (B) Kriging calculation. Gas production is the highest in the southern portion. A north/south low production trend is present in the central, upper two-thirds of Area A.

A

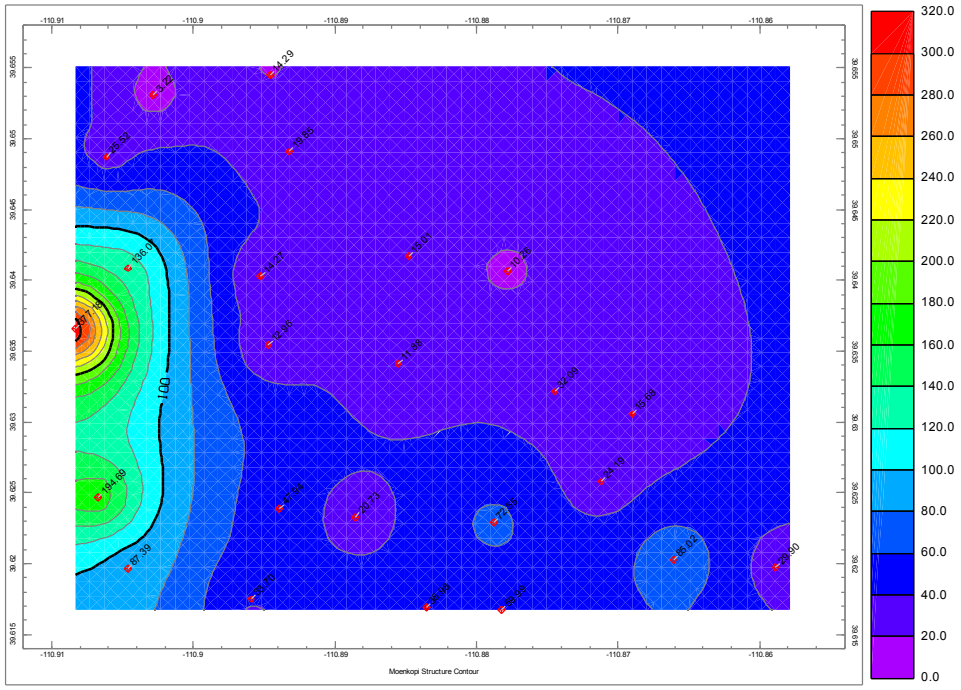

B

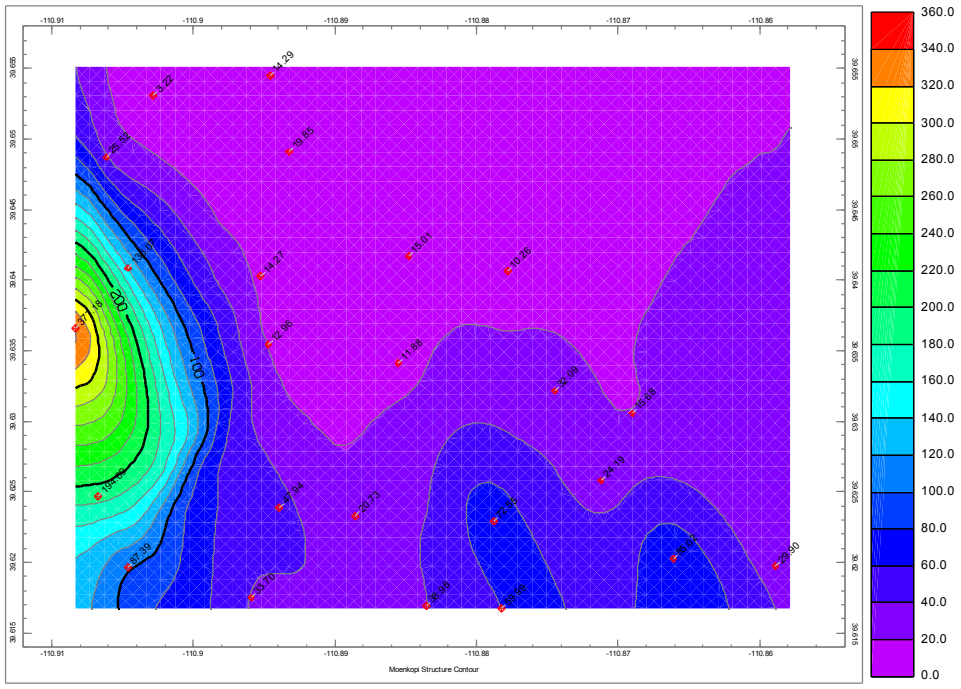

Fig. 3-17. Contour maps of water production, Area A. (A) Inverse distance calculation. (B) Kriging calculation. Two high water producing wells on the western edge of Area A create an apparent high water production trend. This may actual reflect a higher permeability zone, or may be a result of differences in well design.

This range is clearly lower than the ratio between 65 to 1,705 MCFD as found in Area B. A north-trending low production region is apparent on both contour maps for Area A.

In Area A, water production in wells 301, 294, and 408 is significantly higher than the remainder of the wells in Area A. This creates a northwest high water production trend in the west/central portion of our contour maps (Fig. 3-17A and B). All three of these high water producers are located near the fault tip. This may be a result of open coal cleats resulting from increased local tension near the fault tips, or may be created by variations in coal type or reservoir characteristics created during coal deposition. The remainder of the wells in Area A have relatively low water production. The median water production in Area A is 29.90 BWPD; this is low compared to the median in Area B of 64.96 BWPD. Although water production and gas production contour maps share some similar characteristics, only a weak graphical correlation is present, as indicated by a R^2 value of only 0.12 (Fig. 3-10A).

In Area A, total coal thickness ranges between 9.2 and 28.3 feet (2.8 and 8.6 m) (ConocoPhillips, pers. comm., 2003). The median coal thickness in Area A is 16.5 ft. This is low compared to the median coal thickness of 20.5 feet in Area B. Thickness data plotted on Figure 3-18A and B show coal is thickest in the southeast section of Area A, and thinnest in the northwest. The relationship between gas production and coal thickness is plotted on Figure 3-10B. Of the factors we tested for affecting production in Area A, coal thickness has the highest correlation to gas production although the correlation is very weak and the R^2 value is only 0.19.

A

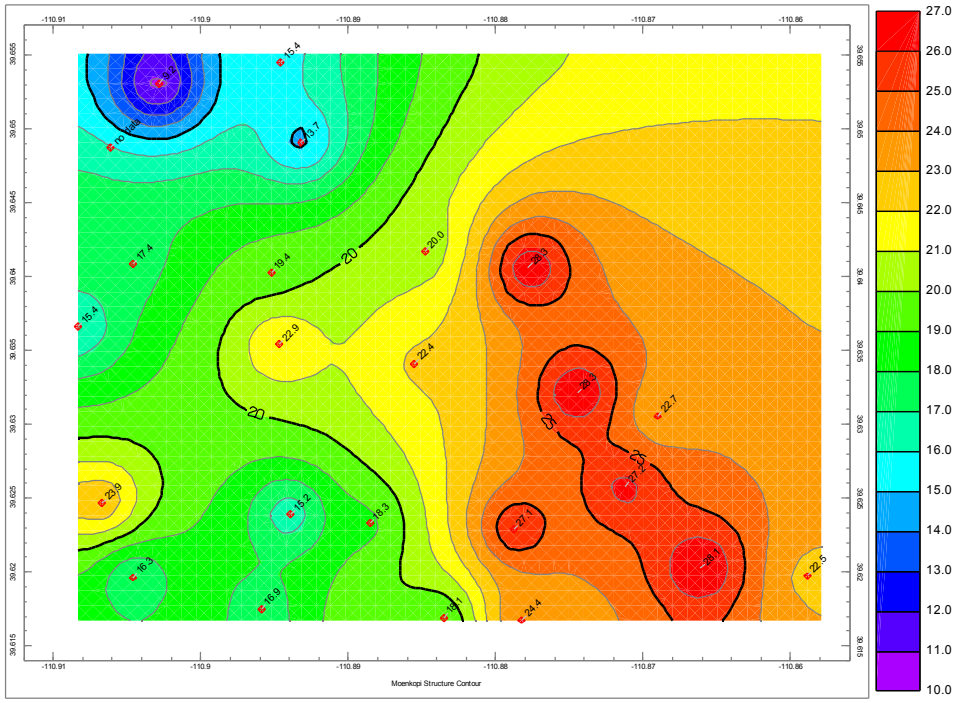

B

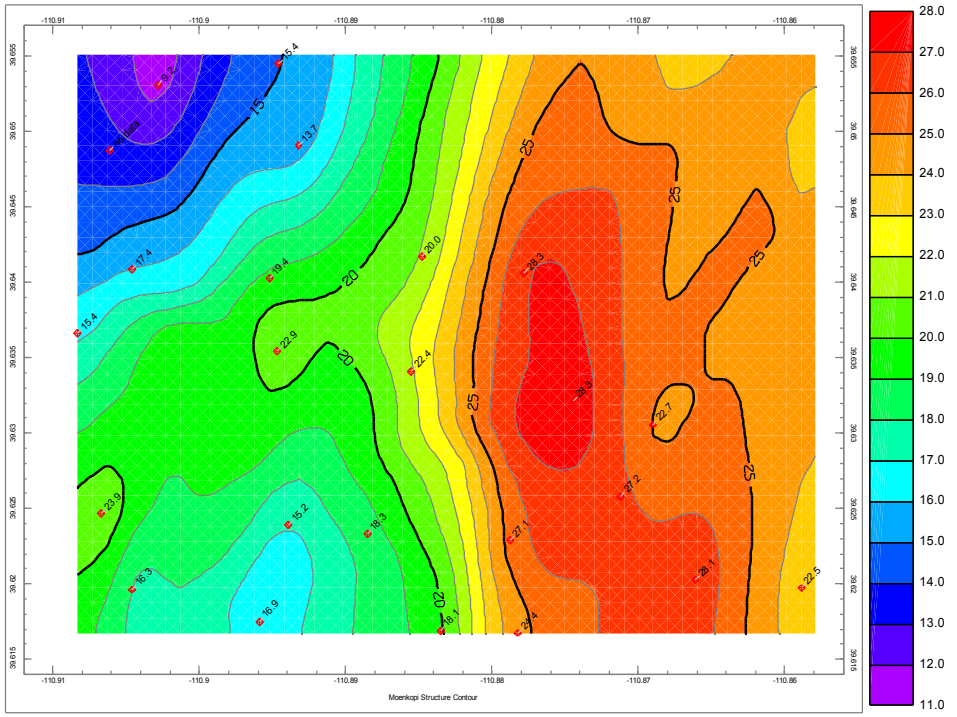

Fig. 3-18. Area A coal thickness. (A) Inverse distance calculation. (B) Kriging calculation. Coal is thickest in the southeast portion of Area A, and thinnest in the northwest.

A

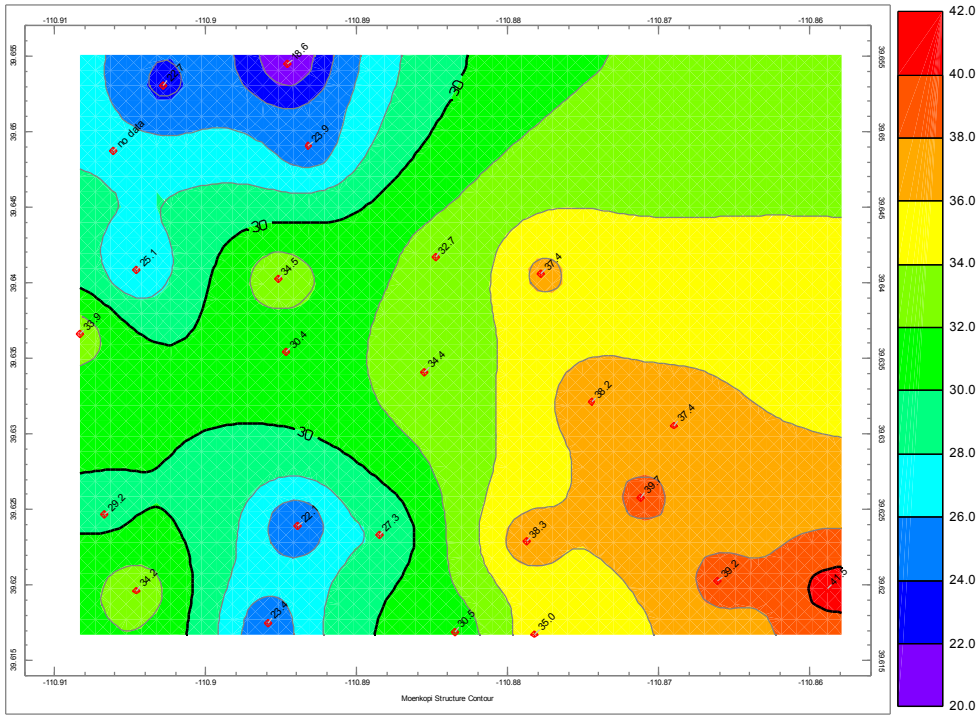

B

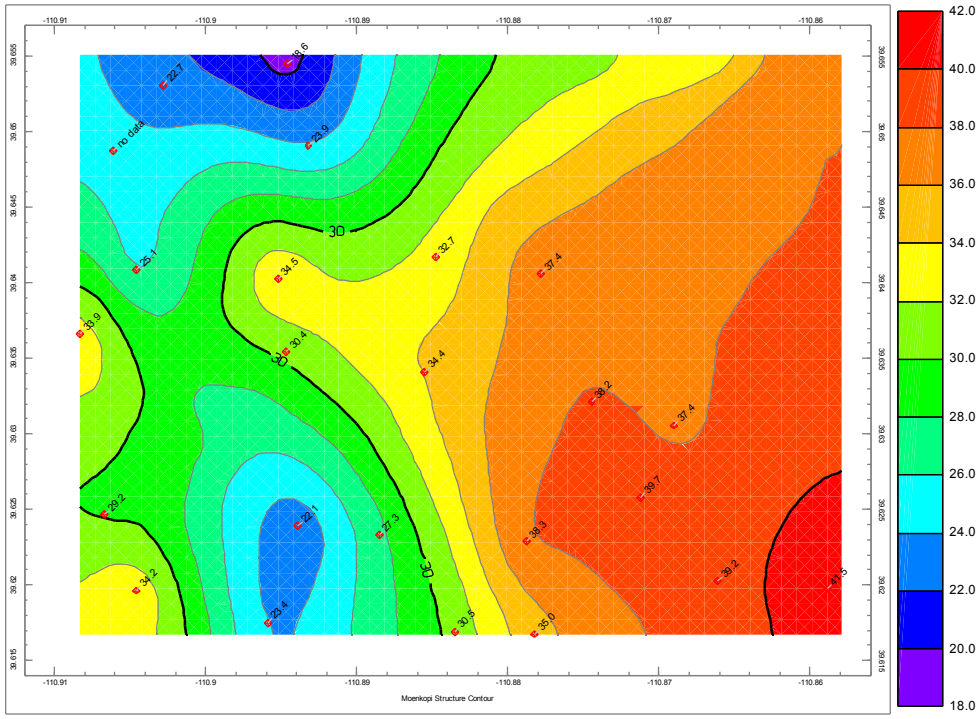

Fig. 3-19. Coal plus carbonaceous shale thickness. (A) Inverse distance calculation. (B) Kriging calculation. Similar to coal thickness maps, coal plus carbonaceous shale reaches maximum thickness in the southeast portion of Area A and is thinnest in the northwest.

A

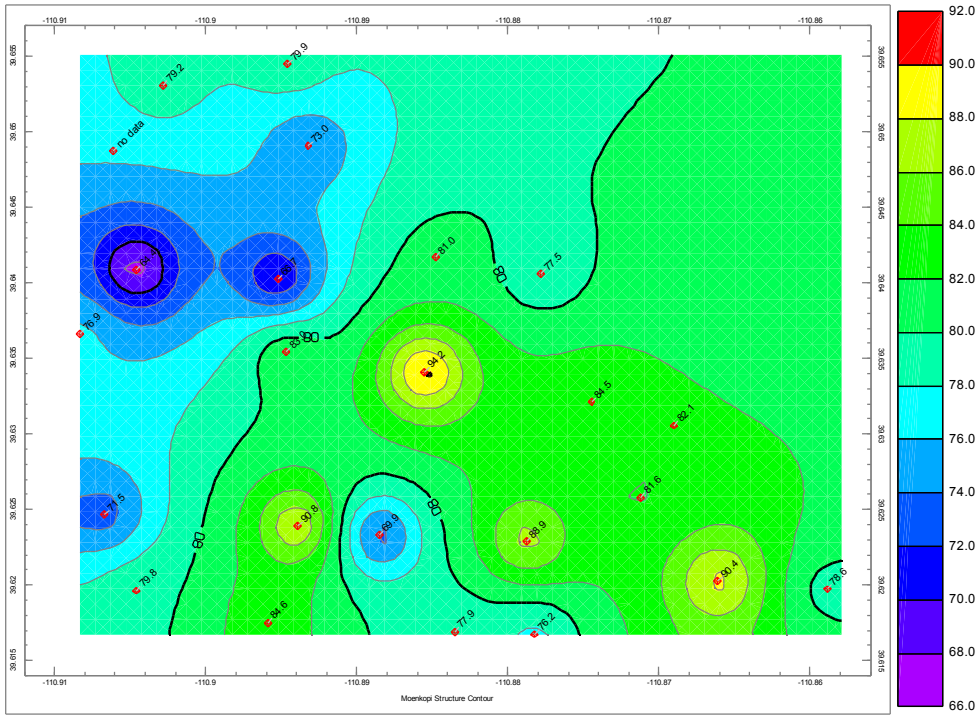

B

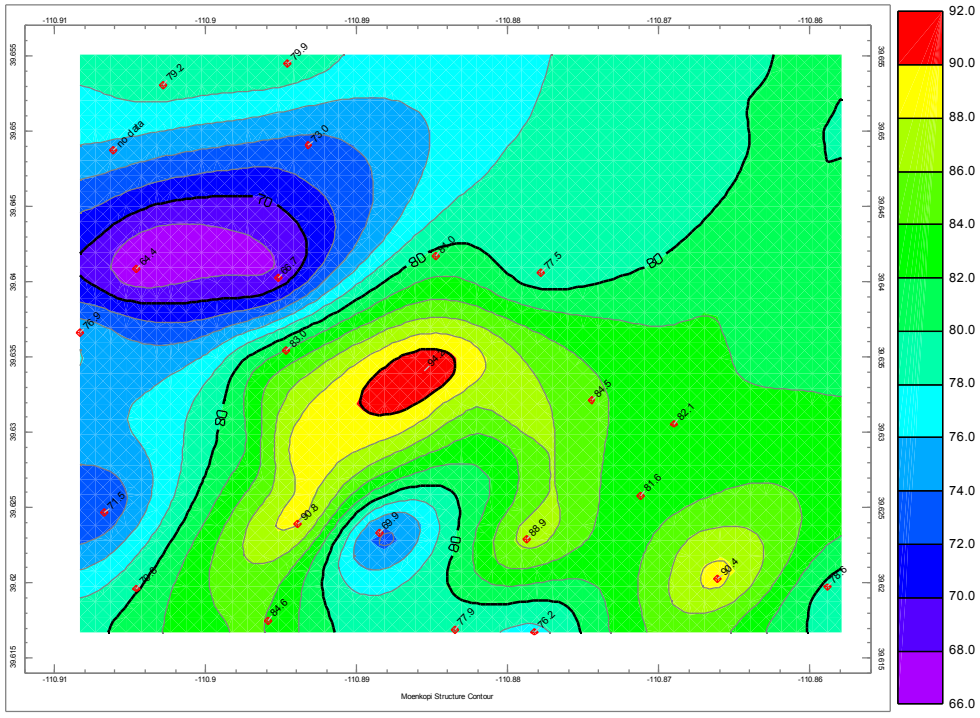

Fig. 3-20. Area A percent clean coal. (A) Inverse distance calculation. (B) Kriging calculation. The cleanest coal is found in the southern portions of Area A, and the least clean coal is present in the west and northwest sections of the area.

We mapped coal plus carbonaceous shale thickness using two techniques in order to examine whether gas production from carb-shales was affecting the overall production trends (Fig. 3-19A and B). Like Area B, the contour maps of coal plus carbonaceous shale are very similar to the coal thickness maps. To graphically display any possible correlation we plotted the gas production as a function of the coal plus carbonaceous shale thickness (Fig. 3-10C). The R^2 value of 0.09 suggests that carbonaceous shale thickness is not as important as coal thickness to overall gas production.

The correlation between percent clean coal and gas production is the lowest of any of the factors analyzed for Area A. A graphical correlation value of only 0.01 can be seen for these two variables on Figure 3-10D. Both contour mapping techniques produce maps that indicate the cleanest coal is found in the southern portions of Area A, and the least clean coal is present in the west and northwest sections of the area (Fig. 3-20A and B).

Interpretations

Area B

In the analyses of the two areas within the Drunkards Wash gas field we examined geologic and production data to determine why Area B is a more prolific producing area that Area A. We found no correlations to gas production among any of the variables examined other than water production in Area B (Fig. 3-10A). Because water and gas production rates are typically reflective of reservoir permeability, we infer

that favorable coal cleat characteristics has developed in Area B as a result of faulting in the area.

In Chapter 2 we showed that fracture density is a function of coal composition (both ash content and maceral composition) and structural position. Where normal faults cut coal stratigraphy, cleat density increases in a damage zone adjacent to the fault. In this vicinity cleat density and cleat height is increased in a fault parallel direction. Perpendicular to the fault, several changes may occur as a function of fault influence. If the throw of the fault does not exceed the coal seam thickness, reservoir connectivity across the fault trace can be maintained. In Area B, where a series a faults offset Ferron stratigraphy by up to 120 feet (37 m), the thin Ferron coal seams are laterally juxtaposed against the adjacent sedimentary rocks. In these locations, gas production perpendicular to the fault strike is limited to the width of the fault block. Upon first thought one expect production to be low as a result of this; however, Area B has good production. High production in Area B may be caused by an increase in permeability parallel to the fault which compensates for production that would have been contributed from direction perpendicular to the fault. Excluding the anomalously high trend in the western portion of the gas production contour map, gas production trends, apparent on figure 3-8 parallel fault trends and support our interpretation that cleat characteristics has been beneficially enhanced near the faults.

Area A

Production in Area A is low relative to production in Area B. The factors examined in our analysis show no strong graphical correlation with gas production (Fig.

3-10A-D), although some common trends are apparent when the factors are mapped. Structure contour maps provided by ConocoPhillips indicate that several faults may be present in Area A. We found that faults are present where ConocoPhillips had indicated, but we have interpreted the fault to be longer, and affecting more Ferron stratigraphy. The larger magnitude of the faults in Area A in conjunction with thin coal beds, create conditions favorable for "joint breakthrough" (see Chapter 2 of this thesis). Due to the magnitude of the faults, a high density of regional fractures and joints are likely present in the stratigraphy adjacent to the Ferron coal. If a larger number of joints breakthrough the Ferron coal in this vicinity, then a conduit for gas migration is present, and coal degasification may be an issue. The likely occurrence of this concept can be seen by comparing the gas production map figure 3-8 and the structure contour map of Area A figure 3-5A. Gas production up-dip of the fault affected zone is significantly better than gas production down-dip. Gas migration conduits formed within the fault damaged zones may have instigated gas migration from the coal, into adjacent formations, from near the fault, and down dip to the fault. This would explain the low gas production trend found in the northern half of Area A.

In the Upper Ferron Sandstone outcrops south of Drunkards Wash, we observed numerous depositional complexities within the Ferron Sandstone Member that could affect coalbed reservoir characteristics. From the wireline logs for Area A and B (can be seen on figures 3-6 and 3-14), it is clear that individual sand and coal sequences do not always correlate to the stratigraphic intervals in adjacent wells. Stratigraphic variances as seen on the well logs are a result of the nature of fluvial deltaic depositional

environments. These variances could create reservoir compartmentalization, changes in coal characteristics, and may explain the presence of some gas production trends in Area A and B found outside the areas that are affected by faulting.

Discussion

Structural control appears to be the primary influence on gas production trends in Area A and B. Faulting has beneficially affected the overall production rates in Area B of the Drunkards Wash field by increasing cleat density and height parallel to the fault trends. Faults in Area A may have detrimentally affected the CBM reservoir. These faults with larger offsets likely have larger associated fracture damaged zones. Reservoir structure and gas production analysis indicate that reservoir degasification is a likely possibility. Furthermore, fracture stimulation, performed during well completion would not be as effective in thin coal beds present in Area A, especially if the induced fracture medium is intercepted by cross cutting joints.

Our analysis indicates that the total coal and carbonaceous shale thickness, and clean coal percentage as tested do not strongly affect gas production trends in Area A or B. From our field research we found that ash layers in clarain-rich coal creates bounding units which confine mechanical and ultimately controls cleat density. To an extent, where a high frequency of ash layers are present, cleat density increases; hence, overall reservoir permeability is increased. In vitrain-rich coals, ash content is a less critical fundamental control on cleat density. Vitrain-rich coals contain a high density of cleats even without a high frequency of ash layers. Since cleat characteristics change with coal

type, clean coal percentages and thickness as determined from analysis of well logs do not provide a predictive tool for estimating gas production trends. A more effective technique would be to determine coal thickness and ash content within each coal lithotype encountered in a well, in order to estimate cleat density and predict high permeability trends within the field. Estimating thickness of coal lithotypes encountered in a well could be performed by well core examination, image logs, or roughly by careful mudlog reporting at the well site.

Conclusions

From outcrop examination of Ferron coals south of the Drunkards Wash field, Utah, we have identified several factors within coal stratigraphy that could either be beneficial or detrimental to gas production in a CBM reservoir. A combination of several factors that decrease reservoir production may be present in Area A. We have suggested that fault induced damaged zones has resulted in reservoir degasification within the thin coals in Area A; however we acknowledge that additional coal type and stratigraphic complexities may be present in this vicinity. Further interpretations regarding the production issues in portions of Drunkards Wash could be made with more data. The availability of high resolution down-hole logs, image logs, mudlogs, magnetic resonance logs or core with coal sections in tact would provide additional information from which a better understanding of coal type, and fracture characteristics could be established.

By examining CBM reservoir analogs, we have gained of valuable understanding of the factors that affect coal bed permeability. Using our knowledge of these factors in conjunction which industry field data from Drunkards Wash, we were able to make

several interpretations concerning production issues in this field. Continued research and application of coal characteristics used in this report, can be used beyond the scope of this study to efficiently explore for, and produce natural gas from all CBM reservoirs.

References

Anderson, P.B., D. Tabet, and G. Hampton, 2003, Coalbed gas deposits of central Utah: AAPG Field Trip #18 Guide, Rocky Mountain Section AAPG.

Anderson, P.B., T.C. Chidsey, Jr., and T.A. Ryer, 1997, Fluvial deltaic sedimentation and stratigraphy of the Ferron Sandstone: Brigham Young University Geology Studies, v. 42, part II, p. 135-154.

Ayers, W.B, Jr., 2002, Coalbed gas systems, resources, and production and a review of contrasting cases from the San Juan and Powder River basins: American Association of Petroleum Geologists Bulletin, v. 86, p. 1853-1890.

Burns, T.D., and R.A. Lamarre, 1997, Drunkards Wash Project: Coalbed methane production from Ferron coals in east-central Utah: Proceedings of the International Coalbed Methane Symposium, University of Alabama, Tuscaloosa, paper 9707, p. 507-520.

Energy Information Administration, 2004, U.S. Crude Oil, Natural Gas Liquid Reserves 2002 annual report. Appendix B. http://www.eia.doe.gov/pub/oil_gas/data/publications/crude.

Gardner, M.H., 1992, Sequence stratigraphy of the Ferron Sandstone, east-central Utah, *in* N. Tyler, M.D. Barton, and R.S Fisher, eds., Architecture and permeability structure of fluvial-deltaic sandstones, east-central Utah: The University of Texas at Austin, Bureau of Economic Geology Guidebook, p. 1-12.

Garrison, J.R., Jr., T.C.V. Van Den Bergh, C. Barker, and D.E. Tabet, 1997, Depositional sequence stratigraphy and architecture of the Cretaceous Ferron Sandstone: Implication for coalbed methane resources-A field excursion: Brigham Young University Geology Studies, v. 42, part II, p. 155-200.

Lamarre, R.A., and T.D. Burns, 1996, Drunkards Wash unit: Coalbed methane production from Ferron coals in east-central Utah: 1996 American Association of Petroleum Geologists, Rocky Mountain Section Meeting-Billings, Montana: American Association of Petroleum Geologists Bulletin v. 80.

Lamarre, R.A., 2001, The Ferron Play: A giant coalbed methane field in east-central Utah: IPAMS Coalbed Methane Symposium, October 16, 2001.

Montgomery, S.L., D.E. Tabet, and C.E. Barker, 2001, Upper Cretaceous Ferron Sandstone: Major coalbed methane play in central Utah: American Association of Petroleum Geologists Bulletin, v. 85, p. 199-219.

Narango, J.C., and D.E. Tabet, Analysis of production and reservoir characteristics from the Drunkards Wash gas field; Utah. Identification of parameters favoring high performing wells. Web site poster. http://www.ugs.state.ut.us/coalbed_gas/pdf/-drunkards_was1.pdf.

Ryer, T.A., 1981, Deltaic coals of the Ferron Sandstone Member of the Mancos Shale: Predictive model for Cretaceous coal-bearing strata of the western interior: American Association of Petroleum Geologists Bulletin, v. 65, p. 2323-2340.

Scott, A. R., 1993, Composition and origin of coalbed gases from selected basins in the United States, *in* D.A. Thompson, ed., Proceedings from the 1993 International Coalbed Methane Symposium, Birmingham, Alabama, v. 1, paper 9370, p. 207-222.

Utah Division of Oil, Gas and Mining, 2004, Gas field statistics. http://ogm.utah.gov/oilgas/STATISTICS/1prod.htm

CHAPTER 4

CONCLUSIONS

The objectives of this project were to identify factors that affect coal cleating and coalbed reservoir permeability, and to determine how these factors affect methane production. Through detailed surveys at outcrops that serve as reservoir analogs and examination of well cores we were able to identify several critical factors that affect the permeability and productivity of a CBM reservoir.

Coal cleats are more abundant than joints in adjacent sedimentary beds, and are the most important feature that affects permeability in coal. Coal composition is one of the primary controls on cleat development and density. Vitrain-rich coals typically contain the highest density of face cleats. Although vitrain-rich coal does not usually have a well-developed butt cleat set the interconnectedness of face cleats is accomplished by the high density of non-oriented conchoidal fractures. In clarain-rich coal both face and butt cleat sets are typically developed. Cleat density in this coal lithotype is controlled by mechanical layer thickness. Mechanical layers are commonly created by a thin interval of a different coal lithotype, a thin ash layer, or adjacent sedimentary beds. Thin mechanical layers contain a higher density of cleats than do thicker ones. Where mechanical layers are very thin (<5 cm), cleat density in clarain coal can equal or exceed cleat density in vitrain-rich coal. When ash content reaches a quantity so that carbonaceous shale is formed, no butt or face cleat set is found. Coal cleats and regional joints commonly terminate upon intersection with carbonaceous shale.

Proximity to structure affects cleat density. Coal permeability is enhanced in a direction parallel to faults within the damage zone as a result of increased cleat density and height. Juxtaposition of stratigraphy across a fault adversely affects reservoir connectedness as fluid or gas migration perpendicular to the fault can be halted. From examination of folds in the Ferron, we found that cleat density is enhanced in the vicinity of the hinge-line of the fold.

The continuation of regional joints from adjacent units into or through a coal zone may affect reservoir performance and productivity. We found that four primary joint continuation patterns are found at joint intersections. These patterns can be predicted based on the thickness of the coal zone and the thicknesses of adjacent units. Understanding how joint intersections behave in a coalbed reservoir provides insight into the vertical connectivity of a reservoir, fluid and gas migration patterns, and may even prove useful when designing fracture stimulation techniques.

We have provided several interpretations concerning the low productivity in Area A of Drunkards Wash based on the results of our fieldwork. In Area A, a combination of several factors likely accounts for the low production rates in this area. We suggest that in addition to faulting, complex fluvial-deltaic stratigraphy may be present in Area A. In Area B, a highly productive zone, we suggest that reservoir permeability has been enhanced as a result of numerous northeast-trending faults.

Understanding coal cleat characteristics and other factors that affect coalbed reservoir permeability may be used to maximize production of future wells, and may be used as a guide for efficient exploitation of new CBM fields. With a large increase in

demand for clean-burning fuels such as natural gas (methane), it is ever more critical to develop each potential source to the highest level of production and efficiency.

APPENDICES

Appendix A

Initial Site Summary Sheets

Ferron Coal: Site 1, Bear Gulch

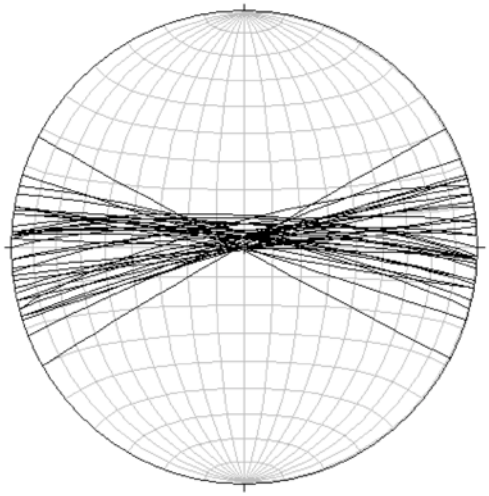

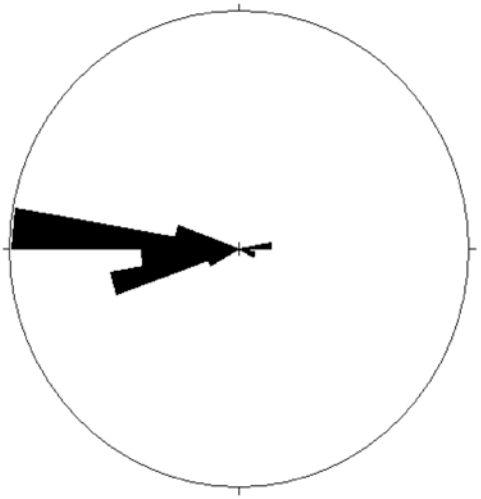

38 primary cleat planes

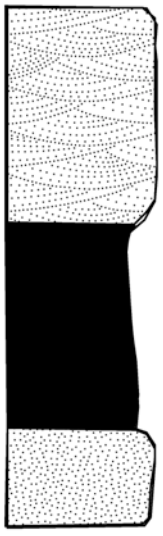

19.25 ft Sandstone

18.5 ft. Coal

7.5 ft Sandstone

Site Data

Bedding: 290, 4 N

Cleat Density: 55 / m

Bed Parting Cleats: 42/m

Coal Zone: Ferron A/C

Overlying Fractures: 11/ 100 ft

Orientation: 030, 90

Underlying Fractures: 19/100 ft

Orientation: 030, 90

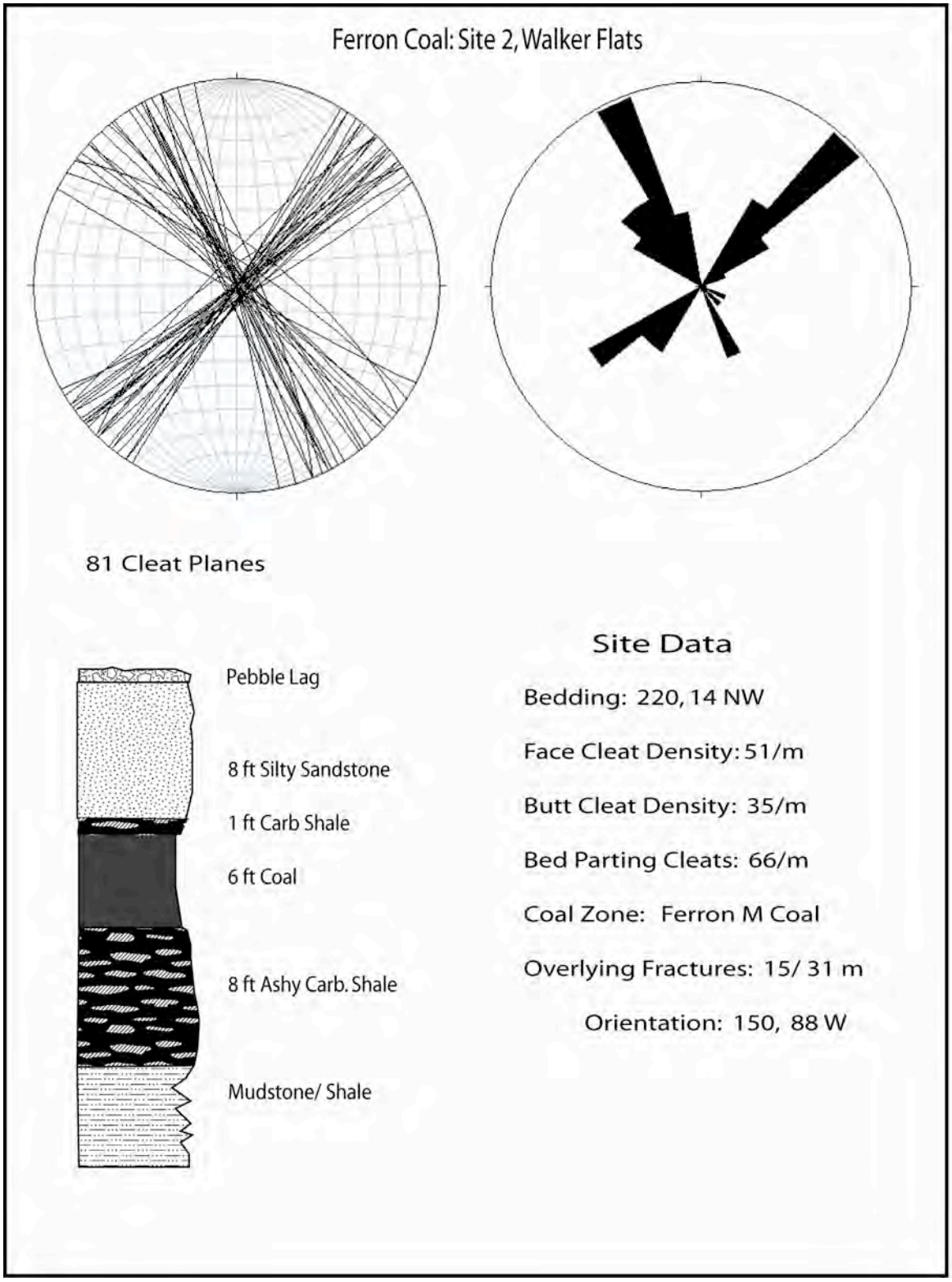
Ferron Coal: Site 2, Walker Flats
81 Cleat Planes
Pebble Lag
8 ft Silty Sandstone
1 ft Carb Shale
6 ft Coal
8 ft Ashy Carb. Shale
Mudstone/ Shale
Site Data
Bedding: 220, 14 NW
Face Cleat Density: 51/m
Butt Cleat Density: 35/m
Bed Parting Cleats: 66/m
Coal Zone: Ferron M Coal
Overlying Fractures: 15/ 31 m
Orientation: 150, 88 W

Site 3 Ferron Coal

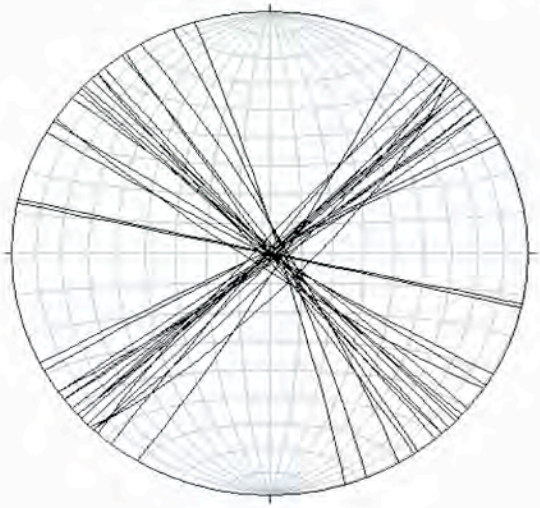

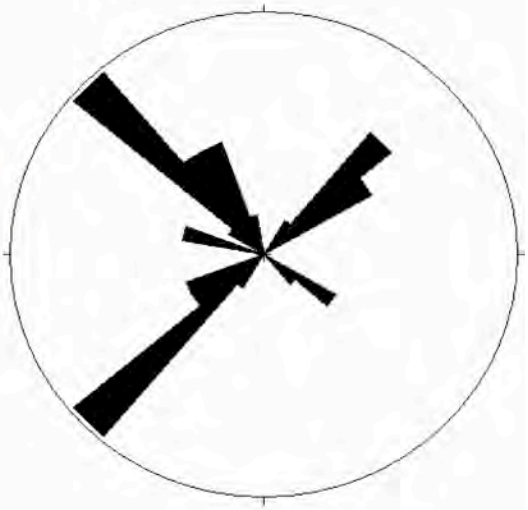

57 Cleat Planes

Pebble Lag

8 ft Silty Sandstone

1 ft Carb Shale

6 ft Coal

8 ft Ashy Carb. Shale

Mudstone/ Shale

Site Data

Bedding: 323, 6 NE

Face Cleat Density: 39/m

Butt Cleat Density: 27/m

Bed Parting Cleats: 58/m

Coal Zone: Ferron M Coal

Overlying Fractures: 15/31m

Orientation: 150, 88 W

Ferron Coals: Miller Canyon C Coal

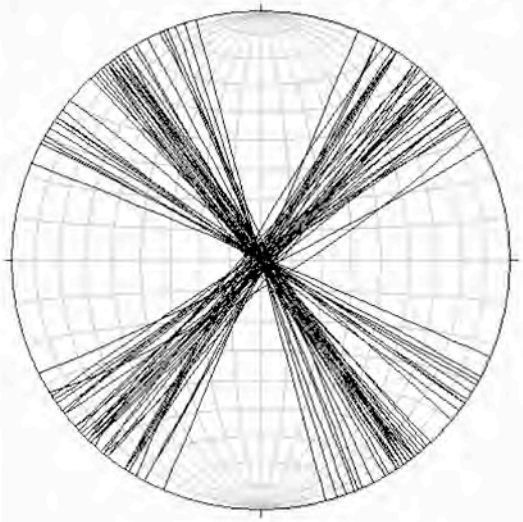

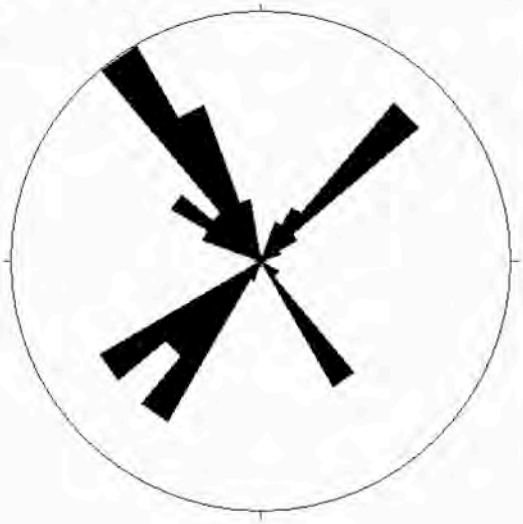

86 Cleat Planes

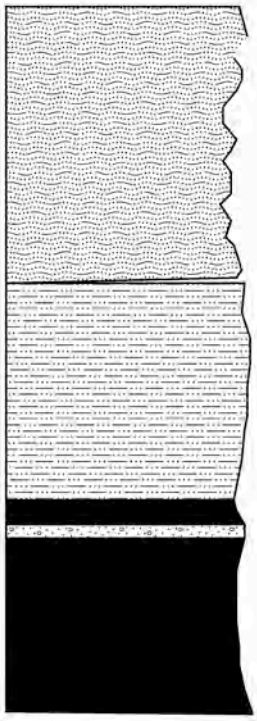

Interbedded
SandstoneMudstone

Mudstone Shale

5 in coal
8 in silty mudstone

6 feet cleat coal

Site Data

Bedding: Horizontal

Face Cleat Density: 31/m

Butt Cleat Density:36/m

Bed Parting Cleats: 70/m

Coal Zone: A coal Zone

Overlying Fracture: 1/m

Orientation: 100, 83 S; 030, 87 S

Underlying Sandstone: 8/10m

Orientations: 115, 83 S: 030, 86 S

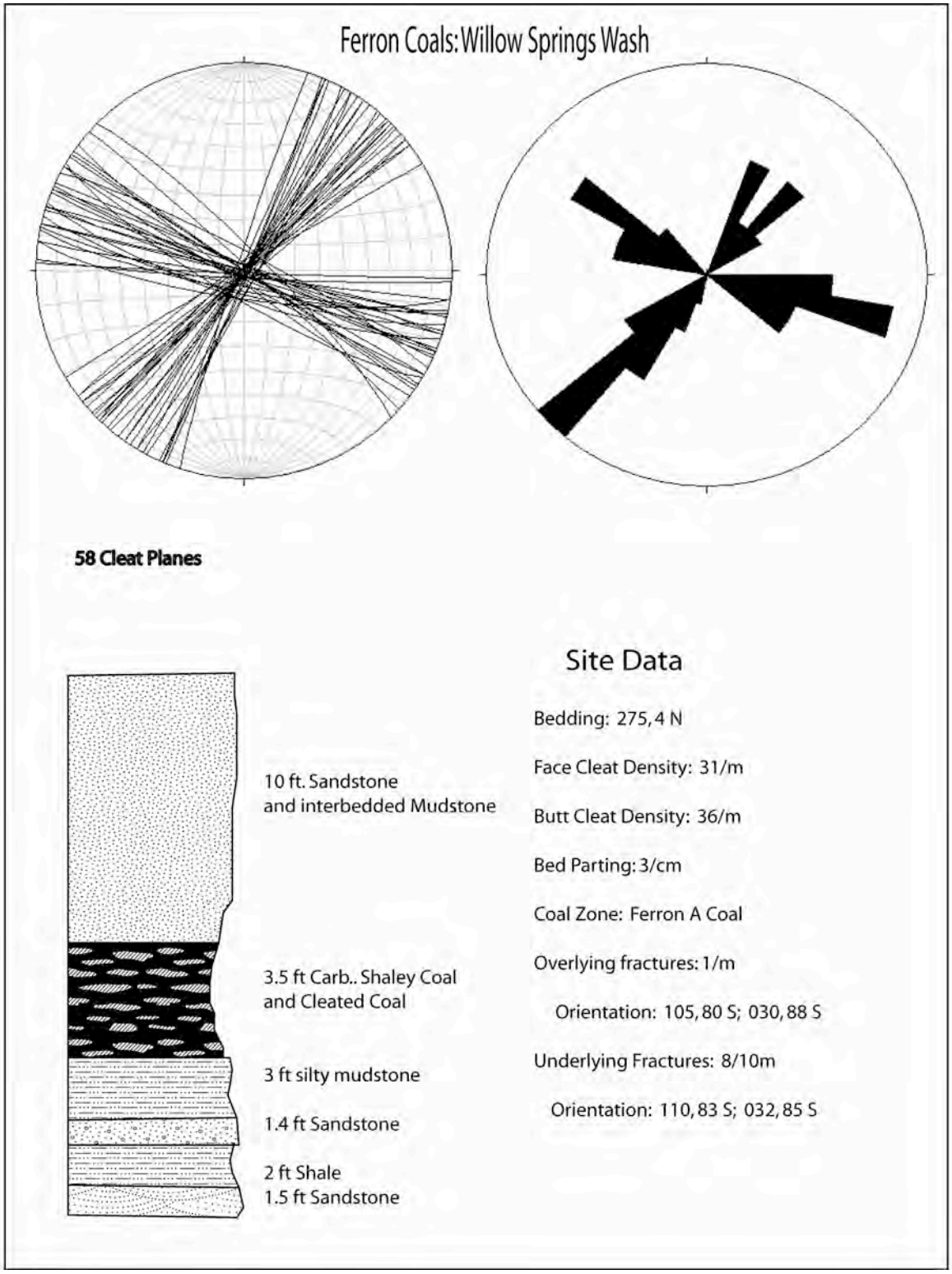
Ferron Coals: Willow Springs Wash
58 Cleat Planes
10 ft. Sandstone
and interbedded Mudstone
3.5 ft Carb.. Shaley Coal
and Cleated Coal
3 ft silty mudstone
1.4 ft Sandstone
2 ft Shale
1.5 ft Sandstone
Site Data
Bedding: 275, 4 N
Face Cleat Density: 31/m
Butt Cleat Density: 36/m
Bed Parting: 3/cm
Coal Zone: Ferron A Coal
Overlying fractures: 1/m
Orientation: 105, 80 S; 030, 88 S
Underlying Fractures: 8/10m
Orientation: 110, 83 S; 032, 85 S

Ferron Coals: I-70 Outcrop

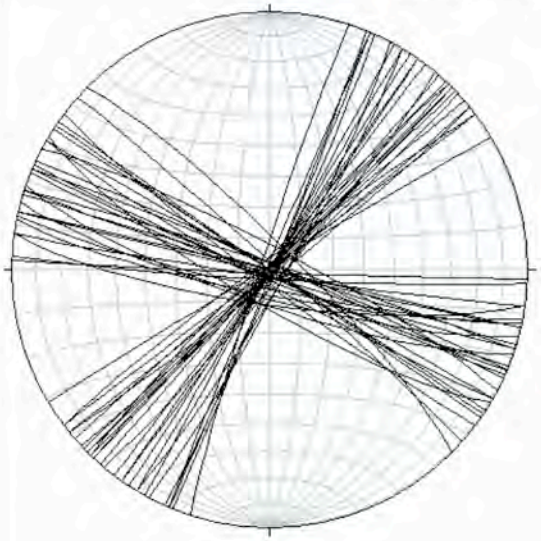

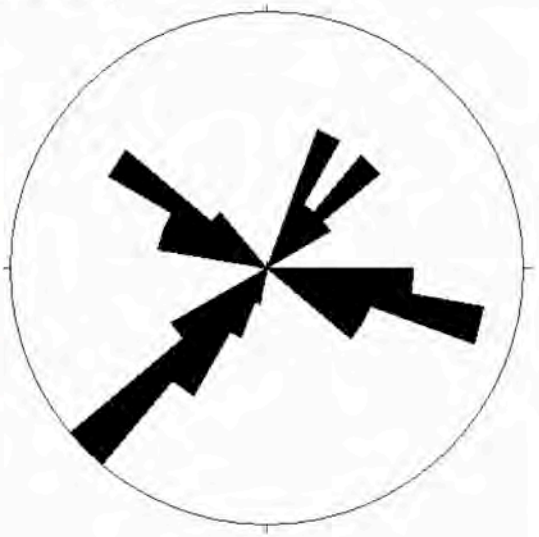

58 Planes

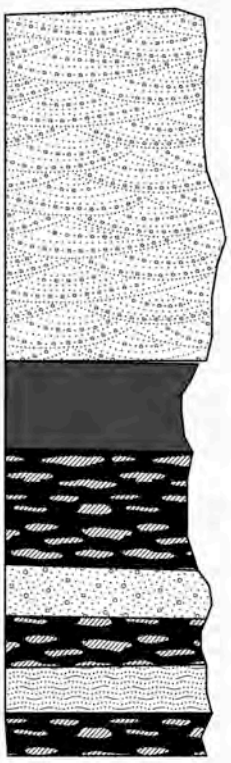

16 ft Sandstone

2.5 ft Cleated Coal

4 ft Carb Sahle

1.25 ft Sandstone

1.5 ft Carb Shale

1.5 ft Shaley Mudstone

1.25 ft Carb Shale

Site Data

Bedding: 347, 3 W

Face Cleat Density: 33/m

Butt Cleat Density: 28/m

Bed Parting Density: 105/m

Overlying Fractures: 7/13m

Orientation: 009, 80 E

Appendix B

Drunkards Wash Field Data

Drunkards Wash: Area A

Area A Mapable Data										
WELL #	LAT	LONG	Ground Level	Depth (ft)	Top (asl)	Water BWPD (cum/mo.)	Gas MCF (cum/mo.)	Coal Thickness (ft)	Coal+Carb-S. (ft)	% Clean Coal
34	39.61751	-110.89591	5871	2238	3633	33.70	86.35	16.9	23.4	84.6%
112	39.61963	-110.90460	5903	2362	3541	87.39	118.39	16.3	34.2	79.8%
113	39.61691	-110.88353	5838	2093	3745	38.98	59.99	18.1	30.5	77.9%
114	39.61675	-110.87822	5801	2080	3721	59.99	193.01	24.4	35.0	76.2%
291	39.62290	-110.87878	6192	2610	3582	72.55	277.37	27.1	38.3	88.9%
292	39.62330	-110.88854	6161	2610	3551	20.73	90.02	18.3	27.3	69.9%
293	39.62391	-110.89391	6147	2628	3519	47.94	54.74	15.2	22.1	90.8%
294	39.62467	-110.90670	6132	2666	3466	194.69	148.27	23.9	29.2	71.5%
301	39.63660	-110.90833	6059	2744	3315	377.18	72.63	15.4	33.9	76.9%
402	39.63056	-110.86901	6217	2576	3641	15.68	24.29	22.7	37.4	82.1%
403	39.64062	-110.87781	5617	2640	2977	10.26	50.28	28.3	37.4	77.5%
404	39.64172	-110.88480	5601	2647	2954	15.01	11.51	20.0	32.7	81.0%
405	39.63411	-110.88552	5742	2639	3103	11.88	39.00	22.4	34.4	94.2%
406	39.63214	-110.87448	5756	2604	3152	32.09	38.66	28.3	38.2	84.5%
407	39.64027	-110.89523	5887	2730	3157	14.27	20.54	19.4	34.5	66.7%
408	39.64086	-110.90459	6040	2780	3260	136.07	139.39	17.4	25.1	64.4%
414	39.63543	-110.89470	5980	2660	3320	12.96	3.00	22.9	30.4	83.0%
510	39.65447	-110.89457	5973	2986	2987	14.29	2.85	15.4	18.6	79.9%
511	39.65308	-110.90282	6047	3020	3027	3.22	5.43	9.2	22.7	79.2%
512	39.64870	-110.90614	6047	2902	3145	25.52	4.18	no data	no data	no data
513	39.64907	-110.89321	5965	2874	3091	19.85	8.05	13.7	23.9	73.0%
536	39.62580	-110.87122	6164	2574	3590	24.19	105.74	27.2	39.7	81.6%
537	39.61972	-110.85889	5722	1986	3736	29.90	30.48	22.5	41.5	78.6%
538	39.62028	-110.86611	5762	2084	3678	85.02	206.81	28.1	39.2	90.4%

Drunkards Wash: Area B

Area B Mapable Data										
WELL #	LAT	LONG	Ground Level	Depth (ft)	Top (asl)	Water BWPD (cum/mo.)	Gas MCF (cum/mo.)	Coal Thickness (ft)	Coal+Carb-S. (ft)	% Clean Coal
2	39.56970	-110.85491	5780	1602	4178	11.80	89.69	32.0	36.0	67.2%
3	39.56934	-110.84640	5714	1520	4194	15.96	242.21	18.5	21.6	70.3%
4	39.56914	-110.86392	5869	1718	4151	30.19	1044.84	33.1	36.8	86.7%
5	39.56247	-110.85517	5734	1672	4062	28.65	509.80	25.2	26.3	91.3%
6	39.57889	-110.85948	5728	1662	4066	37.56	669.97	29.3	36.8	89.7%
7	39.57611	-110.86381	5753	1732	4021	43.37	658.15	31.0	36.0	44.4%
8	39.57365	-110.87427	5796	1906	3890	166.39	1130.66	8.8	10.3	80.0%
9	39.56967	-110.87464	5871	1962	3909	478.06	1484.52	33.5	44.0	82.1%
10	39.56230	-110.85004	5731	1652	4079	25.10	231.38	28.8	32.2	73.3%
11	39.56193	-110.86481	5796	1726	4070	65.86	1043.86	28.4	32.7	81.0%
12	39.58839	-110.84645	5683	1495	4188	94.14	645.82	39.3	44.5	71.2%
13	39.58191	-110.85016	5690	1526	4164	69.85	378.75	22.5	29.5	82.2%
14	39.57303	-110.85035	5835	1456	4379	85.83	488.48	26.4	30.8	74.6%
15	39.59703	-110.85748	5722	1630	4092	42.86	145.36	39.6	46.4	61.1%
16	39.59707	-110.86642	5721	1680	4041	9.99	65.06	39.2	42.9	84.7%
17	39.58968	-110.86714	5752	1674	4078	28.14	493.43	39.5	44.5	76.5%
18	39.58733	-110.85609	5684	1476	4208	182.64	663.52	46.0	52.4	70.7%
19	39.59803	-110.87704	5721	1782	3939	176.73	797.54	24.4	27.8	83.6%
20	39.59711	-110.88654	5831	1931	3900	152.37	915.62	31.6	36.1	72.8%
21	39.58815	-110.88488	5898	1956	3942	704.89	1705.63	21.7	26.2	90.8%
22	39.58971	-110.87651	5820	1844	3976	127.49	789.33	34.4	37.7	63.1%
23	39.58247	-110.87644	5820	1772	4048	7.60	184.83	30.6	37.7	51.3%
24	39.58205	-110.88381	5863	1926	3937	383.36	1678.96	30.4	33.8	78.6%
25	39.57561	-110.88550	5857	1913	3944	94.29	953.74	22.0	28.5	97.7%
26	39.56852	-110.88432	5869	2030	3839	107.20	728.70	33.2	38.9	84.0%
27	39.56188	-110.87861	5914	2001	3913	58.48	878.83	16.2	19.5	77.2%
28	39.56048	-110.88649	5989	2066	3923	37.19	655.22	19.2	21.0	69.8%
33	39.58354	-110.86901	5773	1676	4097	8.37	366.75	24.8	28.5	75.0%
77	39.59578	-110.85045	5700	1510	4190	114.38	276.93	no data	no data	no data
78	39.58482	-110.83627	5619	1254	4365	351.42	523.05	24.5	33.5	87.8%
79	39.56172	-110.84017	5660	1462	4198	11.91	121.80	18.1	21.6	59.1%
125	39.57313	-110.83965	5689	1421	4268	213.58	627.98	19.4	32.0	71.6%
126	39.56604	-110.83845	5656	1433	4223	57.36	275.22	17.5	30.5	40.0%
532	39.59374	-110.84272	5708	1504	4204	135.92	214.66	31.1	40.6	90.8%
533	39.58722	-110.84222	5649	1430	4219	64.96	236.86	27.9	35.4	94.1%